UNIVERSITY OF ZULULAND

Synthesis and characterisation of CdS and PbS nanoparticles in an imidazolium based ionic liquid

By

Zikhona Tshemese

(201640093**)**

BSc. (Hons) (Walter Sisulu University)

THESIS

Submitted in fulfilment of the Requirements for the Degree

MASTER OF SCIENCE

In the field of

CHEMISTRY

Faculty of Science and Agriculture

University of Zululand

Supervisor: Prof. N. Revaprasadu (University of Zululand)

Co-supervisor: Prof. N. Deenadayalu (Durban University of Technology)

DECEMBER 2017

DECLARATION

I hereby declare that the work described in this thesis entitled "**Synthesis and characterization of CdS and PbS nanoparticles in an imidazolium based ionic liquid**" is my own and has not been submitted in any form for another degree or qualification of the University of Zululand or any other University/ Institution of tertiary education. Information derived from the published or unpublished work of others has been acknowledged in the text and a list of references is given.

Name: Zikhona Tshemese

Signature…… Date…….

CERTIFICATION BY SUPERVISOR

This is to certify that this work was carried out by Ms Zikhona Tshemese in the Department of Chemistry, University of Zululand and is approved for submission in fulfilment of the requirement for the degree of Master of Science in Chemistry.

…….

Supervisor

N. Revaprasadu (PhD)

Professor of Inorganic Chemistry

Department of Chemistry, University of Zululand,

KwaDlangezwa, South Africa

…….

Supervisor

N. Deenadayalu (PhD)

Professor of Physical Chemistry

Department of Chemistry, Durban University of Technology,

Durban, South Africa

Dedication

This work is dedicated to all my family members particularly my late father (Mpendulo Tshemese) who unfortunately could not live up to this far, my mother (Nokhethile Tshemese) and my daughter (Hlela Tshemese).

ACKNOWLEDGEMENTS

To God almighty be the glory for his love, mercy and continuous provisions throughout this journey. I am highly indebted to my supervisors Prof. Neerish Revaprasadu and Prof. Nirmala Deenadayalu for their mentorship and expertise throughout my Masters course. I thank the NRF Innovation, NRF/DST South Africa – Egypt Programme and the University of Zululand Research Office for the financial support provided for the study.

A special thanks to my mentor and friend Dr. Sixberth Mlowe, research group members Fr. Charles Gervas, Siphamandla Masikane, Malik Dilshad Khan, Sandile Khoza, Zimele Mzimela, Bongani Msibi, Ginena Shombe; research visitors Dr. Joseph Adekoya, Walter Kun, Kevin Ketchimen; friends Zama Dube, Zamani Ncanana for making this learning curve fun and providing useful suggestions. I also thank the Department of Chemistry as a whole for the support they gave me during my studies especially Welcome Zibane, Judine Govender, Dr Mochane and Dr Linganiso.

My greatest appreciation to the Thermodynamic and Bioprocessing research group from Durban University of Technology Ncomeka Mgxadeni, Ditiro Mashego, Thandeka Mkhize, Siyanda Chule and others for their assistance and friendliness whenever I needed support. I cannot be thankful enough to my family; my mom, Nokwezi Lucwaba, Mthetheleli Tshemese, Mfundo Tshemese, Thulani Tshemese, Yonela Tshemese, Nosipho Nqeketo and Mihla Tshemese; friends Ndzondelelo Bingwa, Tom Were, Vuyo Mangqalaza, Siviwe Qaka, Liso Langabi, Siviwe Stolom, Sanele Mqubi, Ayanda Tungata, Samkelo Ngongo, Luvo Dumani and Lamla Tungata who made the journey worth taking even when the going got tough and during stressful times.

Unizulu MethSSoc branch members (2016/2017 BEC) are equally thanked for the spiritual support and upliftment for the period of my entire programme. “And the congregation of those who believed were of one heart and soul; and not one of them claimed that anything belonging to him was his own, but all things were common property to them”- Acts 4:32.

ABSTRACT

Semiconductor metal sulfides nanoparticles have been prepared using the imidazolium based ionic liquid surfactant as both the stabilizer and growth modifier. The structural and morphological properties of the as-prepared nanoparticles were characterized by X-ray diffraction (XRD), transmission electron microscopy (TEM), scanning electron microscopy (SEM), ultraviolet visible and near infrared radiation (UV-Vis and NIR), photoluminescence and fourier transform infrared spectroscopy (FTIR). Various synthetic methods (thermolysis, microwave and room temperature syntheses) were used and reaction parameters such as temperature and injection protocols, precursor type were varied to study the optical and structural properties of the as-synthesized nanoparticles.

The CdS nanoparticle synthesis was carried by altering the reaction temperature and the injection protocol using single and dual source precursors. Cadmium ethyl xanthate was used as single source precursor whereas cadmium acetate and dodecanethiol were used as dual source molecular precursors in the presence of 1-ethyl-3-methylimidazolium methanesulfonate ionic liquid. XRD studies confirmed the formation of cubic and hexagonal phases for low and high temperatures respectively. The SAED results revealed that the nanoparticles were crystalline and the morphological studies further showed formation of nano-sized particles in the range of 2 – 15 nm, with close to spherical shaped morphologies. Blue-shifted band gaps further confirmed formation of very small CdS nanoparticles, which were temperature dependent.

In the synthesis of PbS nanoparticles, the effect of sulfur source (with the same lead source, lead acetate) was studied for dual source precursors with respect to temperature and lead ethyl xanthate complex was used as single source molecular precursor in the ionic liquid medium. Sodium sulfide and dodecanethiol were used as different sulfur sources. XRD studies confirmed formation of cubic phase of PbS. Electron microscopy analyses showed that the nanoparticle morphologies differed significantly depending on the synthetic factors such as temperature, nature of precursors and ranged from spherical to cubic shapes. TEM images together with SAED patterns revealed crystalline nanoparticles with sizes ranging from 29 to 53 nm. SEM images further confirmed formation of cubic shaped PbS nanoparticles. The study has successfully shown a facile method for the synthesis of CdS and PbS nanoparticles, this method can be used for other nanomaterials as well. Ionic liquids can indeed be used as both media solvents and as stabilizing/capping agents,

replacing the traditionally known solvents. The use of various reaction parameters has led to different morphological and structural properties of the a-synthesized nanoparticles.

Table of Contents

List of Figures **Page**

List of Tables **Page**

List of abbreviations

CdS	Cadmium sulfide
PbS	Lead sulfide
IL	Ionic liquid
[BEIM]BF_4	1-*n*-butyl-3-ethylimidazolium tetrafluoroborate
[BMIM][$MeSO_4$]	1-butyl-3-methylimidazolium methanesulfonate
[BMIM]PF_6	1-n-butyl-3-methylimidazolium hexafluorophosphate
[EMIM] [$EtSO_4$]	1-ethyl-3-methylimidazolium ethyl sulfate
DT	Dodecanethiol
SSP	Single source precursor
MW	Microwave

Techniques and methods

XRD	X-ray diffraction
TEM	Transmission electron microscopy
SEM	Scanning electron microscopy
FTIR	Fourier transform infrared spectroscopy
TGA	Thermogravimetric analysis
PL	Photoluminescence
UV-vis	Ultraviolet visible
SAED	Selected area electron diffraction

Symbols and constants

λ	Wavelength
θ	Theta
Å	Angstom
nm	nanometre
eV	electron volts

CHAPTER ONE

Introduction and literature review

1.1. General introduction

Nanomaterials play a vital role in developing advanced technologies. They are used in energy conversion and storage,[1] and many modern technology devices.[2,3] Cadmium sulfide (CdS) and lead sulfide (PbS) have gained attention because of their interesting properties. They both have tunable band gaps with known values being 2.4 eV for CdS[4] and 0.41 eV for PbS.[5] The cadmium sulfide band gap appears in the visible region which renders it to have high photosensitivity,[6] whereas lead sulfide absorbs light in a wide range of spectrum extending to the infrared region.[7]

Laboratory preparation of these important nanomaterials has been dominated by the use of various solvents which have been proven to be toxic and harmful to the environment.[8] This has led to the need to investigate greener solvents to replace these commonly used solvents. A broad guide into making such materials has been given in green chemistry principles.[9] It is a 12 principle set which concentrates on minimizing the chemical hazards to human and environmental health, finding high quality products, and usage of energy efficient chemical processes.[10] Green chemistry's most crucial aspect is the concept of design. The 12 principles are called design rules which help in achieving the international goal of sustainability.[11] In summary this imparts knowledge about the bitterness of preventing waste than cleaning it up after being formed, designing synthetic methods that maximize the incorporation of all material used in the process into the final product, usage of methodologies that possess little or no toxicity to human health and the environment and designing materials with efficacy of function while reducing toxicity.[12]

There are salts with a melting point below 100 ^{o}C, which are called ionic liquids. These ionic liquids are suitable candidates for the replacement of these hazardous and poisonous organic solvents as they have attracted interest in the last decade with an extended range of green synthesis and applications. They appear to be the subject of many fundamental publications aimed at improving the understanding of these solvents, predicting their physico-chemical properties, describing their increasingly diverse applications and use in analysis, synthesis, catalysis and separation.[13]

The aim of this work is to provide an efficient way of preparing nanosized CdS and PbS nanoparticles stabilized by an imidazolium based ionic liquid. The choice of this ionic liquid class is driven mostly by its interesting properties which include high heat capacity, high density, extremely low volatility, non-flammability, high thermal and electrochemical stability and wide temperature range for liquid state. The 1,3- dialkyl imidazolium based ionic liquids have been investigated as possible electrolytes for lithium and lithium ion cells[14] but in this case they will be used as solvents and/ or capping agents in the synthesis of CdS and PbS nanoparticles. The ionic liquid of choice will also bring about the stability of the nanoparticles as previous studies have shown the effectiveness of this group of ionic liquids to stabilise nanoparticles.[15]

1.2. Literature review

1.2.1. Semiconductors

Significant progress has been made in the preparation of semiconductor nanocrystals with controlled size and shape. It is well-known that nanoparticles with varying shapes and sizes give rise to unique properties which can be harnessed for a myriad of applications. Some of the common shapes of the nanomaterials are highlighted in Figure 1.1. Semiconductors have tunable electronic and spectroscopic properties which make them suitable for applications in optical devices, photovoltaic cells,[4,16] electronic and optoelectronic devices.[17] The interest is given to groups II-VI, III-VI and IV-VI, examples include PbS, ZnS, CdS, Bi_2S_3, Sb_2S_3, HgS, In_2S_3, Ag_2S. These semiconductor chalcogenides have tunable band gap energies.[18] He *et al*. have studied the interactions and organisation of nanoparticles in ionic liquids as an advantage as they reduce the use of toxic organic solvents.[19] Pure nanoparticles with small sizes can be prepared by ionic liquids without any capping and stabilizing agents.[20]

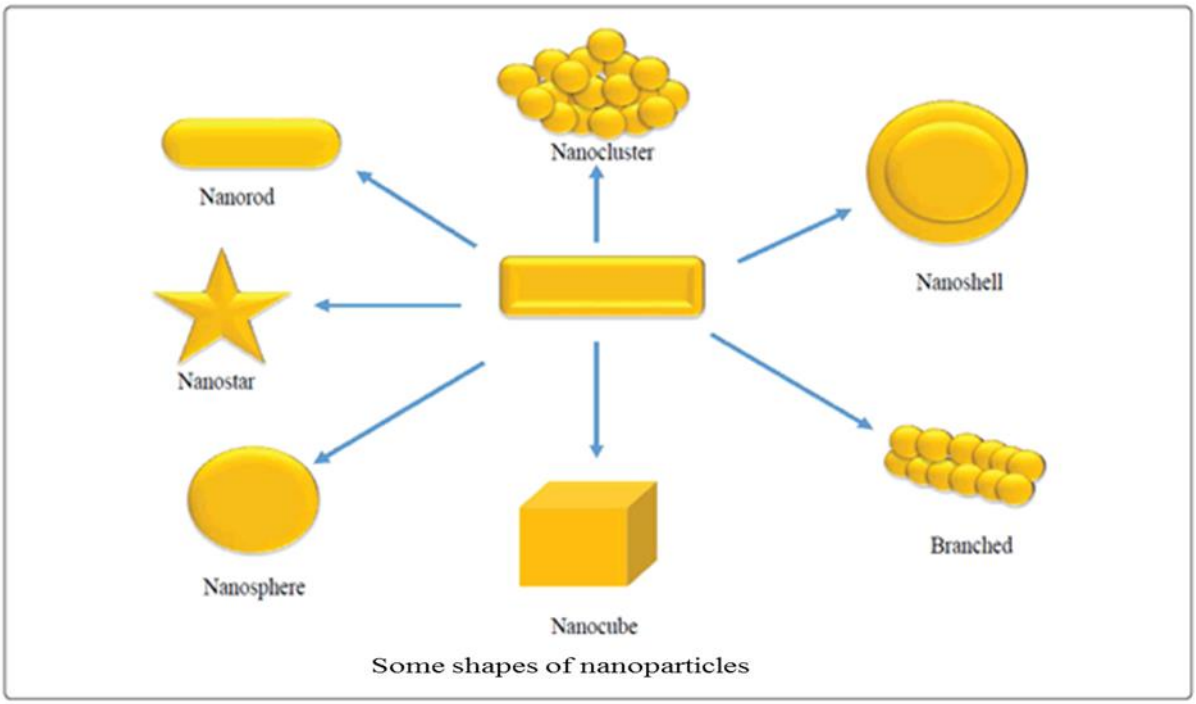

Figure 1.1: Demonstration of various nanoparticle shapes synthesized from the same starting material.[21]

Synthesis of nanomaterials can be achieved by following one of the two universal standard procedures i.e. top-down and bottom-up approach.[22] Under these general standard approaches many synthetic pathways can be employed and amid those reported in the literature; the ionothermal method (Figure 1.2) has potential to be the economically viable.[23] This is due to its low processing temperature and being a green alternative to the conventional solvents.[24,25] Their great structural diversity also makes easy tailoring of their properties for different applications, thus, one can keep the same cation (imidazolium, phosphonium, pyridium) but change only the anion or the alkyl chain to produce different properties. This class of liquids has gained attention in many fields including the synthesis of nanoamaterials.[26] As shown in Figure 1.3, these liquids can be good stabilizers in nanomaterial synthesis and they are known to do the stabilization mechanistically in three ways namely electrostatic, steric and a combination of both steric and electrostatic forces.[27] PbO nanocrystals have been prepared using this class of ionic liquid due to its high thermal stability and wide liquid range.[28] The nanocrystals obtained from this study resembled the PbS crystal structure and a room temperature ionic liquid 1-*n*-butyl-3-ethylimidazolium tetrafluoroborate [BEIM]BF_4 was used in the study.

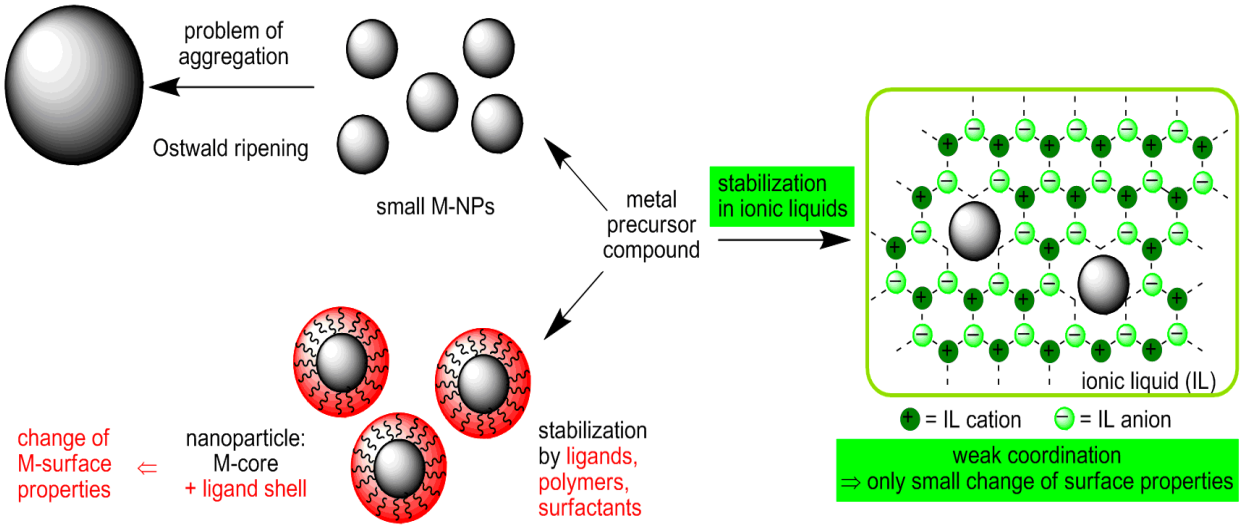

Figure 1.2: A schematic mechanism for the nanoparticle stabilization in ionic liquids during their synthesis.[29]

1.2.2. Cadmium sulfide (CdS)

1.2.2.1. Background

CdS is a group II-VI semiconductor with a band gap of 2.42 eV.[4] This material exists in two natural forms namely, hawleyite and greenockite which differ in crystal structures as shown in Figure 1.3. The latter forms hexagonal crystals with wurzite structure while the former has the cubic (zinc blende) structure (Figure 1.4). Its narrow band gap means it can be used for harvesting visible light.[30] It has been used in non-linear optical devices,[31] photovoltaics[32] and in many fields of applications such as light emitting diodes,[33] and thin film transistors.[34] The ionothermal synthetic method is gaining attention as a green method of synthesizing CdS nanoparticles.[35]

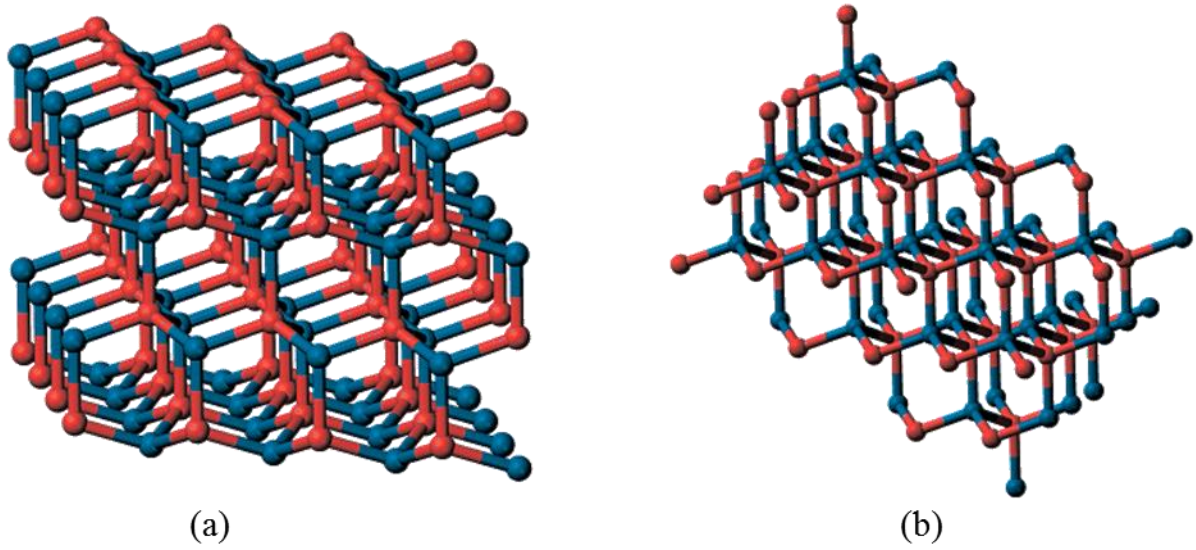

Figure 1.3: Crystal structures of (a) Greenockite (hexagonal) and (b) Hawleyite (cubic) of CdS semiconductor.[36]

Though the imidazolium based ionic liquid(s) have been extensively used as immobilizing agents for transition metal catalyst precursors, only a few reports exists for their use in CdS synthesis.[37,38] Sajjadi *et al.* have studied the aggregation of nanoparticles in aqueous solution of ionic liquids.[39] Imidazolium based ionic liquids with the same anion but different alkyl chains, namely 1-butyl-3-methylimidazolium bromide and 1-methacryloyloxypropyl-3-methylimidazoliumbromide were used in the study. The focal point of the study was on the interactions between ionic liquids and nanoparticles dispersed in aqueous solutions leading to the formation of nanoparticle clusters of finite size. The success of the study was measured by the ability to demonstrate the active participation of the ionic liquid in the formation of the aggregates suspended in aqueous solution filling the inter particle space.

Biswas *et al.* reported the preparation of nanoparticles of hexagonal CdS with a diameter of 3 to 13 nm by the reaction of cadmium acetate dihydrate with thioacetamide in imidazolium [BMIM]-based ionic liquids.[40] By changing the anion of the ionic liquid, different particle sizes were obtained. The authors also report CdS nanoparticles prepared in 1-butyl-3-methylimidazolium methanesulfonate [BMIM][$MeSO_4$]. TOPO was used as a capping agent and the particles that were obtained particularly from this ionic liquid were of 4 nm in size. Thermodynamically stable phases of the metal chalcogenide nanostructures were obtained.

Jiang *et al*. used ionic liquid as precursors for the synthesis of reduced graphene oxide CdS nanocomposites that have enhanced visible light photoactivity.[41] The ionic liquid used in this work was imidazolium based, it was used both as a source of sulfur and as the stabilizing agent. This class of ionic liquid has also been used as green catalysts for the synthesis of stable CdS and ZnO nanoparticles.[42] Low aggregation as a result of ionic liquid presence resulted in small sized and spherical shaped nanoparticles. Ionic liquids have been found to act as remarkable stabilizers for metal nanoparticles by allowing the selection of cationic and anionic species from the huge pool of cations and anions. These solvents also offer selective tuning of metal nanoparticle size and solubility by varying the cationic and anionic moieties owing to their ‘‘tunable nature’’.[27] Imidazolium based ionic liquids have been used as green solvents for the selective recovery of Zn(II), Cd(II), Cu(II) and Fe(III) from hydrochloride aqueous solutions.[43] The group further demonstrated the exciting potential of ionic liquids for use as sole extraction agents in the removal of metal ions, since the modification of their cation and anion composition and the extraction conditions allowed the design of a specific extraction green process for each metal ion.

1.2.2.2. Dual source precursors

Properties of nanomaterials depend on the synthesis procedures and reaction conditions. Synthesis of nanomaterials has been dominated by the use of multiple source precursors, where a metal salt is reacted with a chalcogen source in the presence of a solvent to form desired nanomaterials.[44] Different combinations of the starting materials (precursors) are what affect the size, shape, and consequently the properties of nanomaterials.[45] Most commonly used salts are those of nitrates and acetates.[45] There is also a huge pool of chalcogen sources used in the synthesis of nanomaterials. A thiourea solution has been reported as a sulfur source for the synthesis of CdS nanocrystals.[46] On the other hand, solid Na_2S has also been used as a sulfur source for the synthesis of ZnS in the presence of an ionic liquid.[20]

Chang *et al*. developed a synthetic method for silica CdS nanocomposite spheres. The method used in the study was co-precipitation of cadmium nitrate and ammonium sulfide in the presence of water nanodroplets to produce CdS quantum dots which were incorporated into the silica colloids.[47] Wu *et al*. did a study on preparation of metal chalcogenide nanocrystals using multi precursors. It was found that the absorption of the nanocrystals greatly depended on the size

and shape of material formed.[48] Factors affecting the size and morphology of nanomaterials are temperature, the precursor concentrations and reaction time. In a study conducted by Pal *et al*., different proportions of cadmium nitrate and ammonium sulfide have been utilized to prepare CdS nanoparticles.[49]

1.2.2.3. Single source precursor route

A desirable route for the preparation of nanomaterials has been developed making use of the single source precursors. A complex containing both the metal and chalcogen is decomposed to form the desired nanomaterial. It has been reported that this route give rise to materials with well-defined shapes.[50] The advantages of using this synthetic approach are: it limits the formation of side reactions and eliminates the presence of defects as the metal is already coordinated to the chalcogene source, easier to control the stoichiometry and most complexes (single source precursors) are volatile and they easily decompose to form the desired nanomaterial.[51] The single source precursor needs to be carefully designed and synthesized because of recurrent occurrence of polymeric structures that might result in reduced volatility. Most used single source precursors are those of dithiocarbamates,[52] xanthates,[53] dithioimidodiphosphinates,[54] thiosemicarbazides,[55] thiourea.[56]

Many nanomaterials with high purity and high yield have been synthesized from these complexes, CdS thin films being part of them.[57] In addition to the reaction parameters, the structure and chemical composition of the precursor play a huge role on the properties of the nanomaterial formed.[51] Gaur *et al*. studied the effect of anions on the morphology of CdS nanoparticles synthesized from four cadmium thiourea complexes.[18] The study was carried out in two different methods; thermal decomposition of the single source precursor in a solvent and the solid state which was explored as the suitable strategy. CdS nanoparticles with different morphologies have been synthesized from heterocyclic dithiocarbamates complexes through varying reaction parameters such as temperature and precursor concentration.[58]

1.2.3. Lead sulfide (PbS)

1.2.3.1. Background

Lead sulfide (PbS) is a group IV-VI semiconductor with a cubic crystal structure (shown in Figure 1.4) that is widely studied because of its applications in solar absorbers,[59] LED devices,[60] lasers,[61] optical amplification,[62] optical switches,[63] as gas- sensing agents in the solid- state sensors,[64] biological labelling and medical diagnostics.[65] PbS has a small direct band gap energy, 0.41 eV and large exciton Bohr radius 18 nm.[66] The fact that lead sulfide band gap is small and tunable makes it an interesting semiconductor. Optical absorption and emission in the near infrared region of the spectrum require semiconductors with small bang gap energies, PbS finds potential application in making such devices.[67-69] Nanomaterials with different sizes and shapes give rise to different properties for example nanorods will give different properties from nanocrystals or nanotubes which results in different applications.[64]

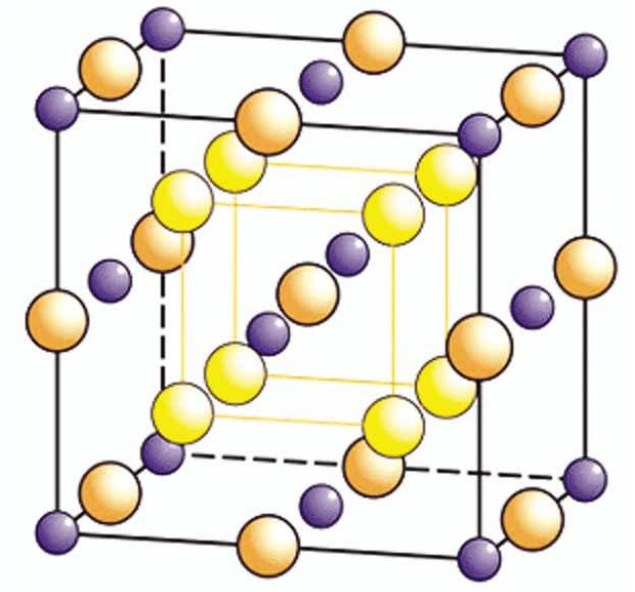

Figure 1.4: Crystal structure of cubic PbS semiconductor.[70]

This chalcogenide (PbS) has been prepared by several methods including solvothermal, microwave irradiation and hydrothermal methods using different starting materials. Using solvothermal synthesis, Cao *et al.* reported on morphology of different shapes of PbS through adjusting the temperature and using different reagents.[71] Ji *et al*. reported on the thioglycolic acid assisted hydrothermal method for the controlled morphology preparation of PbS nanocrystals.[72]

The study revealed that star shaped and rod like nanocrystals through using different sulfur and lead sources were obtained. A study compiled by Querejeta-Fernandez *et al*. was conducted specifically to investigate the formation of star-like lead sulfide superstructures.[73] In a study by Jana *et al*., tetrapod like PbS structures have been prepared using a hydrothermal route.[74] PbS can be synthesized from different halide precursors as in the study done by Yuan *et al.*, where the effect of hard-soft acid-base attributed to the formation of controlled size of nanoparticles.[75] Liu *et al*. gave a report about the photocatalytic activity of PbS quantum dots with an average diameter of 10 nm.[76] Introduction of PbS showed improved photocatalytic activity of Bi_2WO_6. The improved photocatalytic activity was assigned to the unique quantum effects of PbS quantum dots, where PbS quantum dots strongly coupled with Bi_2WO_6 resulted in the enhanced utilization rate of visible light.

The field of nanochemistry has made attempts to synthesize material with less toxicity and that does not endanger human health.[10] In the few reports available about this, Zhao *et al*. reported cubic structured PbS nanocrystals prepared in an ionic liquid, 1-n-butyl-3-methylimidazolium hexafluorophosphate ([BMIM]PF_6).[77] Among imidazolium based ionic liquids, those with halogen containing anions are susceptible to decomposition in the presence of water and form corrosive species like hydrofluoric and phosphoric acid for example in the aforementioned ionic liquid. The 1-ethyl-3-methylimidazolium ethyl sulfate [EMIM] [$EtSO_4$] has been used to prepare PbS nanoparticles with cubic crystal structure.[78]

1.2.3.2. Dual source precursor

Many essential properties and applications of crystals depend strongly on their shapes, sizes and on dimensionalities. These are greatly affected by the route followed into making these materials, reaction parameters which include type of precursors and conditions under which the reactions are performed. There are many reports on multiple precursor synthesis of PbS nanomaterials. The list include Hardman *et al*. who prepared PbS nanoparticles using PbO and TMS as their starting materials.[79] Ultrasound transient absorption measurements were used to study multiple exciton generation in solutions of the synthesized nanoparticles in this study. The $PbBr_2$ has been used with sulfur as the precursor in the fabrication of PbS quantum dots.[75] Using this bromide precursor rendered slow reaction kinetics which led to smaller quantum dots compared to another halide precursor, thus, giving a possible way to control quantum dot growth.

PbS nanowires with ellipse and parallelogram structures which were synthesized from $Pb(NO_3)_2$ and thiourea in ethylenediamine/H_2O as a solvent have been reported.[80] Gonza´lez-Pedro *et al*. have reported on the preparation of high performance PbS quantum dot sensitized solar cells with a 4 % efficiency that was achieved through exploring metal precursor effect.[81] Ji *et al*. used hydrothermal route to control the morphology of PbS nanocrystals.[72] The study was successful through using different precursors i.e lead acetate with thiourea for the synthesis of star-shaped PbS nanocrystals and lead nitrate with sodium sulfide for the synthesis of PbS nanorods. Akhtar *et al.* prepared photoelectrochemically active PbS nanoparticles using dual sources (PbO and TMS) via an environmentally benign route.[67] By carefully changing the reaction conditions they managed to get PbS nanoparticles with well-defined shapes.

1.2.3.3. Single source precursor route

The difficulty in maintaining stoichiometry of some reactions has led to a search of an alternative route into making nanomaterials. Under different molecular precursors reported in literature, star-shaped PbS nanocrystals have been prepared through a hydrothermal process of [bis(thiosemicarbazide)lead(II)]complex.[82] The effect of reaction time was investigated on the morphology of products. A group of mixed ligand single source precursors has been used to synthesize PbS nanocrystals by solvothermal decomposition.[83] Anisotropic PbS nanoparticles were synthesized from lead piperidine and tetrahydroquinoline dithiocarbamate complexes.[84] These complexes were thermolysed in different coordinating solvents and various temperatures. Through using various reaction conditions different morphologies of the as-synthesized material were obtained which ranged from spheres to cubes and rods. Lead xanthate precursors have been reported for the formation of PbS nanomaterials with different shapes, and thin films.[85]

1.2.4. Microwave irradiation

Among many methods that have been used in the synthesis of nanomaterials, microwave assisted reactions have gained attention. This is because of the efficiency of the technique, its advantages include better selectivity, larger reaction yields and increased rates.[86] This synthetic method takes advantage of both single and multiple source precursor use to semiconductor nanomaterial synthesis. Other benefits of this method include performing reactions at low temperatures and for short reaction times,[87] obtaining small particle sizes, and high purity.[88] Metal sulfide synthesis through microwave assisted reactions has been well reported. Murugan *et al*. established a microwave-solvothermal technique for CdS nanocrystalline particles using different solvents for low temperatures.[89] PbS with a cubic phase nanoparticles have been prepared from this method using lead acetate and sulfur powder in a polyethylene glycol solvent.[90]

1.2.5. Ionic Liquids

1.2.5.1.Background

The environment and human health are threatened by use of toxic chemicals. A need of environmentally friendly solvents which can reduce the adverse effects to harm human health and the environment is on the rise. Ionic liquids being molten salts with melting points below 100 ℃ while possessing properties like low viscosity,[91] negligible vapor pressure,[92] non-flamability,[93] high ionic conductivity,[94] good thermal and chemical stability,[19] and tunable solubility for both organic and inorganic molecules have become a central focus as substitutes to the toxic solvents.[23] Ionic liquids offer unique physicochemical properties which lead to them being environmentally friendly and they may lead to new materials that have never been achieved by conventional solvents or even water.

Having a potential to act as a reactant as well as a solvent for a reaction, ionic liquids can be all in one templates, an advantage to reduce the cost of material and bulk usage in processing.[24] Ionic liquids are not just solvents in reactions, they are stabilizing agents and they offer stability in three different forms; electrostatic, steric and electrosteric stabilization.[27] Their low surface tension leads to high nucleation rates and consequently to small nanoparticles. The ionic liquid itself can act as an electronic as well as a steric stabilizer and, thus, can lower particle growth.[95] As highly structured liquids, these solvents have a strong effect on the morphology of the particles formed.[96]

Preparation of soluble and stable metal nanoparticles can be easily done in ionic liquids.[97] Beier *et al*. conducted a study on the preparation of ionic liquid supported Pt nanoparticles as catalysts for enantioselective hydrogenation reactions.[98] At first metallic nanoparticles such as iridium, and palladium were synthesized.[99] A new kind of nanostructures with a variety of morphologies such as Fe nanoparticles, Te, Au and CoPt nanorods, Co nanocubes, TiO_2 hollow microspheres, CuCl nanoplatelets, and ZnO hexagonal micropyramids and hollow mesocrystals have been fabricated by selecting suitable IL reaction systems.[100] New developments of ILs could render many opportunities and challenges for the fabrication of nanoparticles with unique shape and structures. The newly found reaction media still needs to be investigated more widely for other inorganic materials synthesis. A list of common cations and anions is shown in Figure 1.5. A possible combination of these cations and anions is quite high and it presents a great flexibility in their properties.[9,101]

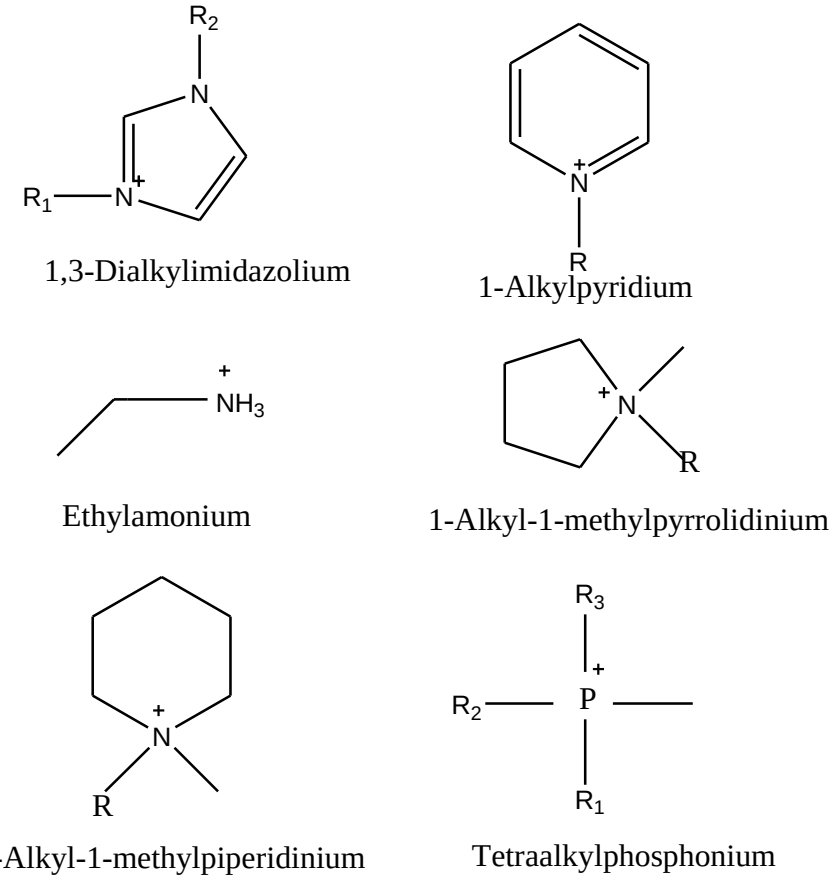

Figure 1.5: List of common cations used to synthesize ionic liquids.

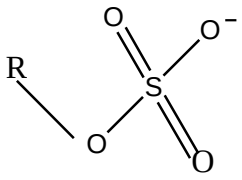

Alkylsulphate

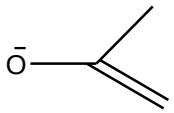

Acetate

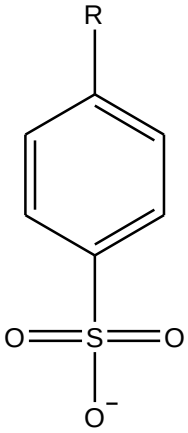

Alkyltosylate

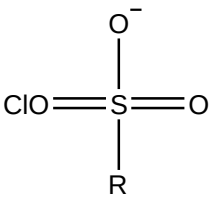

Alkylsulphonate

Cl^-

Chloride

Br^-

Bromide

I^-

Iodide

Figure 1.6: List of common anions used to synthesize ionic liquids.

1.2.5.2.Imidazolium based ILs

Ionic liquids with an imidazolium ring as cation can interact with many different species, as they offer hydrophobic or hydrophilic regions and a high directional polarizability. This is one of the distinct qualities of imidazolium ionic liquids that distinguish them from the typical ion aggregates of which ion pairs and ion triplets are widely recognized examples. The structural organization of these solvents can be used as "entropic drivers" for spontaneous, well-defined, and prolonged ordering of nanoscale structures. Certainly, the unique combination of flexibility towards other molecules and phases plus the strong hydrogen-bond-driven structure makes ionic liquids potential key tools in the preparation of a new generation of chemical nanostructures.[96]

A broad spectrum of high quality nanomaterials have been fabricated in the presence of ionic liquids, the imidazolium class being the most popular. This class of ILs has been used to produce monometallic nanoparticles of Cr, Mo, W, Co, Rh and Ir where the metal carbonyl precursor were decomposed in 1-butyl-3-methylimidazolium tetrafluoroborate ([BMIM][BF_4]). The produced nanoparticles are reported to be stable to oxidation and aggregation below argon atmosphere for six months and the observation was attributed to the IL giving protection to the nanoparticles. The ionic liquid used gave rise to the production of very small nanoparticles with a size of 1- 3 nm, adding to the stability offered by the IL to these nanoparticles their properties were protected and maintained.[9] The imidazolium based IL have been used as great stabilizers to nanoparticles.[102] The stabilization of nanoparticles is governed by repulsive forces provided by the stabilizing agent. Ionic liquids being a kind of stabilizing agents offer the stabilization in three forms, electrostatic, steric stabilization and combination of both electrostatic and steric stabilization.[27] Figure 1.8 shows a structural presentation of the ionic liquid that will be used in this study.

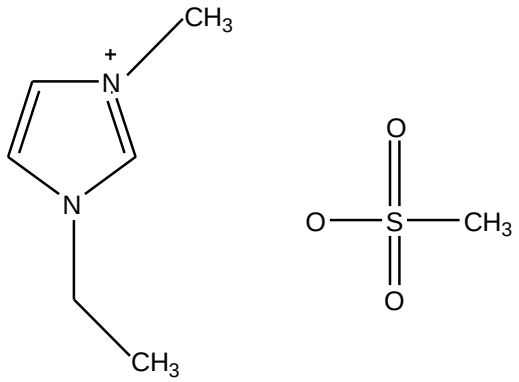

Figure 1.7: Chemical structure of 1-ethyl-3-methylimidazolium methanesulfonate.

1.3. Statement of the research problem

Cadmium sulfide and lead sulfide being the popular group II-IV (former) and IV-VI (latter) semiconductor nanoparticles are presently of great interest among others because of their applications. The preparation of this chalcogenide has been done in organic solvents, most of them are known to be harmful to the environment and that calls for use of green and less harmful solvents. Ionic liquids being called the "designer solvents" seem to be a better replacement to these toxic solvents and they also act as stabilizers in the synthesis of nanomaterials. This study will focus on the use of ionic liquids in the preparation of CdS and PbS nanoparticles. The use of this green method of synthesis with the aim to obtain particles with even better properties will result to extended properties of the products.

1.4. Aim and objectives of the study

The aim of this study is to synthesize CdS and PbS nanoparticles using an imidazolium based ionic liquid as a coordinating solvent and capping agent.

Objectives of the study:

i. To synthesize and control the size of CdS nanoparticles using 1-ethyl-3-methylimidazolium methanesulfonate which is a green solvent and stabilizing agent through the use of various reaction parameters and techniques.
ii. To synthesize and control the size of PbS nanoparticles using the ionic liquid, 1-ethyl-3-methylimidazolium methanesulfonate as a stabilizing agent by using various reaction parameters and techniques.
iii. Characterize the formed nanoparticles using X-ray diffraction, transmission electron microscopy, scanning electron microscopy, UV-visible, photoluminescence and Fourier transform infrared spectroscopy.

1.5. Thesis layout

This thesis is composed of five chapters

Chapter one is an introduction and literature review summarizing the scientific knowledge related to the subjects mentioned in this thesis
Chapter two gives details on the synthesis, results and discussion of cadmium sulfide nanoparticles prepared form single and dual source precursors
Chapter three details about the synthesis, results and discussion of lead sulfide nanoparticles prepared form single and dual source precursors
Chapter four is based on the facile synthesis of these two materials
Chapter five is a summary of the results obtained from this project, challenges and recommendations for future work

1.6. References

(1) Zhang, Q.; Uchaker, E.; Candelaria, S. L.; Cao, G. Nanomaterials for energy conversion and storage. *Chemical Society Reviews* **2013**, *42*, 3127-3171.

(2) Chan, Y.; Steckel, J. S.; Snee, P. T.; Caruge, J.-M.; Hodgkiss, J. M.; Nocera, D. G.; Bawendi, M. G. Blue semiconductor nanocrystal laser. *Applied Physics Letters* **2005**, *86*, 0731021-0731023.

(3) Kershaw, S. V.; Susha, A. S.; Rogach, A. L. Narrow bandgap colloidal metal chalcogenide quantum dots: Synthetic methods, heterostructures, assemblies, electronic and infrared optical properties. *Chemical Society Reviews* **2013**, *42*, 3033-3087.

(4) Ehsan, M. A.; Ming, H. N.; Misran, M.; Arifin, Z.; Tiekink, E. R.; Safwan, A. P.; Ebadi, M.; Basirun, W. J.; Mazhar, M. Effect of AACVD processing parameters on the growth of greenockite (CdS) thin films using a single-source cadmium precursor. *Chemical Vapor Deposition* **2012**, *18*, 191-200.

(5) Mehrabian, M.; Mirabbaszadeh, K.; Afarideh, H. Experimental optimization of molar concentration to fabricate PbS quantum dots for solar cell applications. *Optik-International Journal for Light and Electron Optics* **2015**, *126*, 570-574.

(6) Entezari, M. H.; Ghows, N. Micro-emulsion under ultrasound facilitates the fast synthesis of quantum dots of CdS at low temperature. *Ultrasonics Sonochemistry* **2011**, *18*, 127-134.

(7) Meng, L.; Zhao, F.; Zhang, J.; Luo, R.; Chen, A.; Sun, L.; Bai, S.; Tang, G.; Lin, Y. Preparation of monodispersed PbS quantum dots on nanoporous semiconductor thin film by two-phase method. *Journal of Alloys and Compounds* **2014**, *595*, 51-54.

(8) Duan, H.; Wang, D.; Li, Y. Green chemistry for nanoparticle synthesis. *Chemical Society Reviews* **2015**, *44*, 5778-5792.

(9) Patete, J. M.; Peng, X.; Koenigsmann, C.; Xu, Y.; Karn, B.; Wong, S. S. Viable methodologies for the synthesis of high-quality nanostructures. *Green Chemistry* **2011**, *13*, 482-519.

(10) Akhtar, J.; Malik, M. A.; O'Brien, P.; Wijayantha, K. G. U.; Dharmadasa, R.; Hardman, S. J. O.; Graham, D. M.; Spencer, B. F.; Stubbs, S. K.; Flavell, W. R.; Binks, D. J.; Sirotti, F.; El Kazzi, M.; Silly, M. A greener route to photoelectrochemically active PbS nanoparticles. *Journal of Materials Chemistry* **2010**, *20*, 2336-2344.

(11) Anastas, P.; Eghbali, N. Green chemistry: Principles and practice. *Chemical Society Reviews* **2010**, *39*, 301-312.

(12) Anastas, P. T.; Warner, J. C. Principles of green chemistry. *Green chemistry: Theory and practice* **1998**, 29-56.

(13) Sheldon, R. Catalytic reactions in ionic liquids. *Chemical Communications* **2001**, 2399-2407.

(14) Sutto, T. E.; De Long, H. C.; Trulove, P. C. Physical properties of substituted imidazolium based ionic liquids gel electrolytes. *Journal for Nature Research A* **2002**, *57*, 839-846.

(15) Zheng, W.; Li, D.; Guo, W. Applications of ionic liquids (ILs) in synthesis of inorganic nanomaterials. *Materials Science* **2015**, 94-117.

(16) Feng, X.; Hu, G.; Hu, J. Solution-phase synthesis of metal and/or semiconductor homojunction/heterojunction nanomaterials. *Nanoscale* **2011**, *3*, 2099-2117.

(17) Fan, F.-J.; Wu, L.; Yu, S.-H. Energetic I–III–VI_2 and I_2–II–IV–VI_4 nanocrystals: Synthesis, photovoltaic and thermoelectric applications. *Energy and Environmental Science* **2014**, *7*, 190-208.

(18) Gaur, R.; Jeevanandam, P. Effect of anions on the morphology of CdS nanoparticles prepared via thermal decomposition of different cadmium thiourea complexes in a solvent and in the solid state. *New Journal of Chemistry* **2015**, *39*, 9442-9453.

(19) He, Z.; Alexandridis, P. Nanoparticles in ionic liquids: Interactions and organization. *Physical Chemistry Chemical Physics* **2015**, *17*, 18238-18261.

(20) Kareem, T. A.; Kaliani, A. A. ZnS nanoparticle synthesis in 1-butyl-3-methylimidazolium tetrafluoroborate by simple heating. *Arabian Journal of Chemistry* **2015**.

(21) Alaqad, K.; Saleh, T. Gold and silver nanoparticles: Synthesis methods, characterization routes and applications towards drugs. *Journal of Environmental Analytical Toxicology* **2016**, *6*, 2161-0525.

(22) Habiba, K.; Makarov, V. I.; Weiner, B. R.; Morell, G. Fabrication of nanomaterials by pulsed laser synthesis. *Manufacturing Nanostructures* **2014**, 263-292.

(23) Eshetu, G. G.; Armand, M.; Ohno, H.; Scrosati, B.; Passerini, S. Ionic liquids as tailored media for the synthesis and processing of energy conversion materials. *Energy and Environmental Science* **2016**, *9*, 49-61.

(24) Duan, X.; Ma, J.; Lian, J.; Zheng, W. The art of using ionic liquids in the synthesis of inorganic nanomaterials. *Crystal Engeneering Communication* **2014**, *16*, 2550-2559.

(25) Nagaraju, G.; Ravishankar, T.; Manjunatha, K.; Sarkar, S.; Nagabhushana, H.; Goncalves, R.; Dupont, J. Ionothermal synthesis of TiO_2 nanoparticles: Photocatalytic hydrogen generation. *Materials Letters* **2013**, *109*, 27-30.

(26) Andanson, J.-M.; Baiker, A. Interactions of 1-ethyl-3-methylimidazolium trifluoromethanesulfonate ionic liquid with alumina nanoparticles and organic solvents studied by infrared spectroscopy. *The Journal of Physical Chemistry C* **2013**, *117*, 12210-12217.

(27) Manojkumar, K.; Sivaramakrishna, A.; Vijayakrishna, K. A short review on stable metal nanoparticles using ionic liquids, supported ionic liquids, and poly (ionic liquids). *Journal of Nanoparticle Research* **2016**, *18*, 1-22.

(28) Juan, C. L.; Mao, Z. S.; Shen, W. Z.; Jun, Z. Z.; Xin, D. H. Preparation of PbS-type PbO nanocrystals in a room-temperature ionic liquid. *Materials Letters* **2005**, *59*, 3119-3121.

(29) Janiak, C. Ionic liquids for the synthesis and stabilization of metal nanoparticles. *Journal for Nature Research B* **2013**, *68*, 1059-1089.

(30) Chronopoulos, D. D.; Karousis, N.; Zhao, S.; Wang, Q.; Shinohara, H.; Tagmatarchis, N. Photocatalytic application of nanosized CdS immobilized onto functionalized MWCNTs. *Dalton Transactions* **2014**, *43*, 7429-7434.

(31) Tripathi, S.; Kaur, R. Investigation of non-linear optical properties of CdS/PS polymer nanocomposite synthesized by chemical route. *Optics Communications* **2015**, *352*, 55-62.

(32) Xiong, S.; Xi, B.; Qian, Y. CdS hierarchical nanostructures with tunable morphologies: Preparation and photocatalytic properties. *The Journal of Physical Chemistry C* **2010**, *114*, 14029-14035.

(33) Lin, Y.; Zhang, Y.; Zhao, J.; Gu, P.; Bi, K.; Zhang, Q.; Chu, H.; Zhang, T.; Cui, T.; Wang, Y. White-light-emitting diodes using GaN-excited CdSe/CdS/ZnS quantum dots. *Particuology* **2014**, *15*, 90-93.

(34) Duan, X.; Niu, C.; Sahi, V.; Chen, J.; Parce, J. W.; Empedocles, S.; Goldman, J. L. High-performance thin-film transistors using semiconductor nanowires and nanoribbons. *Nature* **2003**, *425*, 274-278.

(35) Devendran, P.; Alagesan, T.; Pandian, K. Single pot microwave synthesis of CdS nanoparticles in ionic liquid and their photocatalytic application. *Asian Journal of Chemistry* **2013**, *25*, S79-S82.

(36) Lohninger, H. Teach/me: Data Analysis. *Springer* **1999**.

(37) Suarez, P. A.; Dullius, J. E.; Einloft, S.; De Souza, R. F.; Dupont, J. The use of new ionic liquids in two-phase catalytic hydrogenation reaction by rhodium complexes. *Polyhedron* **1996**, *15*, 1217-1219.

(38) Chauvin, Y.; Mussmann, L.; Olivier, H. A novel class of versatile solvents for two-phase catalysis: Hydrogenation, isomerization, and hydroformylation of alkenes catalyzed by rhodium complexes in liquid 1, 3-dialkylimidazolium salts. *Angewandte Chemie International Edition in English* **1996**, *34*, 2698-2700.

(39) Sajjadi, H.; Modaressi, A.; Magri, P.; Domańska, U.; Sindt, M.; Mieloszynski, J.-L.; Mutelet, F.; Rogalski, M. Aggregation of nanoparticles in aqueous solutions of ionic liquids. *Journal of Molecular Liquids* **2013**, *186*, 1-6.

(40) Biswas, K.; Rao, C. N. R. Use of ionic liquids in the synthesis of nanocrystals and nanorods of semiconducting metal chalcogenides. *Chemistry–A European Journal* **2007**, *13*, 6123-6129.

(41) Jiang, N.; Xiu, Z.; Xie, Z.; Li, H.; Zhao, G.; Wang, W.; Wu, Y.; Hao, X. Reduced graphene oxide–CdS nanocomposites with enhanced visible-light photoactivity synthesized using ionic-liquid precursors. *New Journal of Chemistry* **2014**, *38*, 4312-4320.

(42) Rajathi, K.; Kumar, V. Green synthesis of stable ZnO and CdS nanoparticles using room temperature ionic liquids and their characterization. *Journal of Chemical and Pharmaceutical Research* **2015**, *7*, 855-859.

(43) de los Ríos, A. P.; Hernández-Fernández, F.; Alguacil, F.; Lozano, L.; Ginestá, A.; García-Díaz, I.; Sánchez-Segado, S.; López, F.; Godínez, C. On the use of imidazolium and ammonium-based ionic liquids as green solvents for the selective recovery of Zn (II), Cd (II), Cu (II) and Fe (III) from hydrochloride aqueous solutions. *Separation and Purification Technology* **2012**, *97*, 150-157.

(44) Epifani, M.; Giannini, C.; Manna, L. A novel synthesis of CdSe nanocrystals. *Materials Letters* **2004**, *58*, 2429-2432.

(45) Didenko, Y. T.; Suslick, K. S. Chemical aerosol flow synthesis of semiconductor nanoparticles. *Journal of the American Chemical Society* **2005**, *127*, 12196-12197.

(46) Mirnaya, T.; Asaula, V.; Volkov, S.; Tolochko, A.; Melnik, D.; Klimusheva, G. Synthesis and optical properties of liquid crystalline nanocomposites of cadmium octanoate with CdS quantum dots. *Physics and Chemistry of Solids* **2012**, 131-135.

(47) Chang, S.-y.; Liu, L.; Asher, S. A. Preparation and properties of tailored morphology, monodisperse colloidal silica-cadmium sulfide nanocomposites. *Journal of the American Chemical Society* **1994**, *116*, 6739-6744.

(48) Yu, W. W.; Qu, L.; Guo, W.; Peng, X. Experimental determination of the extinction coefficient of CdTe, CdSe, and CdS nanocrystals. *Chemistry of Materials* **2003**, *15*, 2854-2860.

(49) Pal, U.; Loaiza-González, G.; Bautista-Hernández, A.; Vázquez-Cuchillo, O. Synthesis of CdS nanoparticles through colloidal rout. *Superficies y Vacío* **2000**, *11*, 40-43.

(50) Nair, P. S.; Scholes, G. D. Thermal decomposition of single source precursors and the shape evolution of CdS and CdSe nanocrystals. *Journal of Materials Chemistry* **2006**, *16*, 467-473.

(51) Barreca, D.; Gasparotto, A.; Maragno, C.; Tondello, E. CVD of nanosized ZnS and CdS thin films from single-source precursors. *Journal of the Electrochemical Society* **2004**, *151*, G428-G435.

(52) Shen, S.; Zhang, Y.; Peng, L.; Xu, B.; Du, Y.; Deng, M.; Xu, H.; Wang, Q. Generalized synthesis of metal sulfide nanocrystals from single-source precursors: Size, shape and chemical composition control and their properties. *Crystal Engeneering Communication* **2011**, *13*, 4572-4579.

(53) Nair, P. S.; Radhakrishnan, T.; Revaprasadu, N.; Kolawole, G.; O'Brien, P. Cadmium ethylxanthate: A novel single-source precursor for the preparation of CdS nanoparticles. *Journal of Materials Chemistry* **2002**, *12*, 2722-2725.

(54) Fan, D.; Afzaal, M.; Mallik, M. A.; Nguyen, C. Q.; O'Brien, P.; Thomas, P. J. Using coordination chemistry to develop new routes to semiconductor and other materials. *Coordination Chemistry Reviews* **2007**, *251*, 1878-1888.

(55) Nair, P. S.; Radhakrishnan, T.; Revaprasadu, N.; Kolawole, G. A.; O'Brien, P. A single-source route to CdS nanorods. *Chemical Communications* **2002**, 564-565.

(56) Moloto, M.; Revaprasadu, N.; O'brien, P.; Malik, M. N-alkylthioureacadmium (II) complexes as novel precursors for the synthesis of CdS nanoparticles. *Journal of Materials Science: Materials in Electronics* **2004**, *15*, 313-316.

(57) Yoon, S. H.; Lee, S. S.; Seo, K. W.; Shim, I. Preparation of CdS thin films through MOCVD method, using Cd-S single-source precursors. *Bulletin-Korean Chemical Society* **2006**, *27*, 2071-2073.

(58) Mthethwa, T.; Pullabhotla, V. R.; Mdluli, P. S.; Wesley-Smith, J.; Revaprasadu, N. Synthesis of hexadecylamine capped CdS nanoparticles using heterocyclic cadmium dithiocarbamates as single source precursors. *Polyhedron* **2009**, *28*, 2977-2982.

(59) McMahon, T. J.; Jasperson, S. N. PbS–Al Selective Solar Absorbers. *Applied Optics* **1974**, *13*, 2750-2751.

(60) Nyamen, L. D.; Pullabhotla, V. S. R.; Nejo, A. A.; Ndifon, P. T.; Warner, J. H.; Revaprasadu, N. Synthesis of anisotropic PbS nanoparticles using heterocyclic dithiocarbamate complexes. *Dalton Transactions* **2012**, *41*, 8297-8302.

(61) Preier, H.; Bleicher, M.; Riedel, W.; Maier, H. Double heterojunction PbS-$PbS_{1-x}Se_x$-PbS laser diodes with cw operation up to 96 K. *Applied Physics Letters* **1976**, *28*, 669-671.

(62) Dong, G.; Wu, B.; Zhang, F.; Zhang, L.; Peng, M.; Chen, D.; Wu, E.; Qiu, J. Broadband near-infrared luminescence and tunable optical amplification around 1.55 μm and 1.33 μm of PbS quantum dots in glasses. *Journal of Alloys and Compounds* **2011**, *509*, 9335-9339.

(63) Sathyamoorthy, R.; Kungumadevi, L. Facile synthesis of PbS nanorods induced by concentration difference. *Advanced Powder Technology* **2015**, *26*, 355-361.

(64) Karami, H.; Ghasemi, M.; Matini, S. Synthesis, characterization and application of lead sulfide nanostructures as ammonia gas sensing agent. *International Journal of Electrochemical Science* **2013**, *8*, 11661-11679.

(65) Nyamen, L. D.; Revaprasadu, N.; Ndifon, P. T. Low temperature synthesis of PbS and CdS nanoparticles in olive oil. *Materials Science in Semiconductor Processing* **2014**, *27*, 191-196.

(66) Mehrabian, M.; Mirabbaszadeh, K.; Afarideh, H. Experimental optimization of molar concentration to fabricate PbS quantum dots for solar cell applications. *Optik-International Journal for Light and Electron Optics* **2015**, *126*, 570-574.

(67) Akhtar, J.; Malik, M. A.; O'Brien, P.; Wijayantha, K.; Dharmadasa, R.; Hardman, S. J.; Graham, D. M.; Spencer, B. F.; Stubbs, S. K.; Flavell, W. R. A greener route to photoelectrochemically active PbS nanoparticles. *Journal of Materials Chemistry* **2010**, *20*, 2336-2344.

(68) Das, A.; Wai, C. M. Ultrasound-assisted synthesis of PbS quantum dots stabilized by 1, 2-benzenedimethanethiol and attachment to single-walled carbon nanotubes. *Ultrasonics Sonochemistry* **2014**, *21*, 892-900.

(69) Tavakoli, M. M. Surface engineering of PbS colloidal quantum dots using atomic passivation for photovoltaic applications. *Procedia Engineering* **2016**, *139*, 117-122.

(70) Sadovnikov, S. I.; Gusev, A. I.; Rempel, A. A. Nanostructured lead sulfide: Synthesis, structure and properties. *Russian Chemical Reviews* **2016**, *85*, 731-758.

(71) Cao, Y.; Hu, P.; Jia, D. Solvothermal synthesis, growth mechanism, and photoluminescence property of sub-micrometer PbS anisotropic structures. *Nanoscale Research Letters* **2012**, *7*, 1-8.

(72) Ji, Y.; Yang, D. R.; Zhang, H.; Ma, X. Y.; Xu, J.; Que, D. L. Morphology control of PbS nanocrystals by a novel hydrothermal process. *Trans Tech Publication*, **2004**, *99*, 197-202.

(73) Querejeta-Fernández, A.; Hernández-Garrido, J. C.; Yang, H.; Zhou, Y.; Varela, A.; Parras, M.; Calvino-Gámez, J. J.; González-Calbet, J. M.; Green, P. F.; Kotov, N. A. Unknown aspects of self-assembly of PbS microscale superstructures. *American Chemical Society Nano* **2012**, *6*, 3800-3812.

(74) Jana, S.; Goswami, S.; Nandy, S.; Chattopadhyay, K. Synthesis of tetrapod like PbS microcrystals by hydrothermal route and its optical characterization. *Journal of Alloys and Compounds* **2009**, *481*, 806-810.

(75) Yuan, L.; Patterson, R.; Cao, W.; Zhang, Z.; Zhang, Z.; Stride, J. A.; Reece, P.; Conibeer, G.; Huang, S. Air-stable PbS quantum dots synthesized with slow reaction kinetics via a $PbBr_2$ precursor. *Royal Society of Chemistry Advances* **2015**, *5*, 68579-68586.
(76) Liu, L.; Wang, Y.; An, W.; Hu, J.; Cui, W.; Liang, Y. Photocatalytic activity of PbS quantum dots sensitized flower-like $Bi_2 WO_6$ for degradation of rhodamine B under visible light irradiation. *Journal of Molecular Catalysis A: Chemical* **2014**, *394*, 309-315.
(77) Zhao, X.-L.; Wang, C.-X.; Hao, X.-P.; Yang, J.-X.; Wu, Y.-Z.; Tian, Y.-P.; Tao, X.-T.; Jiang, M.-H. Synthesis of PbS nanocubes using an ionic liquid as the solvent. *Materials Letters* **2007**, *61*, 4791-4793.
(78) Behboudnia, M.; Habibi-Yangjeh, A.; Jafari-Tarzanag, Y.; Khodayari, A. Facile and room temperature preparation and characterization of PbS nanoparticles in aqueous [EMIM][$EtSO_4$] ionic liquid using ultrasonic irradiation. *Bulletin of the Korean Chemical Society* **2009**, *30*, 53-56.
(79) Hardman, S. J.; Graham, D. M.; Stubbs, S. K.; Spencer, B. F.; Seddon, E. A.; Fung, H.-T.; Gardonio, S.; Sirotti, F.; Silly, M. G.; Akhtar, J. Electronic and surface properties of PbS nanoparticles exhibiting efficient multiple exciton generation. *Physical Chemistry Chemical Physics* **2011**, *13*, 20275-20283.
(80) Yu, D.; Wang, D.; Meng, Z.; Lu, J.; Qian, Y. Synthesis of closed PbS nanowires with regular geometric morphologies. *Journal of Materials Chemistry* **2002**, *12*, 403-405.
(81) González-Pedro, V.; Sima, C.; Marzari, G.; Boix, P. P.; Giménez, S.; Shen, Q.; Dittrich, T.; Mora-Seró, I. High performance PbS quantum dot sensitized solar cells exceeding 4% efficiency: The role of metal precursors in the electron injection and charge separation. *Physical Chemistry Chemical Physics* **2013**, *15*, 13835-13843.
(82) Salavati-Niasari, M.; Sobhani, A.; Davar, F. Synthesis of star-shaped PbS nanocrystals using single-source precursor. *Journal of Alloys and Compounds* **2010**, *507*, 77-83.
(83) Mandal, T.; Piburn, G.; Stavila, V.; Rusakova, I.; Ould-Ely, T.; Colson, A. C.; Whitmire, K. H. New mixed ligand single-source precursors for PbS nanoparticles and their solvothermal decomposition to anisotropic nano-and microstructures. *Chemistry of Materials* **2011**, *23*, 4158-4169.

(84) Nyamen, L. D.; Pullabhotla, V. R.; Nejo, A. A.; Ndifon, P. T.; Warner, J. H.; Revaprasadu, N. Synthesis of anisotropic PbS nanoparticles using heterocyclic dithiocarbamate complexes. *Dalton Transactions* **2012**, *41*, 8297-8302.

(85) Clark, J. M.; Kociok-Köhn, G.; Harnett, N.; Hill, M.; Hill, R.; Molloy, K. C.; Saponia, H.; Stanton, D.; Sudlow, A. Formation of PbS materials from lead xanthate precursors. *Dalton Transactions* **2011**, *40*, 6893-6900.

(86) Caponetti, E.; Martino, D. C.; Leone, M.; Pedone, L.; Saladino, M. L.; Vetri, V. Microwave-assisted synthesis of anhydrous CdS nanoparticles in a water–oil microemulsion. *Journal of Colloid and Interface Science* **2006**, *304*, 413-418.

(87) Zhu, J.; Zhou, M.; Xu, J.; Liao, X. Preparation of CdS and ZnS nanoparticles using microwave irradiation. *Materials Letters* **2001**, *47*, 25-29.

(88) Liao, X.-H.; Zhu, J.-J.; Chen, H.-Y. Microwave synthesis of nanocrystalline metal sulfides in formaldehyde solution. *Materials Science and Engineering: B* **2001**, *85*, 85-89.

(89) Murugan, A. V.; Sonawane, R.; Kale, B.; Apte, S.; Kulkarni, A. V. Microwave–solvothermal synthesis of nanocrystalline cadmium sulfide. *Materials Chemistry and Physics* **2001**, *71*, 98-102.

(90) Ding, T.; Zhang, J.-R.; Long, S.; Zhu, J.-J. Synthesis of HgS and PbS nanocrystals in a polyol solvent by microwave heating. *Microelectronic Engineering* **2003**, *66*, 46-52.

(91) Seddon, K. R. Ionic liquids for clean technology. *Journal of Chemical Technology and Biotechnology* **1997**, *68*, 351-356.

(92) Earle, M. J.; Esperança, J. M.; Gilea, M. A.; Lopes, J. N. C.; Rebelo, L. P.; Magee, J. W.; Seddon, K. R.; Widegren, J. A. The distillation and volatility of ionic liquids. *Nature* **2006**, *439*, 831-834.

(93) Ye, C.; Liu, W.; Chen, Y.; Yu, L. Room-temperature ionic liquids: A novel versatile lubricant. *Chemical Communications* **2001**, 2244-2245.

(94) Noda, A.; Hayamizu, K.; Watanabe, M. Pulsed-gradient spin− echo 1H and 19F NMR ionic diffusion coefficient, viscosity, and ionic conductivity of non-chloroaluminate room-temperature ionic liquids. *The Journal of Physical Chemistry B* **2001**, *105*, 4603-4610.

(95) Mudring, A.-V.; Alammar, T.; BACKER, T.; Richter, K. Nanoparticle synthesis in ionic liquids. *Oxford University Press* **2009**, *1030*, 177-188.

(96) Nan, A.; Liebscher, J. Ionic liquids as advantageous solvents for preparation of nanostructures. *InTech* **2011**, *129*, 287-303.

(97) Scholten, J. D.; Leal, B. C.; Dupont, J. Transition metal nanoparticle catalysis in ionic liquids. *American Chemical Society Catalysis* **2011**, *2*, 184-200.

(98) Beier, M. J.; Andanson, J.-M.; Mallat, T.; Krumeich, F.; Baiker, A. Ionic liquid-supported Pt nanoparticles as catalysts for enantioselective hydrogenation. *American Chemical Society Catalysis* **2012**, *2*, 337-340.

(99) Antonietti, M.; Kuang, D.; Smarsly, B.; Zhou, Y. Ionic liquids for the convenient synthesis of functional nanoparticles and other inorganic nanostructures. *Angewandte Chemie International Edition* **2004**, *43*, 4988-4992.

(100) Yao, K.; Lu, W.; Wang, J. Ionic liquid-assisted synthesis, structural characterization, and photocatalytic performance of CdS nanocrystals. *Materials Chemistry and Physics* **2011**, *130*, 1175-1181.

(101) Sharma, R.; Mahajan, R. K. Influence of various additives on the physicochemical properties of imidazolium based ionic liquids: A comprehensive review. *Royal Society of Chemistry Advances* **2014**, *4*, 748-774.

(102) Andreev, A.; Lipovskii, A. Anisotropy-induced optical transitions in PbSe and PbS spherical quantum dots. *Physical Review B* **1999**, *59*, 15402-15404.

CHAPTER TWO

Synthesis of CdS nanoparticles

2.1. Introduction

In recent years safer and simpler ways of synthesizing cadmium chalcogenides nanomaterials have been actively investigated, cadmium sulfide being part of them.[1,2] This is because these materials are good candidates for electronic and optical devices and the fact that they can be easily reduced in dimensions, which helps in reducing the size of electronic devices.[3-5] The structure of the nanomaterial plays a vital role in shaping its electronic properties, the same material can exhibit different structures upon size reduction depending on the preparation conditions.[6] Thus, the focus of many researchers is on developing preparation methods or protocols which will lead to the exhibition of new functional features in these materials.[7] A wide range of synthetic procedures for these materials have been reported in literature. These include chemical precipitation,[8] laser ablation,[9] solvothermal,[10] mesoporous copolymer template, hydrothermal, one pot synthesis, photochemical and colloidal route.[11]

CdS is a II-VI semiconductor with size dependable properties.[12,13] It has a large tunable band gap value (E_g) 2.42 eV as a bulk material, this band gap allows light emission between blue and red wavelengths.[3] As a result of this large band gap energy, CdS nanoparticles are used in hetero junction solar cells as window materials.[14,15] In these hetero junction (p-n) solar cells, CdS is usually used as the n-type material together with other p-type materials like indium phosphide, gallium arsenide, cadmium telluride etc.[16] However, it is possible to obtain both types of conductivities (n or p type) from CdS through doping. For the n-type it can be doped by B, In, Cu, Al and Ga, while for the p-type Au and Ag can be used.[17] Other photovoltaic applications of CdS include electrical driven lasers,[18] photodetectors,[19] light emitting diodes,[20] field effect transistors[21] etc.

CdS exists in three crystal structures which are cubic zinc blende,[22] high pressure rock-salt[23] and the hexagonal wurtzite phase.[24] The hexagonal wurtzite phase is the most stable phase out of the three and the easiest to prepare, and as a result, it is the most studied. This phase has been observed in both bulk CdS and in nanocrystalline size, whereas cubic (metastable) and rock-salt phases are only observed in nanocrystalline materials.[25-27] Many research outputs have been reported on different synthetic methods which give rise to different properties. The structure of the

nanocrystalline material including size, shape and the dimensions plays a key role in determining their physical properties.[28,29] In each of the synthetic procedures mentioned above, it is possible to use either single or dual source molecular precursors. In this study both single and dual source precursors were used for the hot injection method. The advantages and shortcomings of each of the precursor type are given in detail in chapter 1.

In chemistry, most of species are studied in solutions, as much as any liquid can be used as a solvent, very few are generally used. The list of detrimental chemicals consists highly of solvents, this is because solvents are used in large amounts and they are commonly explosive liquids that are difficult to handle. The introduction of cleaner technologies is becoming a major concern to both industry and academia and as such a search for alternatives to these "traditionally" used solvents has been a priority. Fused salts are liquids comprising of only ions, these can be used as replacements to the conventional solvents. Ionic liquids that are liquid at and below room temperature can be synthesized through a careful choice of starting materials.[30] There have been review reports on the potential of ionic liquids use as solvents in synthesis and catalysis.[31,32] Ionic liquids are classified as green solvents and/or capping agents in semiconductor nanomaterial synthesis. Many nanomaterials have been prepared from them including CdS,[33-36] however there has been no report of this particular ionic liquid (1-ethyl-3-methylimidazolium methanesulfonate) for CdS nanoparticles. The aim of the study is to investigate the effect of ionic liquid on both physical and chemical properties of the CdS nanoparticles.

2.2. Experimental section

2.2.1. Materials

Cadmium acetate dihydrate 98 %, 1-dodecanethiol 98 %, 1-ethyl-3-methylimidazolium methanesulfonate 95 % and potassium ethyl xanthogenate 96% were purchased from Sigma-Aldrich. Acetone and ethanol were supplied by Prestige laboratory and were used as received without any further purification.

2.2.2. Methods

2.2.2.1. Synthesis of CdS nanoparticles from dual source precursors

Three approaches were employed to synthesize CdS nanoparticles using 1-ethyl-3-methylimidazolium methanesulfonate as a coordinating solvent. In all the methods, CdS nanoparticles were synthesized based on high temperature thermolysis protocols and each approach is given in detail as follows: in method (**1**), a mixture of cadmium acetate dihydrate (0.0302 g, 0.113 mmol) and 1-ethyl-3-methylimidazolium methanesulfonate (3.5 mL) were heated in a three necked flask to a temperature of either 190 °C, 230 °C or 270 °C. To the heated mixture, 2 mL of 1-dodecanethiol was injected while maintaining the temperature for 1h, 2h and 4h, after which the sample was cooled to about 70 °C. The sample was then washed several times with ethanol and acetone and subsequently dried in a desiccator.

For method (**2**), a 2 mL solution of 1-dodecanethiol was first heated in a three necked flask to the temperatures of 190 °C, 230 °C and 270 °C. Then cadmium acetate dihydrate (0.0302 g, 0.113 mmol) and 1-ethyl-3-methylimidazolium methanesulfonate (3.5 mL) were added to the heated liquid. The product was washed several times with ethanol and acetone and subsequently dried in a desiccator.

In method (**3**), Cadmium acetate dihydrate (0.0302 g, 0.113 mmol), ionic liquid (3.5 mL) and dodecanethiol (2 mL) were all mixed in a three necked flask and heated to the desired temperatures i.e. 190 °C, 230 °C and 270 °C. The reaction was maintained at the particular temperature for 1h, 2h and 4h. The product was washed several times with ethanol and acetone and subsequently dried in a desiccator.

The expected nanoparticle formation can be represented by the following equation:

$$Cd(CH_3COO)_2 + C_{12}H_{12}S \xrightarrow{\text{ionic liquid}} CdS + \text{negligible bi products} \quad (2.1)$$

The chemical equilibrium of this reaction can be described by the equation:

$$CdS \rightleftharpoons Cd^{+} + S^{-} \quad (2.2)$$

This chemical equilibrium is a function size of the crystallites.

2.2.2.2. Synthesis of cadmium ethyl xanthate: $Cd(C_2H_5OCS_2)$

Cadmium ethyl xanthate was prepared according to the method reported in literature.[37] The reaction is given as follows:

$$Cd(CH_3COO)_{2(aq)} + 2(KS_2COC_2H_5)_{(aq)} \rightarrow Cd(S_2COC_2H_5)_{(s)} + 2CH_3COOK \quad (2.3)$$

In a reaction vessel, 2.7 g (10 mmol) of $Cd(CH_3COO)$ was dissolved in 20 mL of distilled water. To this solution, 3.2 g (20 mmol) of $KS_2COC_2H_5$ in 30 mL of distilled water was added dropwise. A pale yellow precipitate immediately formed which was filtered, washed with distilled water and dried. Yield: 96 %. Elemental analysis: $C_6H_{10}CdO_2S_4$: Calculated (%): C, 20.31; H, 2.84; S, 28.16; Cd, 46.09. Found (%): C, 20.32; H, 2.67; S, 28.49; Cd, 46.18.

2.2.2.3. Synthesis of CdS nanoparticles from single source precursor ($Cd(C_2H_5OCS_2)$)

The CdS nanoparticles were prepared by injection of the cadmium ethyl xanthate into the hot ionic liquid at a required temperature under nitrogen atmosphere, a method adopted from a study by Trindade *et al.*[38]

In a typical preparation, $Cd(C_2H_5OCS_2)$ (0.198 g, 0.56 mmol) was dispersed in 2 mL of ionic liquid/ dodecanethiol. This solution was then injected in 5 mL of the hot IL while stirring at 190, 230 and 270 °C. The reaction would be allowed to continue for 30 minutes for each of the reaction temperatures. The reaction vessel was a three necked flask which was equipped with a condenser, rubber septum connecting the nitrogen gas tube on one end and another rubber septum connecting a thermometer on the other end.

2.2.3. Characterization techniques

2.2.3.1. CHNS/O analyser

Elemental microanalyses were performed on a Perkin-Elmer automated model 2400 series II for the samples' atomic composition. This technique provides a highly sensitive analysis of how much does the sample have C, H, N, S/O. It is mostly used to determine the complexes' purity.

2.2.3.2. Infra-red analysis

Infra-red spectra were recorded on a Bruker FT-IR Tensor 27 spectrophotometer equipped with a standard ATR crystal cell detector. Analyses were performed in the 200- 4000 cm^{-1} range.

2.2.3.3. Thermogravimetric analysis (TGA)

Thermogravimetric analyses were carried out at 20 ℃/min heating from 30 ℃ to 700 ℃ under N_2 gas flow rate of 10 mL/min using a Perkin Elmer Pyris 6 TGA equipped with a closed perforated ceramic pan.

2.2.3.4. Optical measurements

Optical measurements were done using a Varian Cary 50 UV–visible spectrophotometer. The samples were placed in silica cuvette (1 cm path length), using ethanol as a reference solvent. Photoluminescence of the particles was analysed using a Perkin-Elmer, LS55 Luminescence spectrophotometer.

2.2.3.5. Powder X-ray diffraction (pXRD)

Powder diffraction patterns were recorded in the high angle 2θ range of 20–70° using a Bruker AXS D8 diffractometer equipped with a nickel filtered Cu Kα radiation (λ = 1.5418 Å) at 40 kV, 40 mA and at room temperature. The scan speed and step sizes were 0.5 min^{-1} and 0.01314 respectively.

2.1.1.1. Transmission electron microscopy (TEM) and high resolution TEM (HRTEM)

Samples were allowed to dry completely at room temperature and viewed using a JEOL 1400 TEM and JEOL 2100 HRTEM. Viewing was done at an accelerating voltage of 120 kV (TEM) and 200 kV (HRTEM), and images captured digitally using a Megaview III camera; stored and measured using soft imaging systems iTEM software (TEM) and Gatan camera and Gatan software (HRTEM).

Table 2.1: Summary of methods and parameters used in the preparation of CdS nanoparticles in 1-ethyl-3-methylimidazolium methanesulfonate.

Precursor type and name	**Method used**	**Reaction temperature (℃)**
Dual sources: cadmium acetate + dodecanethiol	Heat up, hot injection	190, 230, 270
SSP: cadmium ethyl xanthate	Hot injection	190, 230, 270

2.3. Results and discussions

2.3.1. Synthesis of CdS nanoparticles from dual source precursors

Method 1

The ionic liquid (1-ethyl-3-methylimidazolium methanesulfonate) shown in Figure 1.7 was used as a reaction medium, stabilizing agent and as a capping agent for all reactions. Reactions were carried out at three different temperatures (190 °C, 230 °C and 270 °C) to observe the effect of temperature on the properties of the nanoparticles. Figure 2.1 shows XRD patterns of the as prepared CdS nanoparticles from the three temperatures. For all the temperatures studied, the same crystal phase has been obtained as shown by the XRD patterns. This is a cubic phase and it has been obtained with different crystallite sizes for each of the individual temperatures. The difference in peak broadness signifies that the crystallite sizes are different which could be resulting from the temperature influence. Nanoparticles obtained at 270 ℃ are larger in size (compared to lower temperatures), this can be attributed to the agglomeration of small individual particles which leads to clusters. The highest peak intensity shows that the preferred growth is in the (111) plane for all three temperatures. The diffraction peaks of this crystal phase can be indexed to (111), (220) and (311) (Card No. 01-080-0019). The crystallite sizes calculated from the Scherrer equation (eqn. 4) using the diffraction pattern perpendicular to (111) plane were found to be 2.40 nm, 2.68 nm, 2.53 nm for 190 °C, 230 °C and 270 °C, respectively.

$$d = \frac{K\,\lambda}{B\,cos\theta} \qquad (2.4)$$

$$= \frac{0.98\,\lambda}{B\,cos\theta}$$

where:

- d is the mean size of the ordered (crystalline) domain which may be smaller or equal to the grain size;
- K is the dimensionless shape factor, with a value close to unity;
- λ is the X-ray wavelength,
- B is the line broadening at half maximum intensity (FWHM) after subtracting the instrumental line broadening in radians;

- θ is the Bragg angle (in degrees).

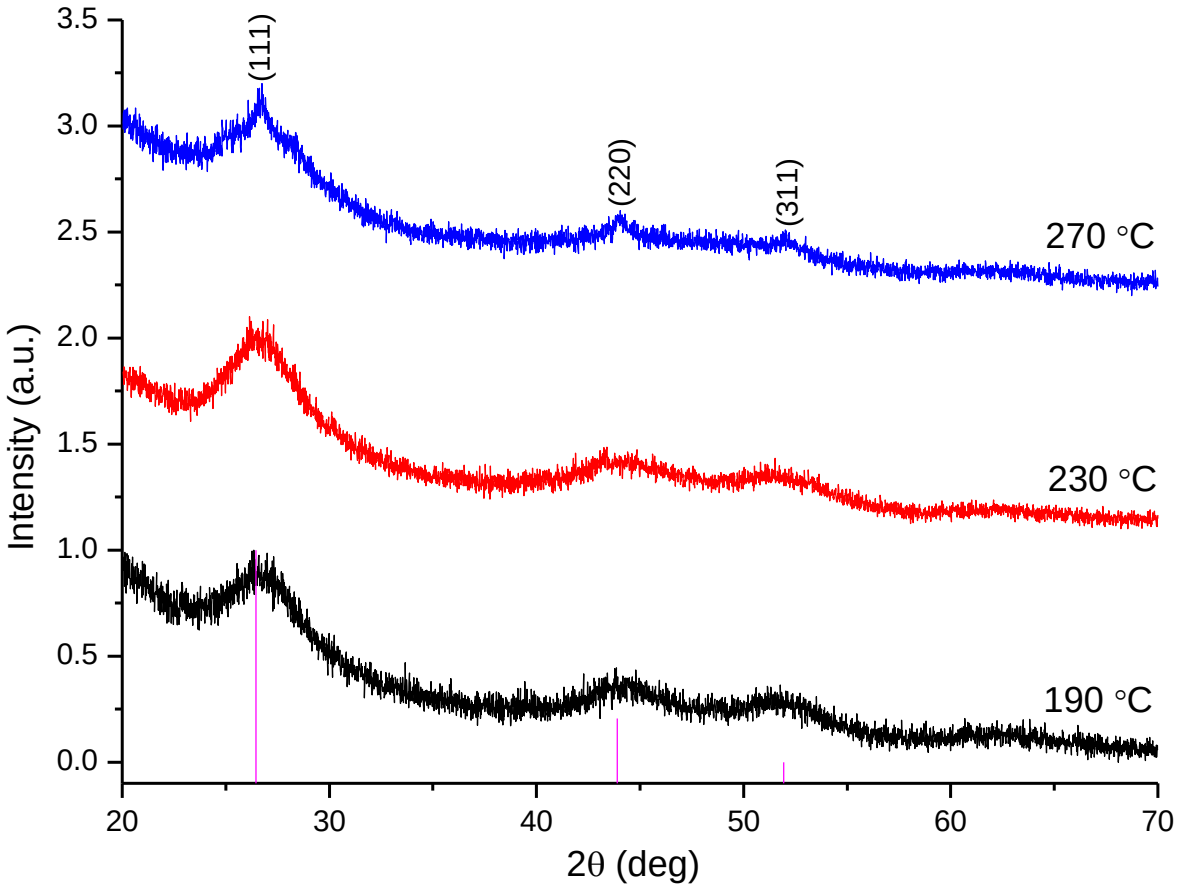

Figure 2.1: XRD patterns of CdS nanoparticles synthesized by method 1 at 190 °C, 230 °C and 270 °C.

Ultra violet visible spectra shown in Figure 2.2 display a blue shift for all the nanoparticles obtained in this study. The band gap energies extrapolated from the Tauc plot have been found to be 3.12 eV, 2.90 eV, 2. 88 eV for temperatures 190 °C, 230 °C and 270 °C, respectively. Comparing these band gaps to the bulk CdS (2.42 eV), it can be seen that very small (nano-sized) particles were synthesized which exhibit strong quantum confinement effects.[39] The redshift in band gap absorption observed between 190 °C and 270 °C is attributed to the fast particle growth which might be escalated by the increase in temperature.

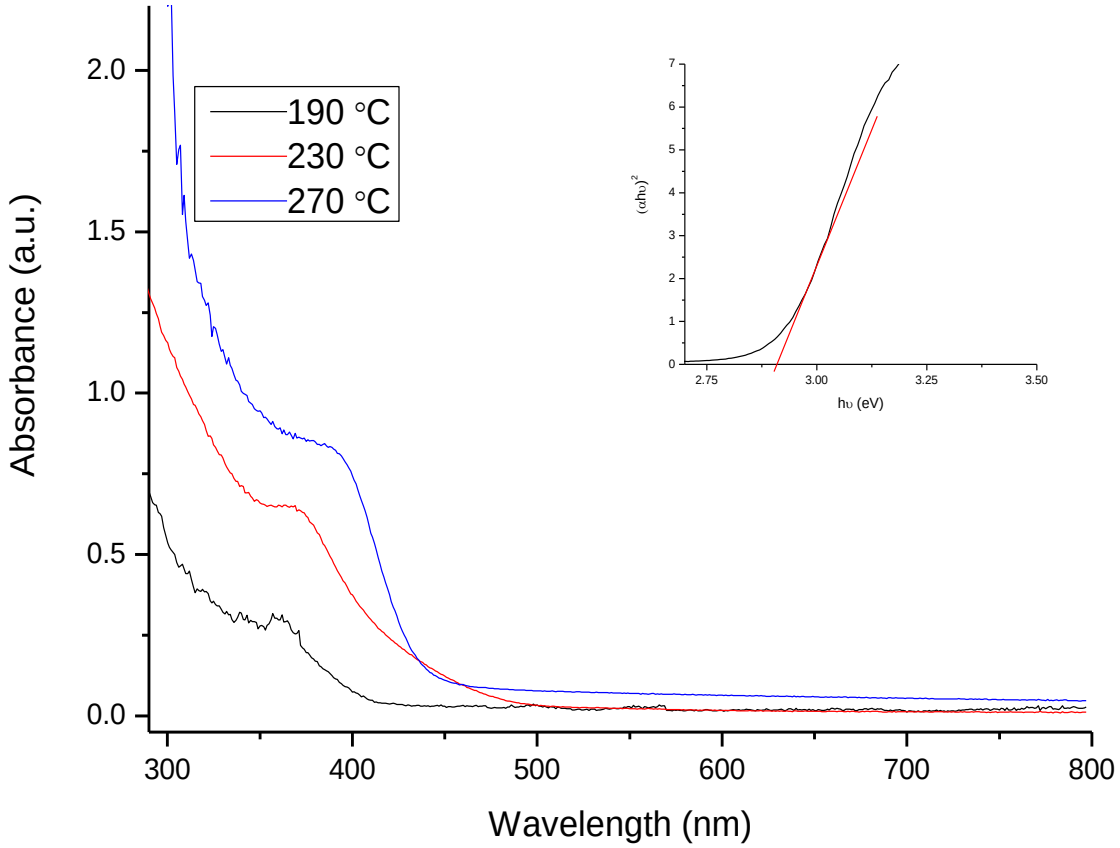

Figure 2.2: UV-visible spectra of CdS nanoparticles synthesized by method 1 at 190 °C, 230 °C and 270 °C. Inset: Tauc plot of nanoparticles prepared at 190 °C.

The photoluminescence spectra of CdS nanoparticles prepared form method 1 are shown in Figure 2.3. These photoluminescence properties were investigated at 320 nm wavelength. Three different emission peaks which are located at 528 nm, 535 nm and 533 nm are observed for temperatures 190 °C, 230 °C and 270 °C individually. These are termed "green band luminescence" and they are due to interstitial sulfur positions.[40] The emission centred at 535 nm indicates short emission which can be used for opto-electronic applicaions.[29] Biswas and co-workers have also reported a similar trend on the CdS nanoparticles prepared on the imidazolium based ionic liquids.[35] This correlates with the XRD and UV-visible results reported earlier in the study.

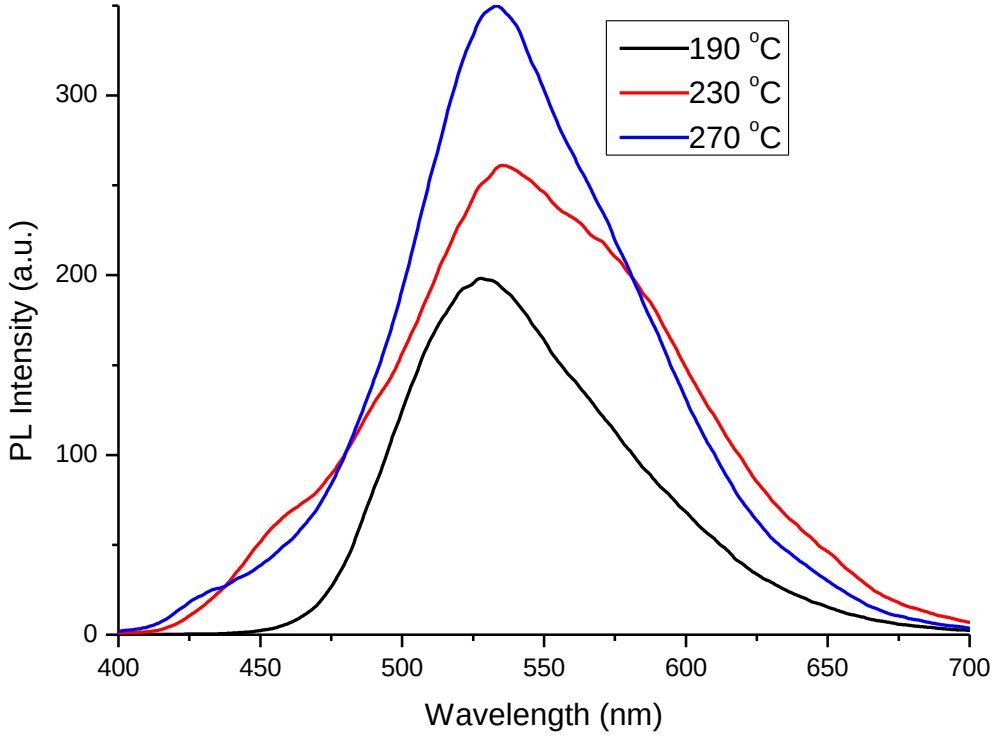

Figure 2.3: PL spectra of CdS nanoparticles synthesized by method 1 at 190 °C, 230 °C and 270 °C.

The obtained TEM images and the corresponding histogram are illustrated in Figure 2.4. From the images, spherical nanoparticles were obtained with very small sizes, this is in agreement with the prior mentioned results i.e. the broadness of the XRD peaks and the blue shift in the UV-vis spectra. However, the trend is in the opposite direction (the smallest particle size is found from high temperature). These sizes were measured and found to be 4.32 ±1.58 nm, 4.30 ± 1.85 nm and 2.30 ± 0.33 nm for 190 °C, 230 °C and 270 °C respectively. The histogram shows a relatively narrow homogeneous distribution for the sample prepared at 190 °C.

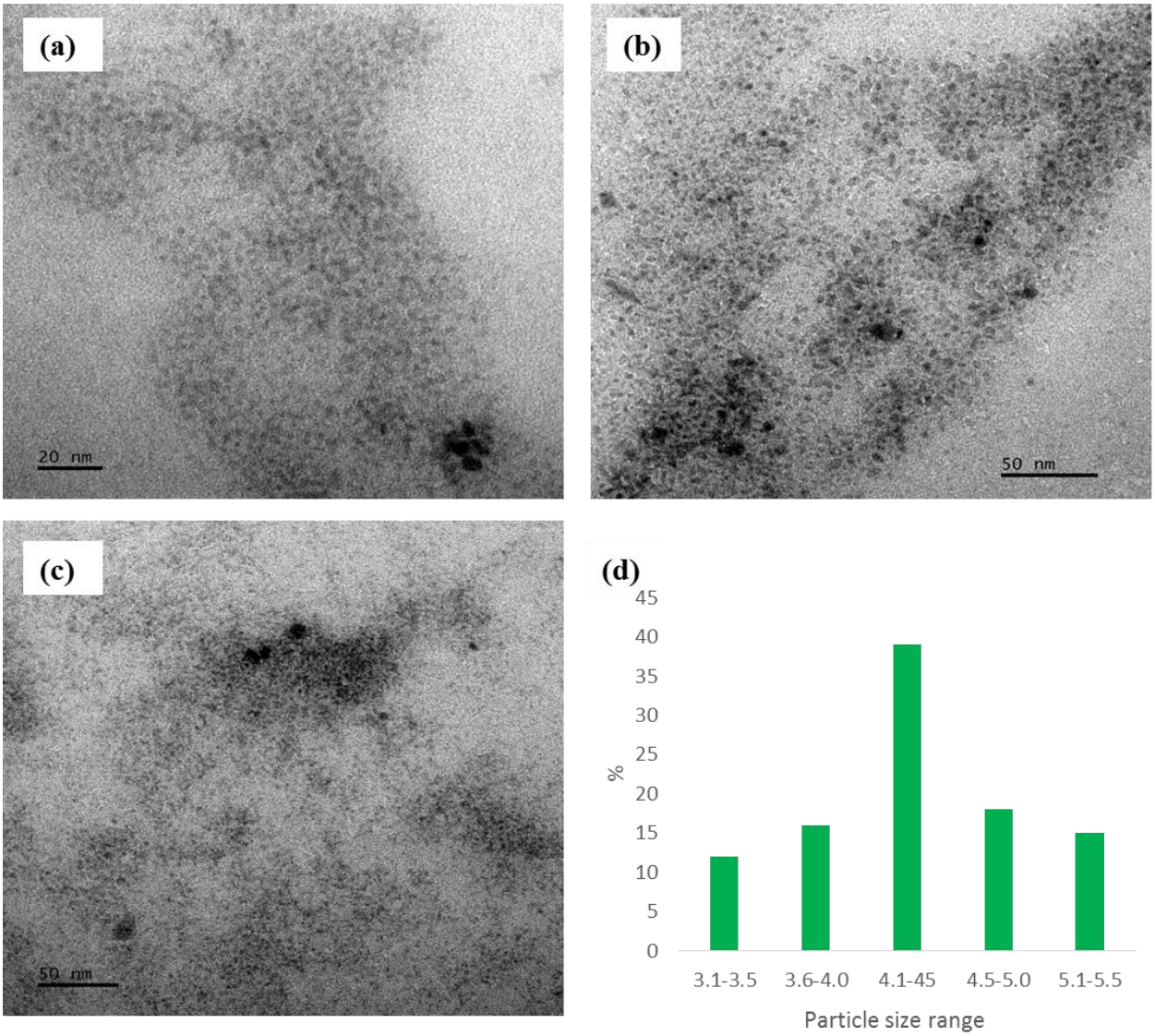

Figure 2.4: TEM images of CdS nanoparticles synthesized by method 1 at (a) 190 °C, (b) 230 °C, (c) 270 °C and (d) representative histogram obtained from 190 °C sample .

Method 2

A different approach was employed where the same quantities of the materials used in method 1 were also used and this is called method 2. In this method, a known amount of dodecanethiol was heated in a three necked flask equipped with a rubber septum on one neck with a thermometer, a condenser and another rubber septum with a nitrogen gas inlet on the third neck. In a separate vessel, a known amount of lead acetate was being dispersed in 1-ethyl-3-methylimidazolium methanesulfonate. When the heating reaches the targeted temperature (190 °C, 230 °C, 270 °C), it would be kept stable for a few minutes and then the solution of lead acetate and the ionic liquid would be injected to the hot solvent. The XRD patterns in Figure 2.5 show a significant effect of the temperature on the crystal phase i.e. when the temperatures are low there exist only a cubic crystal phase while when the temperature is increased a different phase is observed, hexagonal crystal phase. The cubic crystal phase indices are as mentioned in method 1. However, the hexagonal phase can be indexed to (100), (002), (101), (110), (103) and (112) (Card No. 01-080-0006). The wide peaks in XRD pattern are consistent with characteristic wurzite nanocrystallites in the nanosize system.[41,42] The crystal growth preference is towards the (002) direction. The crystallite sizes calculated from Scherrer equation (eqn. 2.4) were 2.92 nm and 2.40 nm for 190 °C and 230 °C respectively while the size was found to be 15.66 nm for 270 °C.

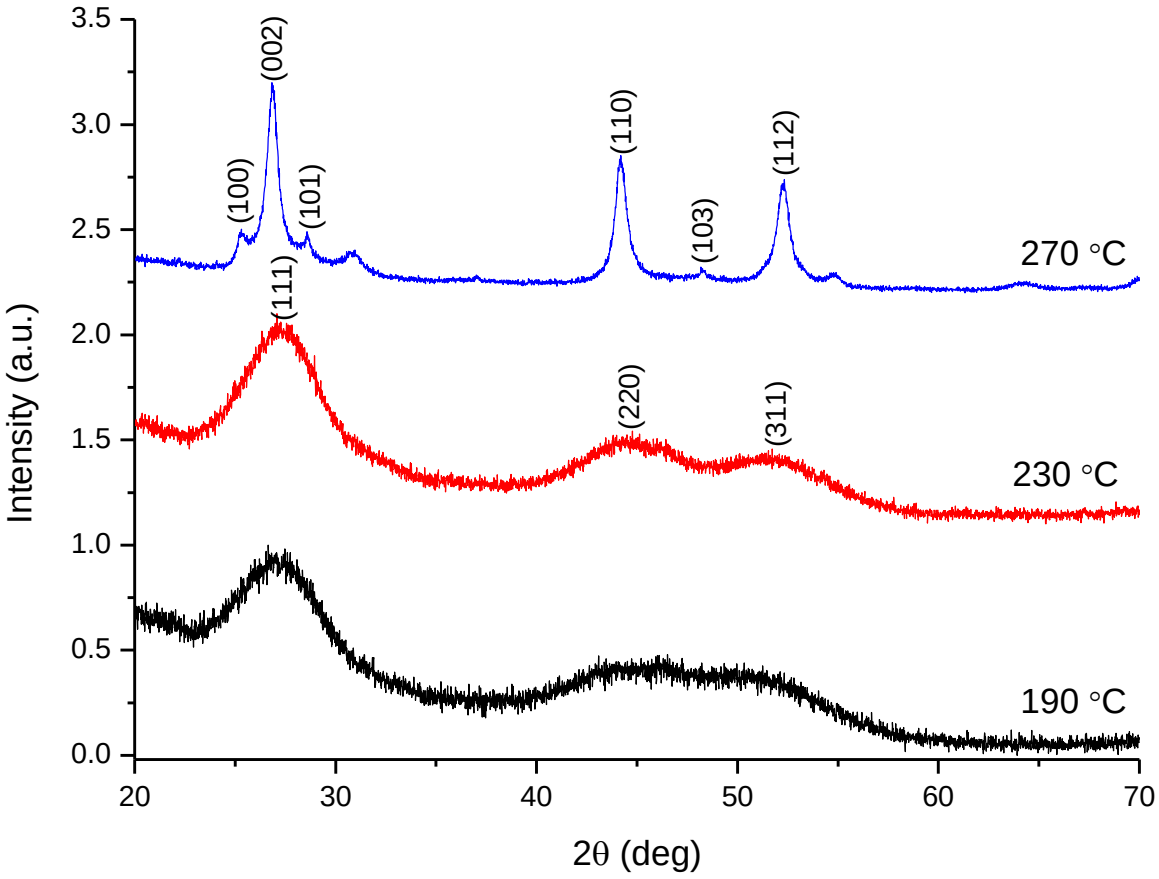

Figure 2.5: XRD patterns of CdS nanoparticles synthesized by method 2 at 190 °C, 230 °C and 270 °C.

Ultraviolet visible spectra of CdS nanoparticles prepared using method 2 at three temperatures is shown in Figure 2.6. The particles formed by this method resemble those formed from the first method except that for 270 °C the Tauc plot could not give a pronounced band gap energy extrapolation. These band gap energies are 3.08 eV and 2.96 eV for 190 °C and 230 °C respectively. The sharp absorption peaks in these two temperatures are blue shifted and the broad absorption of the higher temperature is slightly red shifted which reveals a much larger particle size compared to the former.

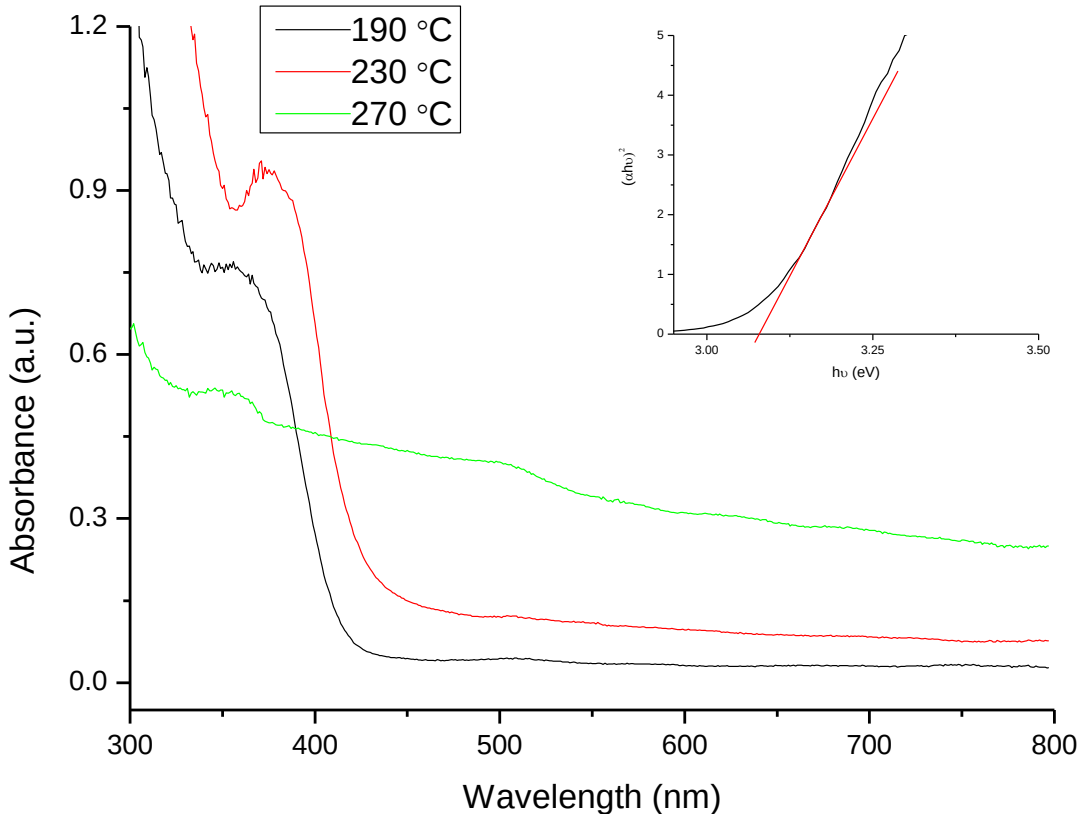

Figure 2.6: UV-visible spectra of CdS nanoparticles synthesized by method 2 at 190 °C, 230 °C and 270 °C. Inset: Tauc plot of nanoparticles prepared at 190 °C.

Photoluminescence spectra of the particles synthesized form method 2 are shown in Figure 2.7 below. Different excitation wavelengths were used for the materials synthesized from this method, 230 nm, 300 nm and 320 nm for 190 °C, 230 °C and 270 °C separately. For 190 °C, a prominent emission peak is observed around 530 nm, this is known as green band luminescence.[43] The are two other peaks located at 402 nm and 428 nm which can be assigned to band edge emission. An acceptor level peak is located at 460 nm which is agreement with previous reported literature,[44] A well-defined green emission band at 529 nm and a noticeable peak is detected at the same range for 270 °C.

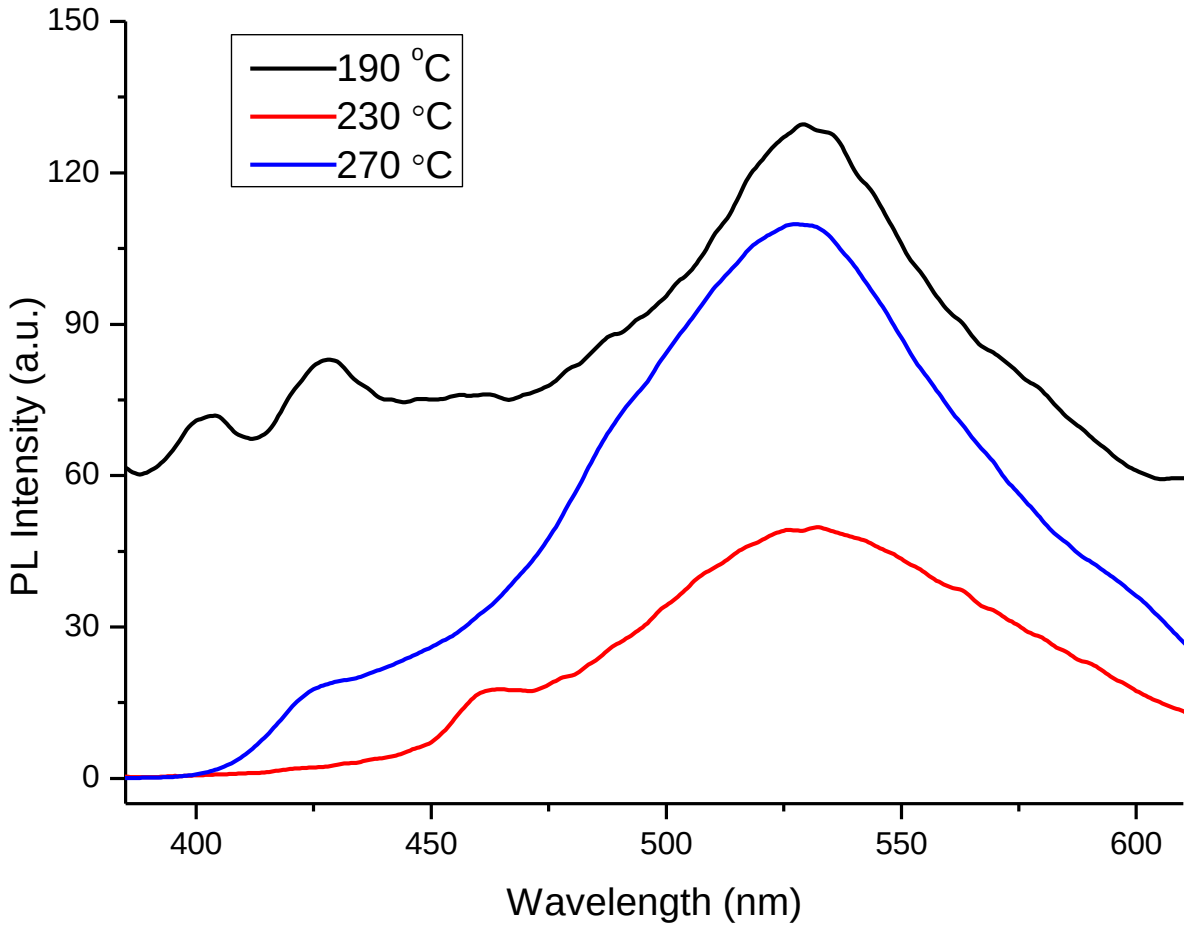

Figure 2.7: PL spectra of CdS nanoparticles synthesized by method 2 at 190 °C, 230 °C and 270 °C.

TEM images and their representative histogram of nanoparticles synthesized by method 2 are shown in Figure 2.8. The temperature effect observed here follows the same sequence as that of method 1. The estimated particle sizes range from 4.8 ± 0.35- 11.50 ± 1.63 nm which complement the results obtained from earlier analyses (XRD, UV-vis and PL). The histogram shows estimated particle sizes between 9.1 and 12.5 nm with a mean of 11.50 for 270 °C.

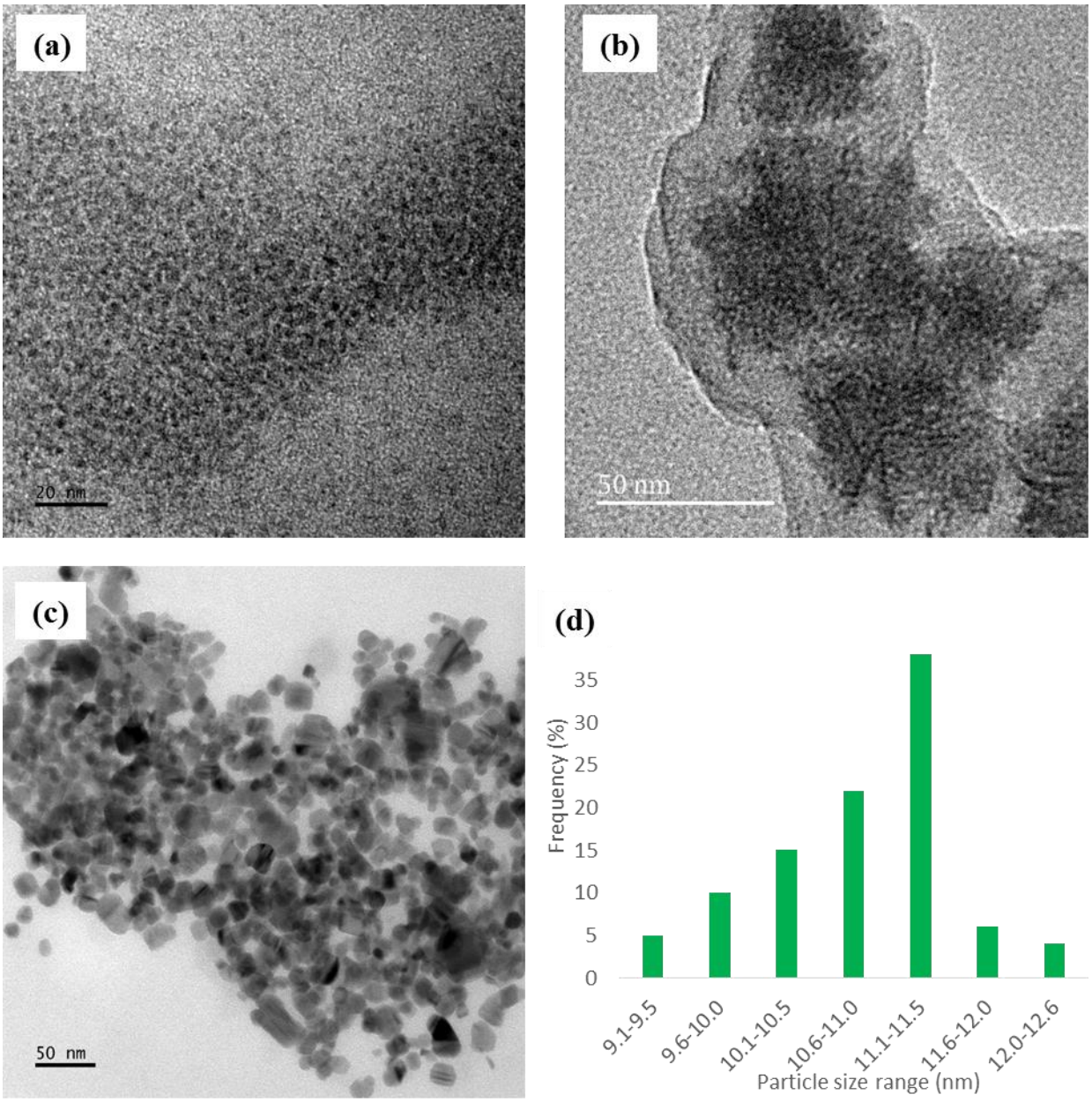

Figure 2.8: TEM images CdS nanoparticles synthesized by method 2 at (a) 190 °C, (b) 230 °C, (c) 270 °C and (d) representative histogram obtained from 270 °C sample.

Method 3

In this methosd, the precursors were mixed with the solvent (1-ethyl-3-methylimidazolium methanesulfonate) in a reaction vessel and heated to the desired temperature. The reaction would be maintained at the particular temperature for a certain period of time afterwhich a resultant product is obtained. The product would then be washed, centrifuged and dried for analysis. The XRD patterns of CdS nanoparticles synthesized by method 3 are shown in Figure 2.9. The patterns in the diffractogram reveal the formation of two crystal phases which are influenced by the reaction temperature. A change in crystal phase is observed after ample elevation in temperature. The diffraction patterns of CdS from the first two temperatures (190 °C and 230 °C) are of the same phase. This also had an effect on the crystallite sizes as it is evidenced by the peak breadth of the patterns. There is a linear relationship between the reaction temperature and crystallite size, as shown in Figure 2.10. The sizes of these nanoparticles were calculated from the Scherrer equation and found to be 3.33 nm, 7.69 nm and 9.92 nm for 190 °C, 230 °C and 270 °C respectively.

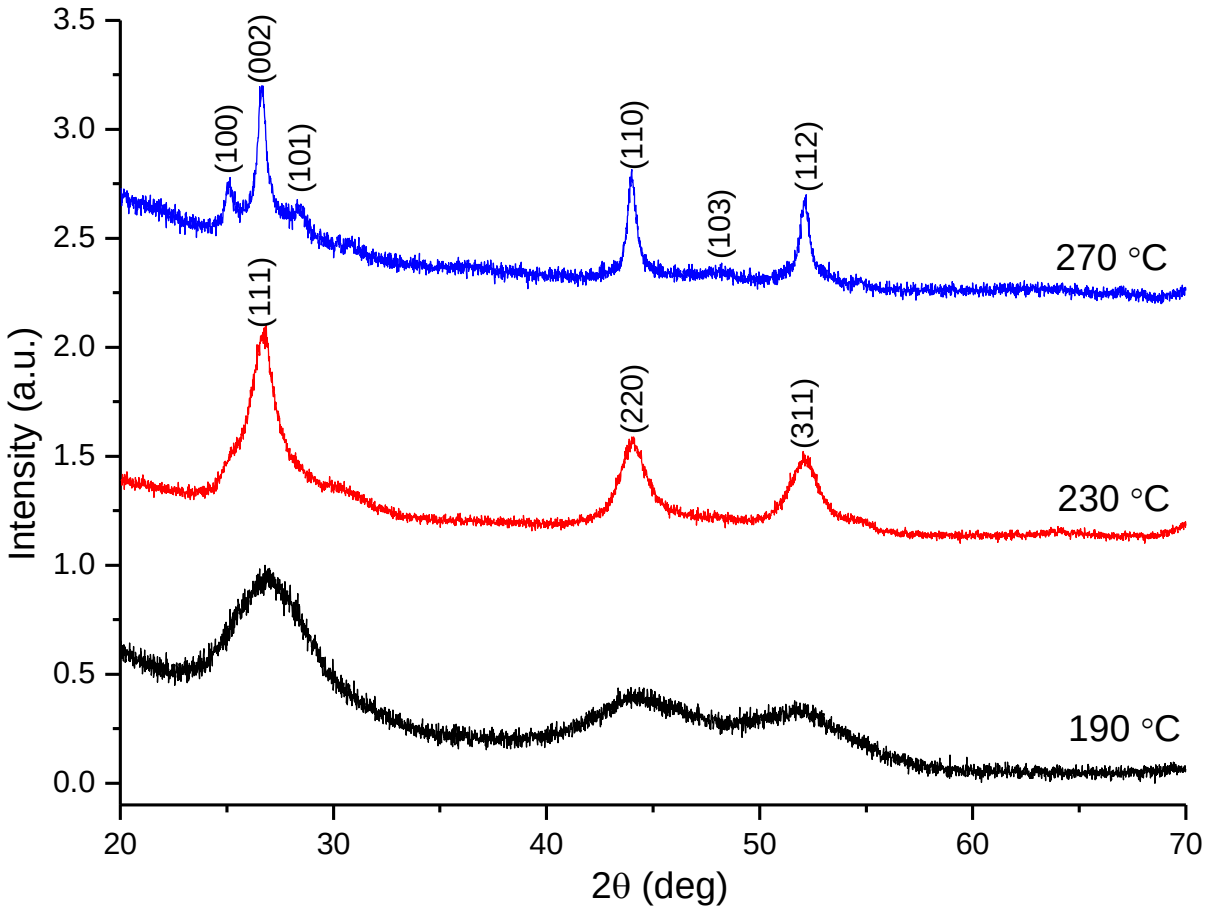

Figure 2.9: XRD patterns of CdS nanoparticles synthesized by method 3 at 190 °C, 230 °C and 270 °C.

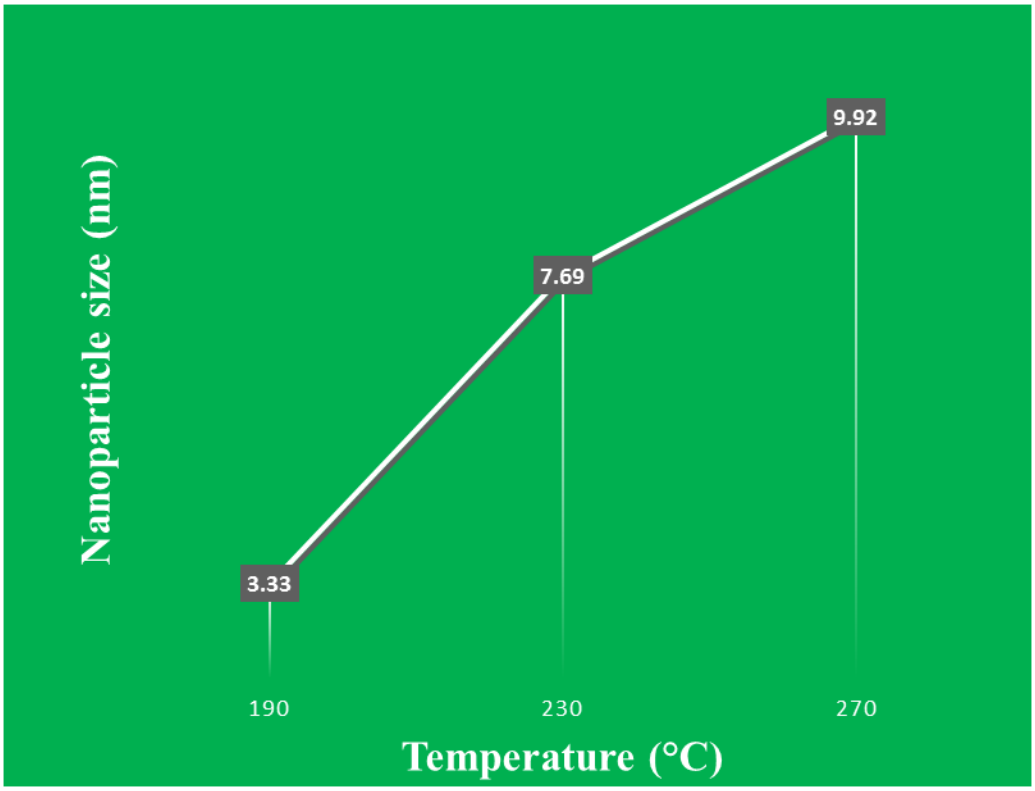

Figure 2.10: A plot of reaction temperature vs nanoparticle size for CdS nanoparticles prepared by method 3.

The UV- vis spectra in Figure 2.11 displays a clear absorption peak for the particles obtained at 190 °C whereas those obtained from higher temperatures (230 °C and 270 °C) show broad bands with no pronounced peaks. The broad band on the particles from 230 °C is more blue-shifted compared to the rest of the set and hence its band gap energy is 3.45 eV (inset in Figure 2.11). The highest reaction temperature gave a red shift and this is in line the prior results which is marked by narrow XRD peaks. What can be deduced from these results is that the nanoparticle growth is accelerated by the elevation in temperature.

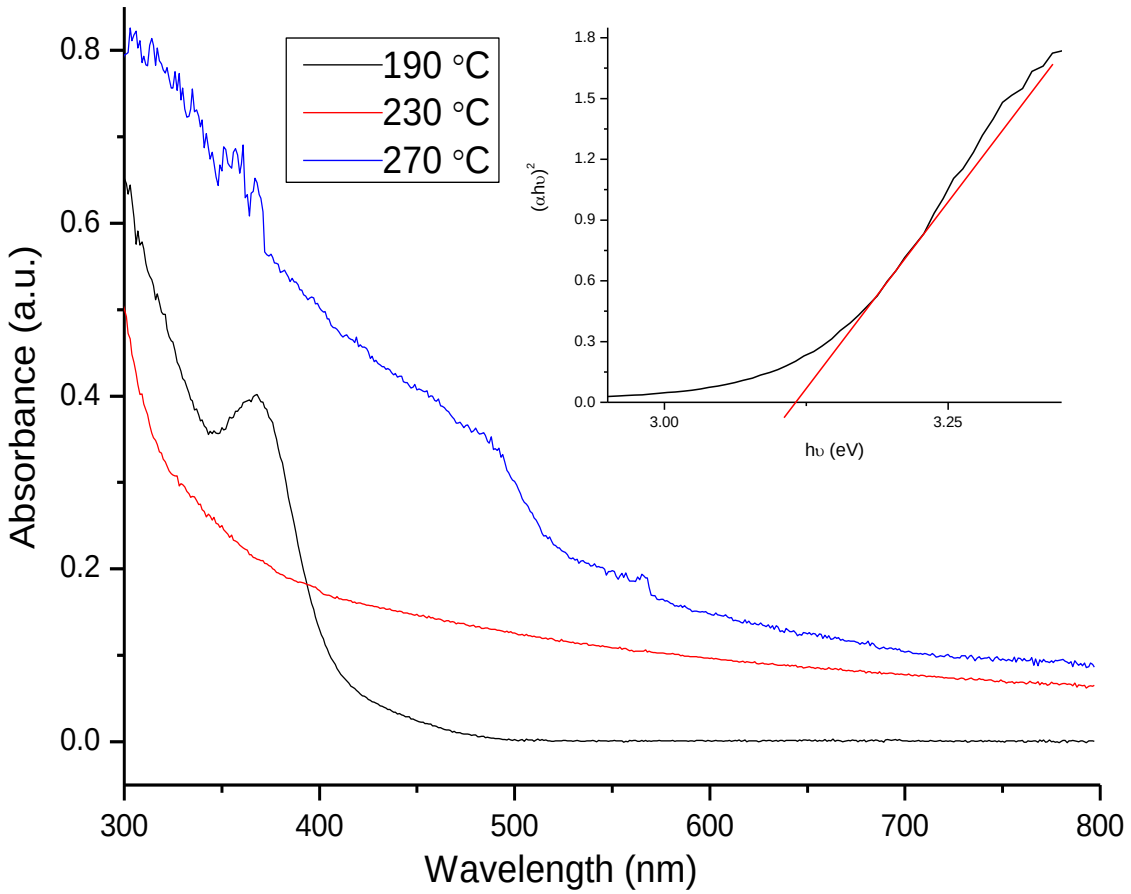

Figure 2.11: UV-visible spectra of CdS nanoparticles synthesized by method 3 at 190 °C, 230 °C and 270 °C. Inset: Tauc plot of nanoparticles prepared at 190 °C.

Figure 2.12 below is a display of the photoluminescence spectra of CdS nanoparticles. There are two major peaks with weak emissions for 190 °C and 230 °C at 427 nm and 530 nm respectively while only one peak observed for 270 °C which is further red shifted and is located at 532 nm. But these are blue shifted compared to other research findings of the same material.[45] These nanoparticles show colour emissions which are size dependent and the increase in temperature resulted in particle growth, and then Stokes shift was experienced. The presence of multiple peaks may be due to the surface damages of the nanoparticle structure.[46] The TEM images shown in Figure 2.13 show a growth of larger nanoparticles from lower to higher temperature. Highly crystalline material was obtained from the analysed samples as evidenced by the selective area electron diffraction (SAED) patterns (Figure 2.13c).

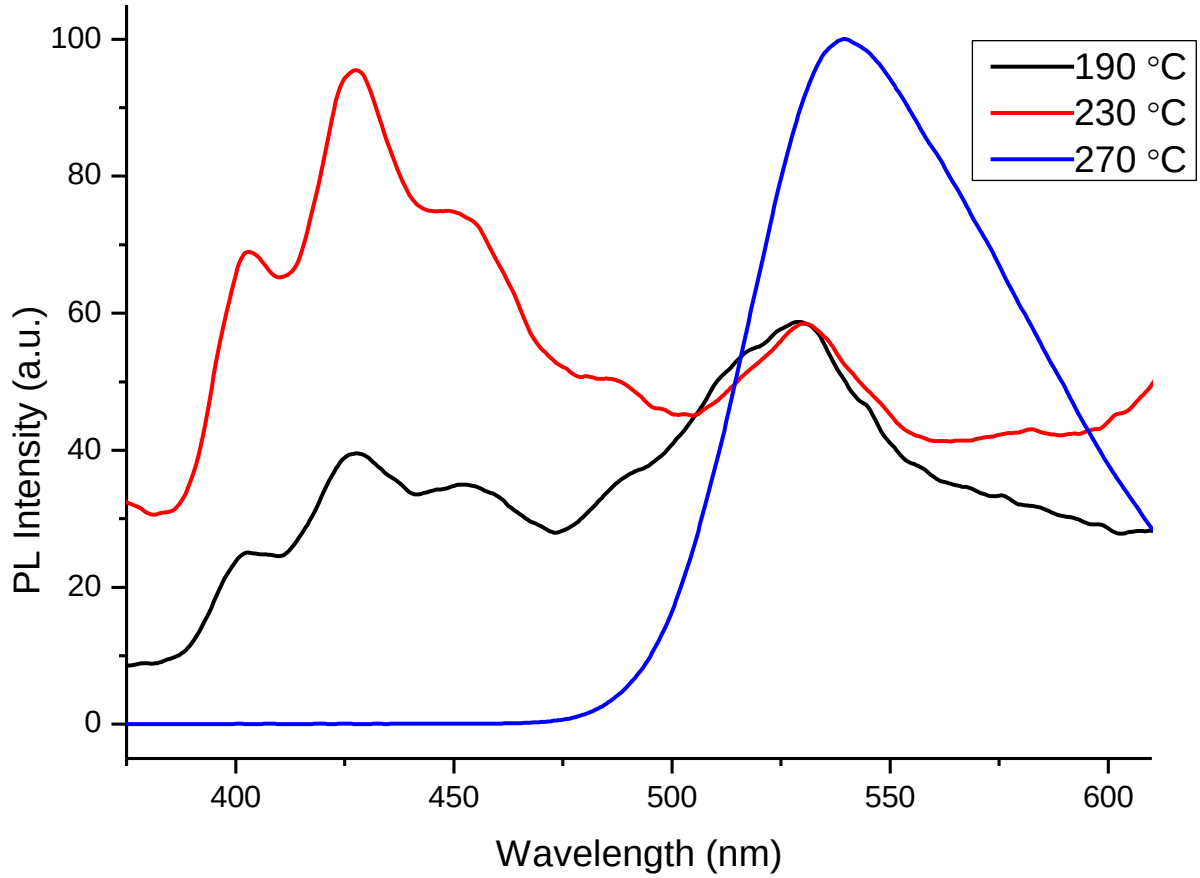

Figure 2.12: PL spectra of CdS nanoparticles synthesized by method 3 at 190 °C, 230 °C and 270 °C.

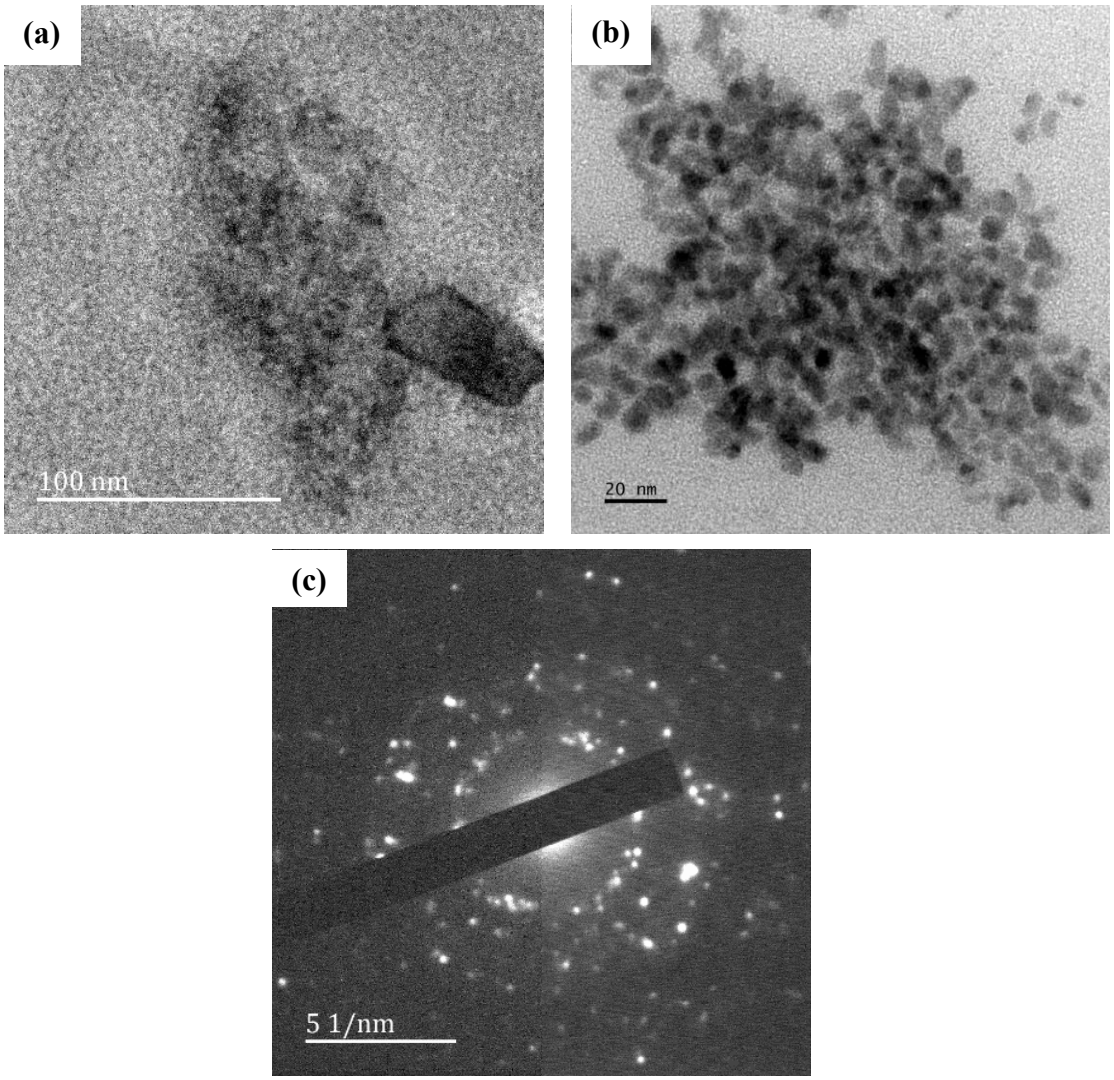

Figure 2.13: TEM images of CdS nanoparticles synthesized by method 3 at (a) 190 °C, (b) 230 °C and (c) SAED for 270 °C.

Table 2.2: Summary of band gap analysis from Tauc plots for all three methods for each of the preparation temperatures.

Method used	**Temperature of reaction**		
	190 °C	**230 °C**	**270 °C**
1	3.25 eV	2.999 eV	2.89 eV
2	3.08 eV	2.96 eV	Not defined
3	3.13 eV	3.45 eV	2.83 eV

2.3.2. Synthesis of CdS nanoparticles from a single source precursor (cadmium ethyl xanthate)

The existence of metal xanthates traces back to 1815 but thorough structural studies have been done three decades ago.[47] The bonding mode of xanthates is expected to look like those of dithiocarbamate complexes, however this is not the case. In the xanthate complex, the cadmium atom is surrounded by four sulfur atoms which are nearly tetragonally arranged around it. The structural difference from dithiocarbamates is that each sulfur atom is attached to a different xanthate group which then bridges two adjacent cadmium atoms and results in a two dimensional network.[37] As a simple single source precursor, cadmium ethyl xanthate has been used for the fabrication of CdS nanoparticles in this section. The results of the as-prepared nanoparticles are detailed below. For comparison purposes, 1-dodecanethiol was used as an extra sulfur source in some cases to see its effect on the phase and morphology of the nanoparticles.

Thermogravimetric analysis (TGA) offers understanding about the decomposition of precursors and what products might be expected. TGA of the cadmium ethyl xanthate complex reveals a one-step decomposition with weight loss between ca. 137 ℃ and 175 ℃ (Figure 2.14). The solid decomposition residue amounts to 43.43 % for the xanthate adduct which is close to the calculated value of 40.72% for CdS for this complex. Previous studies on the cadmium ethyl

xanthate complexes have a one-step decomposition with a rapid weight loss of 57 % between 145 ℃ and 165 ℃.[48]

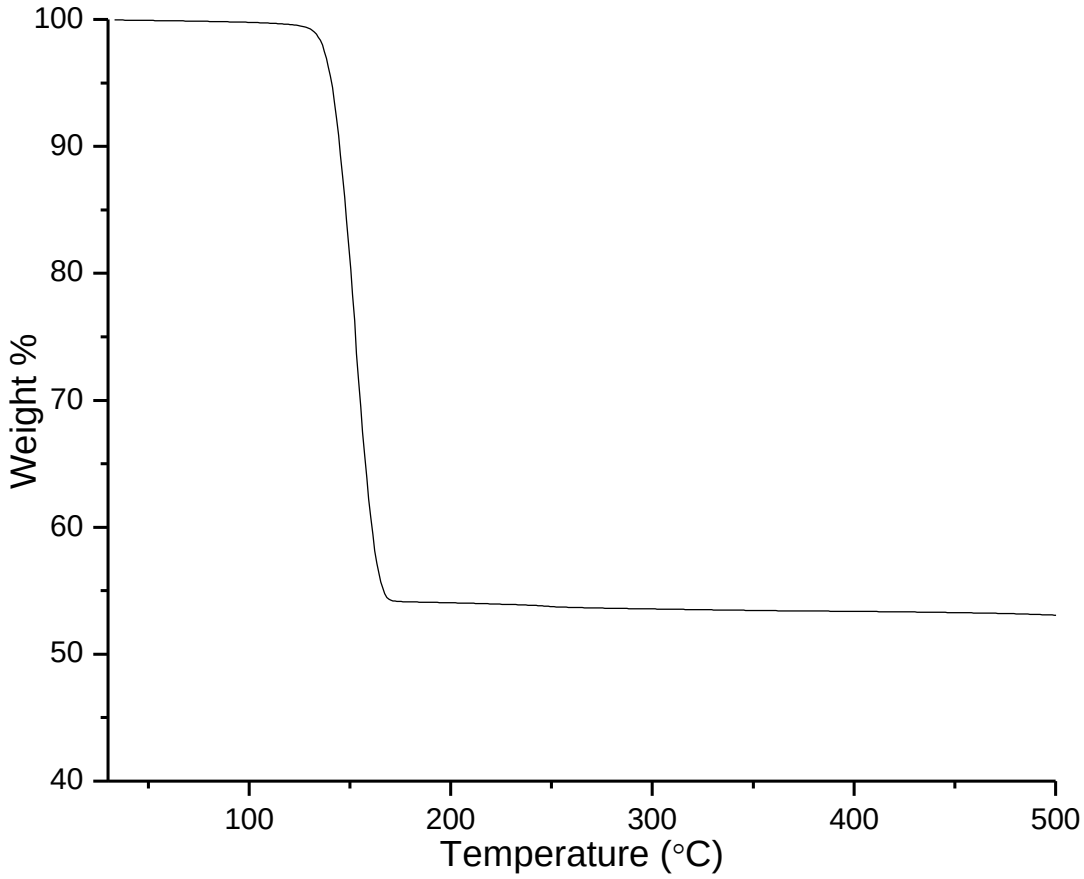

Figure 2.14: TGA curve for the decomposition of cadmium ethyl xanthate.

Cadmium ethyl xanthate was used for the preparation of CdS nanoparticles in the ionic liquid medium (1-ethyl-3-methylimidazolium methanesulfonate) because the ionic liquid can act as both the capping agent and the medium of reaction. It was then decided to introduce 1-dodecanethiol in the study to see its effect on the morphology of the nanoparticles. Two reactions were carried out with the same quantities and at the same temperature for the same duration. One reaction with 1-dodecanethiol and the other without it, while both 1-ethyl-3-methylimidazolium methanesulfonate and lead ethyl xanthate are common parameters. The whole preparation was accomplished by following injection protocols which have been previously published by Mthethwa *et al.* and Nyamen *et al.*[41,49]

Powder XRD patterns of the CdS nanoparticles synthesized from this method are shown in Figure 2.15. The patterns reveal a formation of cubic crystal phase of both products (a) and (b). The intensity of these patterns differ with respect to reaction parameters, therefore, the absence or presence of 1-dodecanethiol has an effect on this factor. Crystal growth preference is slightly towards the (111) direction in both patterns.

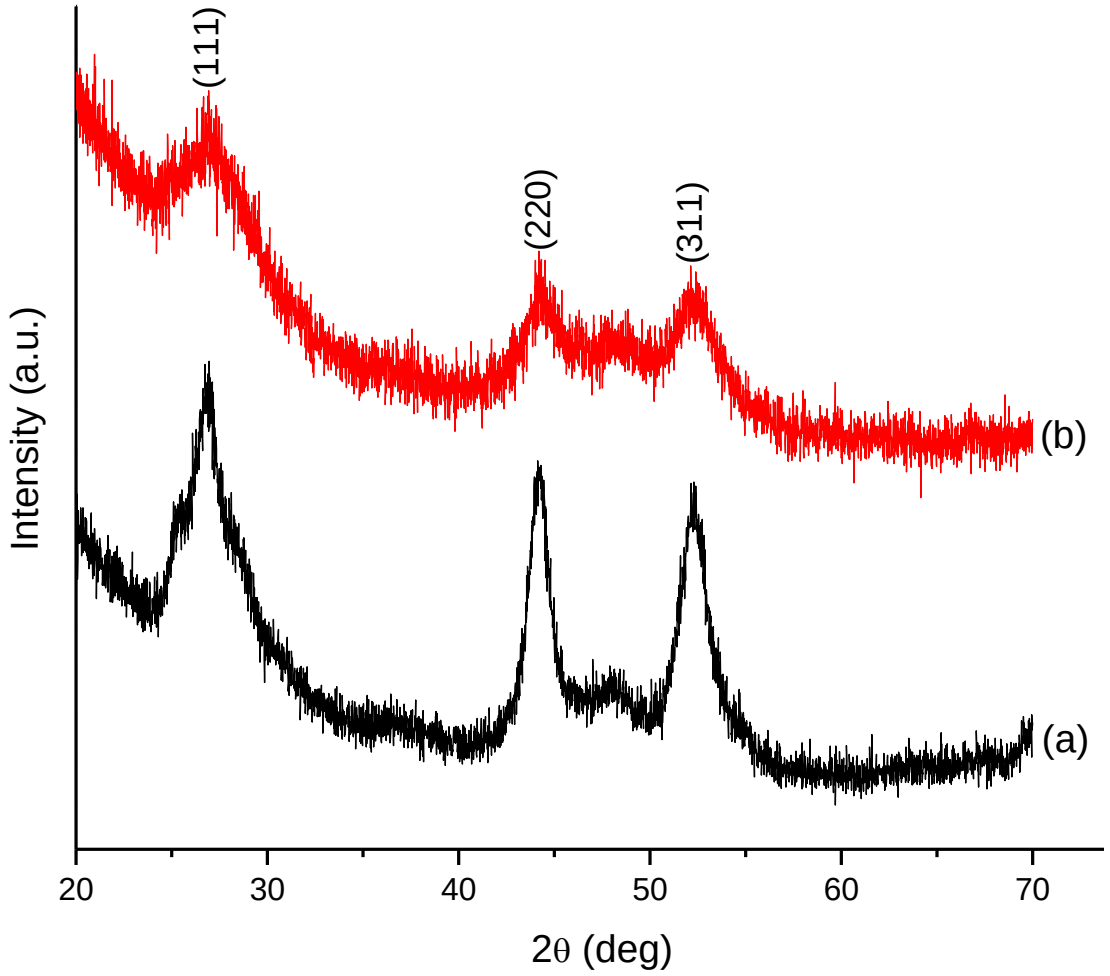

Figure 2.15: XRD patterns of CdS nanoparticles prepared at 190 ℃ (a) without DT and (b) with DT.

Figure 2.16 is an illustration of UV-visible spectra of the nanoparticles synthesized at 190 ℃. A sharp band edge recognised for nanoparticles prepared without 1-dodecanethiol (Figure 2.16(a)) is an indication of smaller nanoparticle sizes compared to their respective set. Likewise the broadening of the band edge suggests relatively bigger nanoparticles (Figure 2.16(b)). The band gap value estimated from the Tauc plot (inset) is 2.15 eV for the sample prepared without DT.

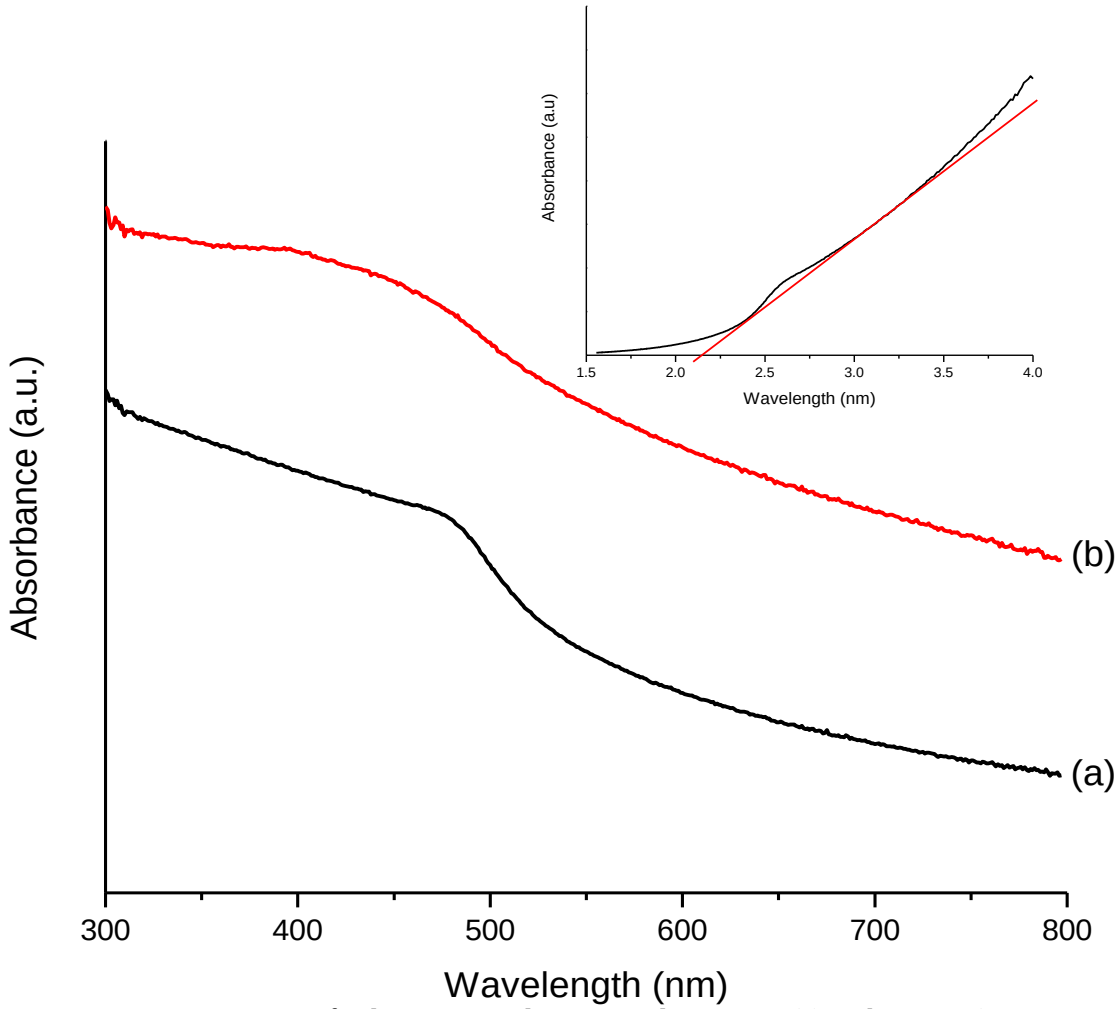

Figure 2.16: UV-vis spectra of CdS nanoparticles prepared at 190 °C (a) without DT (inset Tauc plot) and (b) with DT.

PL spectra of nanoparticles from cadmium ethyl xanthate synthesized at 190 ℃ is shown in Figure 2.17. The spectrum labelled (a) shows an emission at around 500- 512 nm (inset of Figure 2.17). A red shift from 512 nm to 535 nm suggests that upon addition of dodecanethiol to the system increases the particle size.[50,51] TEM was used to find the direct size and structure of the obtained nanoparticles. Figure 18 (a) is a representative TEM image of CdS nanoparticle with its corresponding SAED. It shows monodisperse small and spherical nanoparticles, the fact that the nanoparticle sizes are small is an indication that they were well dispersed in the solution.[52] This result is consistent with the earlier analysis obtained from XRD where the peak broadness signifies small particle sizes. Again, the SAED result, Figure 2.18 (b) confirms the crystallinity of the nanoparticles which was earlier seen from XRD.

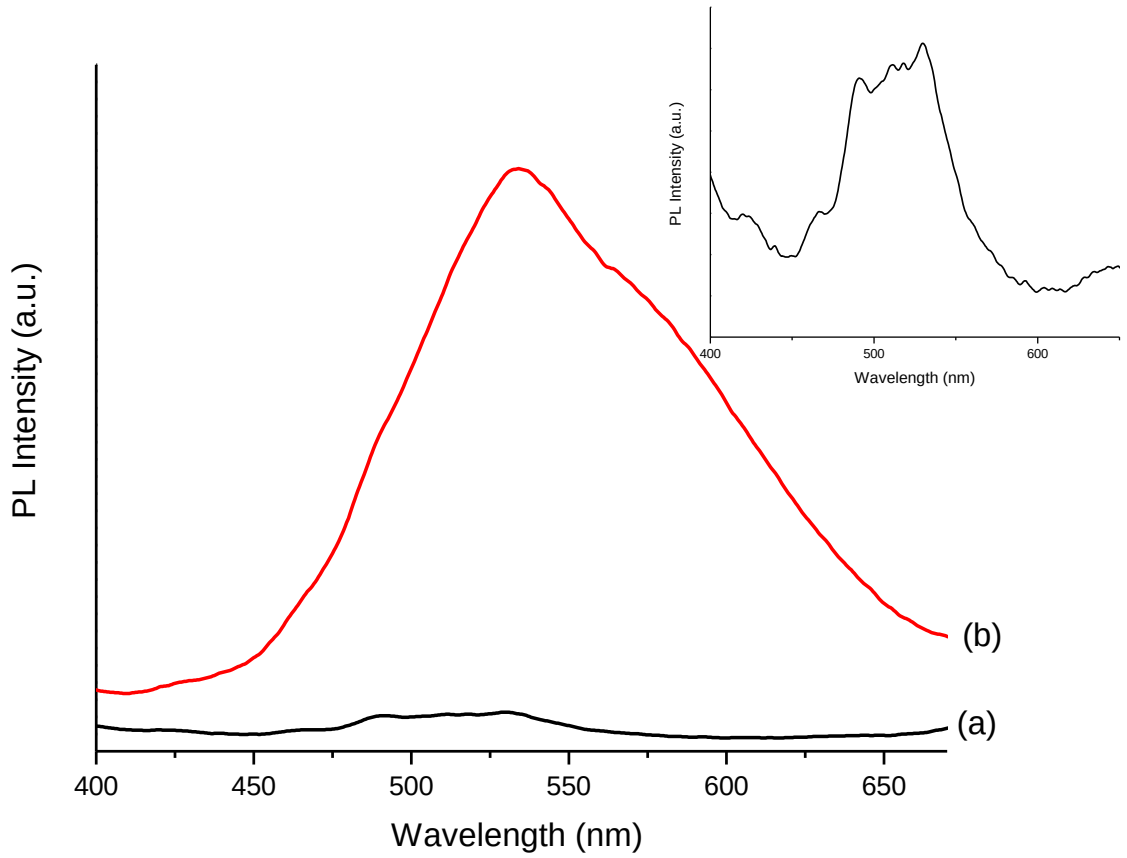

Figure 2.17: PL spectra of CdS nanoparticles prepared at 190 °C (a) without DT and (b) with DT, inset is a zoomed spectrum of (a).

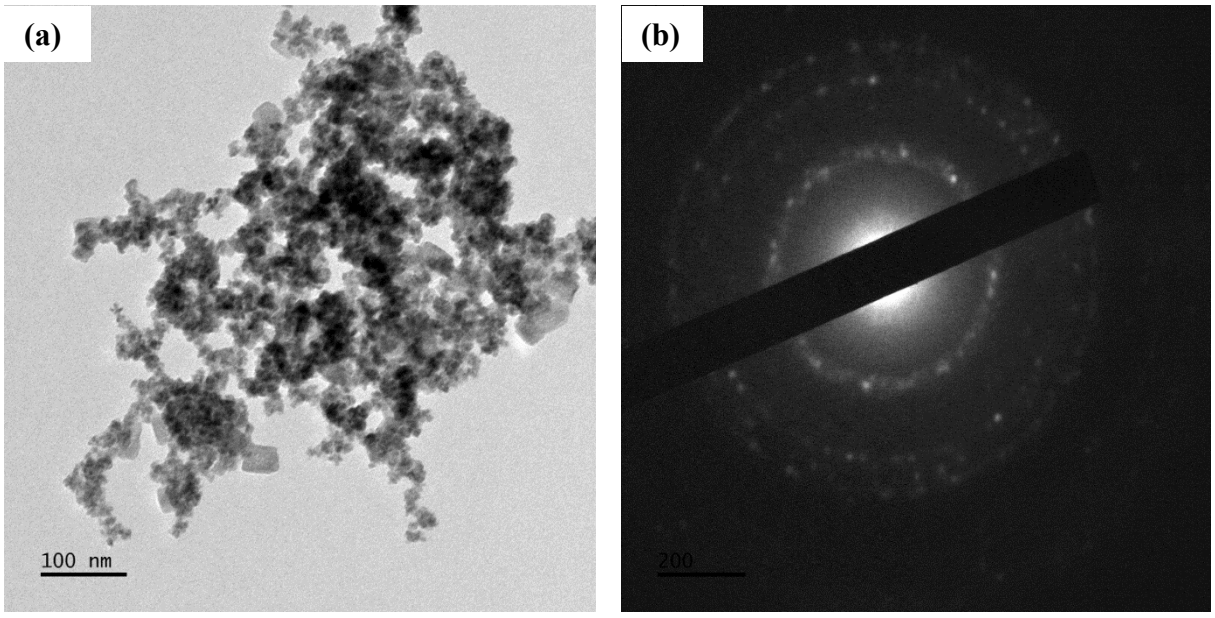

Figure 2.18: TEM image of CdS nanoparticles prepared from SSP at (a) 190 °C and (b) its corresponding SAED.

A comparative study was carried out where temperature would be varied while keeping other reaction parameters constant. This sub-section is focused on reaction carried at 230 ℃. XRD results clearly show a phase transformation from hexagonal (Figure 2.19(a)) to cubic on addition of excess sulfur Figure 2.19(b). The growth preference is towards the (111) plane for the cubic structured crystals while it is (110) for the hexagonal phase. The crystallite size can be estimated to be smaller in the cubic phase structures because of a broader peak breadth.

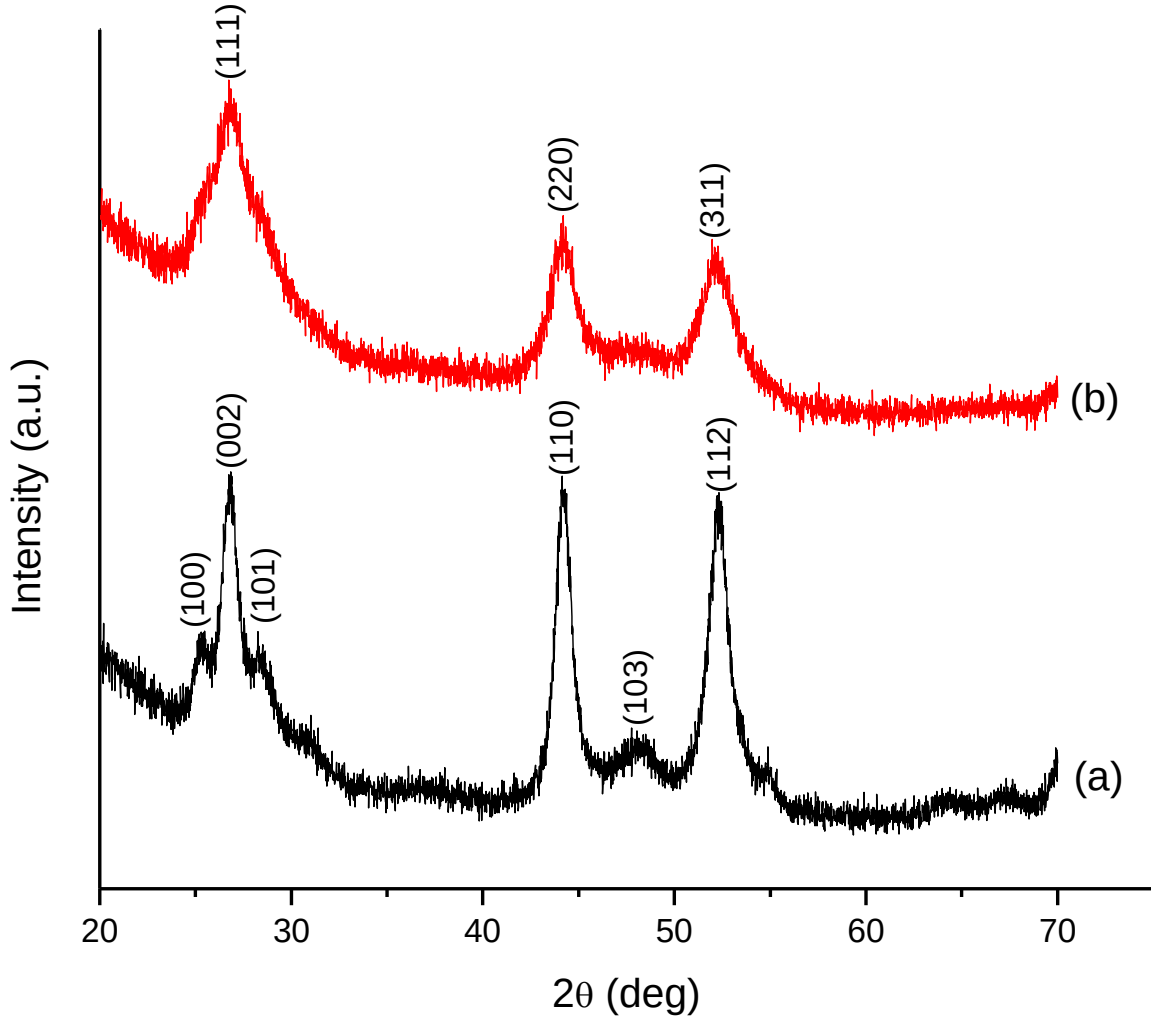

Figure 2.19: XRD patterns of CdS nanoparticles synthesized at 230 ℃ (a) without DT and (b) with DT.

From the UV-visible spectra in Figure 2.20, a sharper absorption band edge is observed for the nanoparticles with dodecanethiol which is the opposite of what was observed in the earlier results (190 ℃). The band gap was estimated to be 1.8 eV from the Tauc plot (inset).

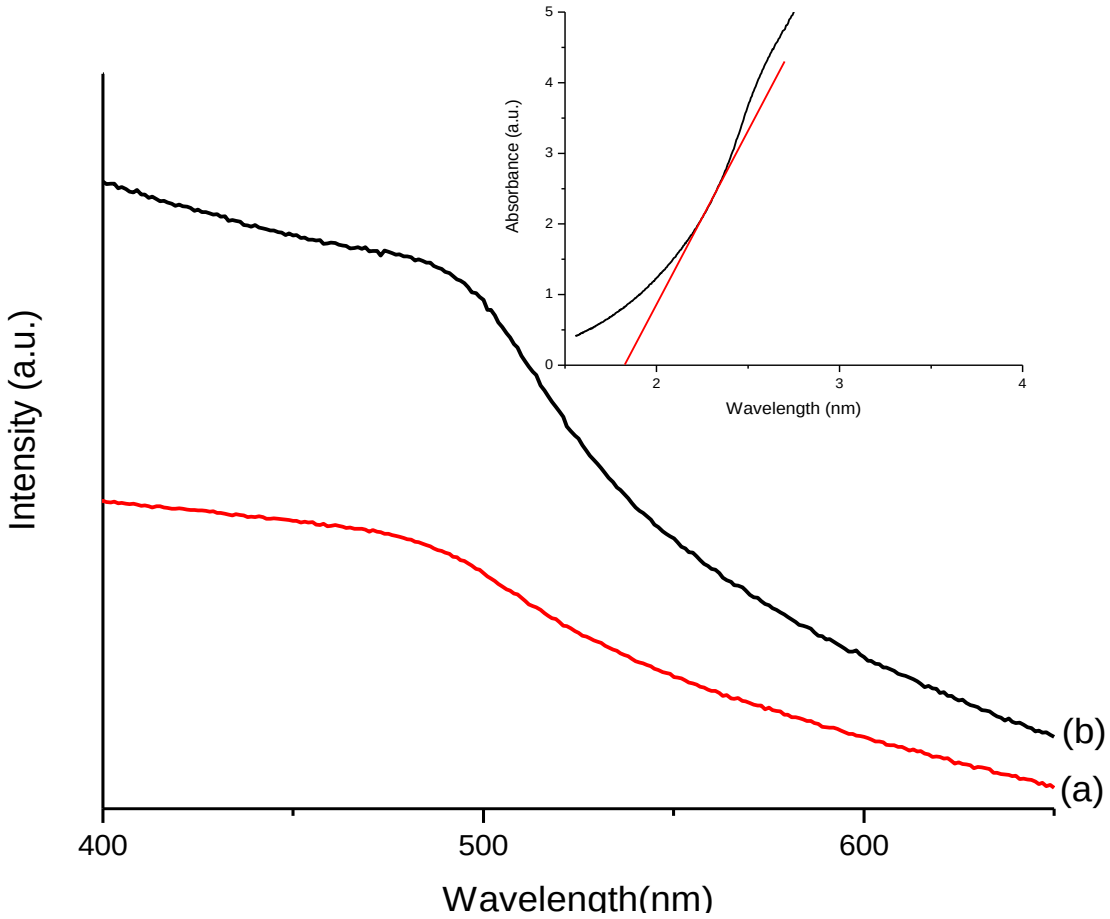

Figure 2.20: UV-vis spectra of CdS nanoparticles prepared at 230 °C (a) without DT and (b) with DT (inset Tauc plot).

PL spectra outlined in Figure 2.21 exhibit poor emission for both as synthesized particles. This emission is comparable to the other reported CdS nanomaterials PL spectra.[35,53] Previous studies have proposed that the photoluminescence phenomena give rise to emission as result of trapped holes where shallow traps result in emission at higher energy.[50] The well-known green emission has been observed at 530 nm with no change even after the addition of dodecanethiol.

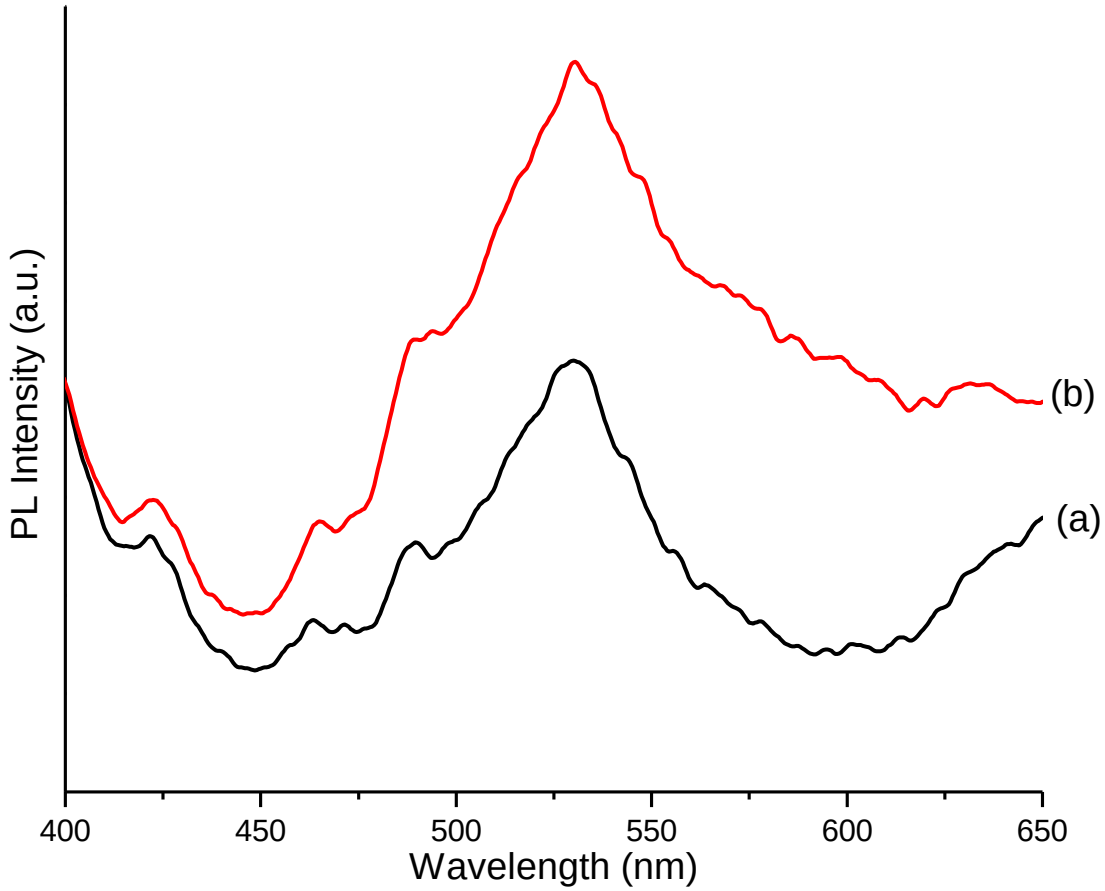

Figure 2.21: PL spectra of CdS nanoparticles prepared at 230 °C (a) without DT and (b) with DT.

TEM images of the prepared nanoparticles are shown in Figure 2.22. The particles obtained from the synthesis without DT appear to be larger than those of the relative set. An assumption is that DT could have self-capped the nanoparticles because it is an organic compound with a long chain which is often used as the capping agent. It might have substituted the ionic liquid capping the nanoparticles. The mechanism for this "assumption" still needs to be looked into. The SAED of the analysed samples shows that the particles are crystalline.

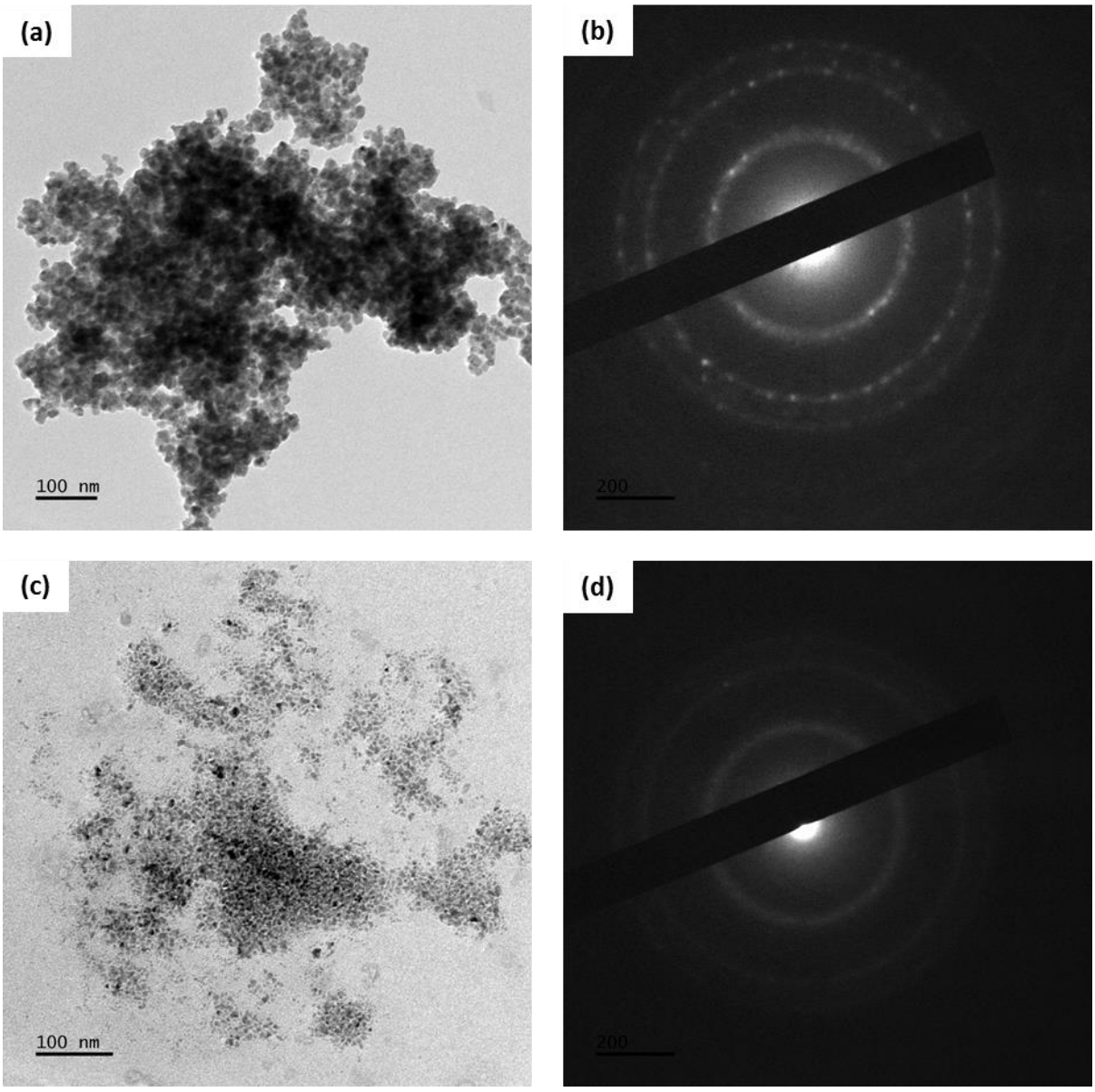

Figure 2.22: TEM images of CdS nanoparticles prepared from SSP at 230 ℃ (a) without DT, (c) with DT and their corresponding SAED (b) and (d) respectively.

Powder XRD patterns of CdS nanoparticles synthesized from the xanthate precursor are demonstrated in Figure 2.23. From the patterns, a clear phase revolution was observed for which a hexagonal and cubic phase could be distinguished without any trace of impurities from the samples. The fact that there might be co-existence of both cubic and hexagonal phase nanoparticles cannot be avoided because the position (2θ values) of some hexagonal peaks coincide with those of the cubic phase. The XRD peaks show that particles obtained from Figure 2.23 (b) are smaller than the corresponding particles.

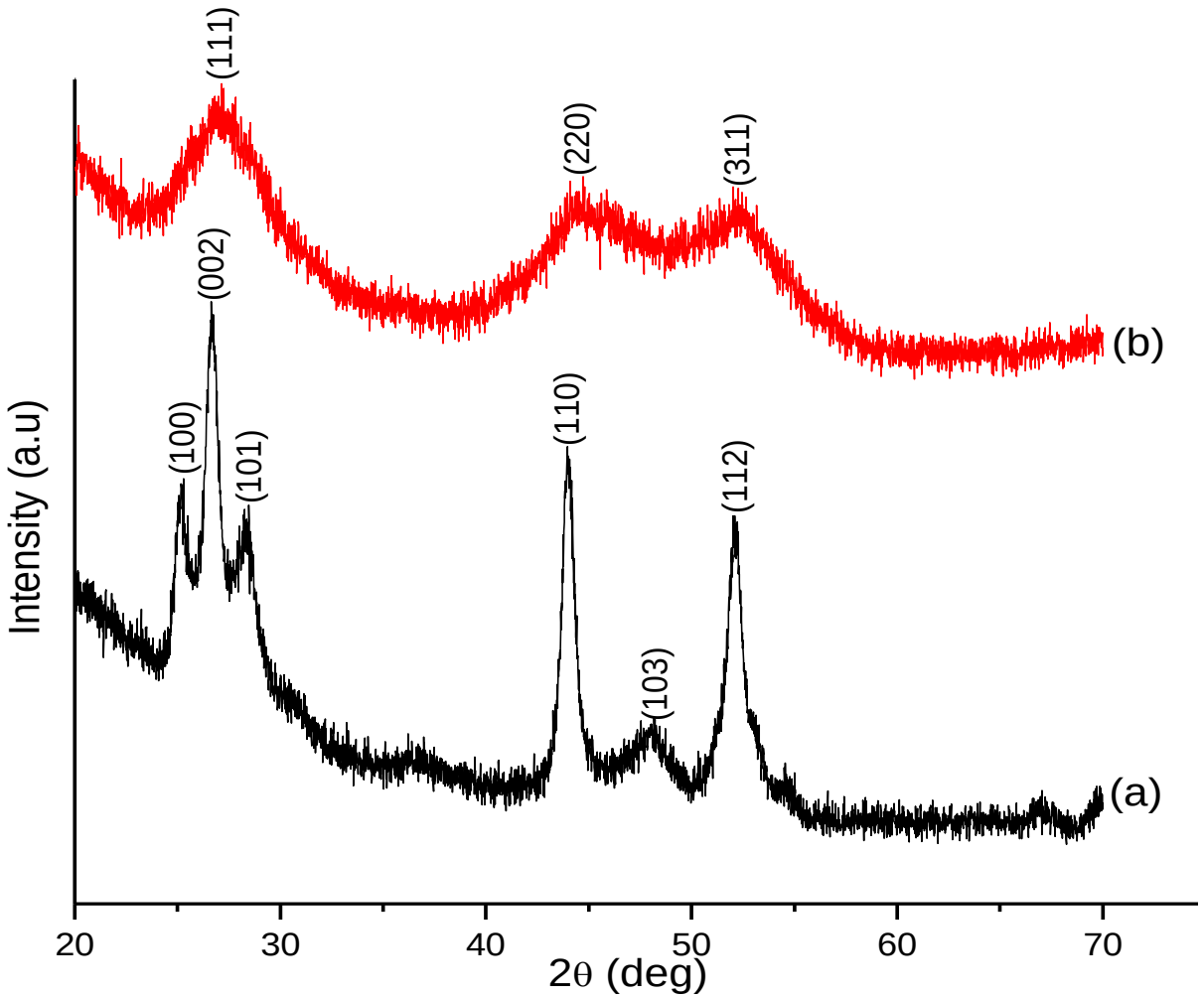

Figure 2.23: XRD patterns of CdS nanoparticles prepared at 270 °C (a) without DT and (b) with DT.

The formation of CdS nanoparticles was examined by UV-Vis absorption spectroscopy and the results are shown in Figure 2.24. The difference in absorption bands/edges (bathochromic shift) indicates a difference in sizes of these nanoparticle. A very sharp absorption edge is observed for the particles prepared without DT and the band gap extrapolation was found to be 3.05 eV from the Tauc plot (inset in Figure 2.24).

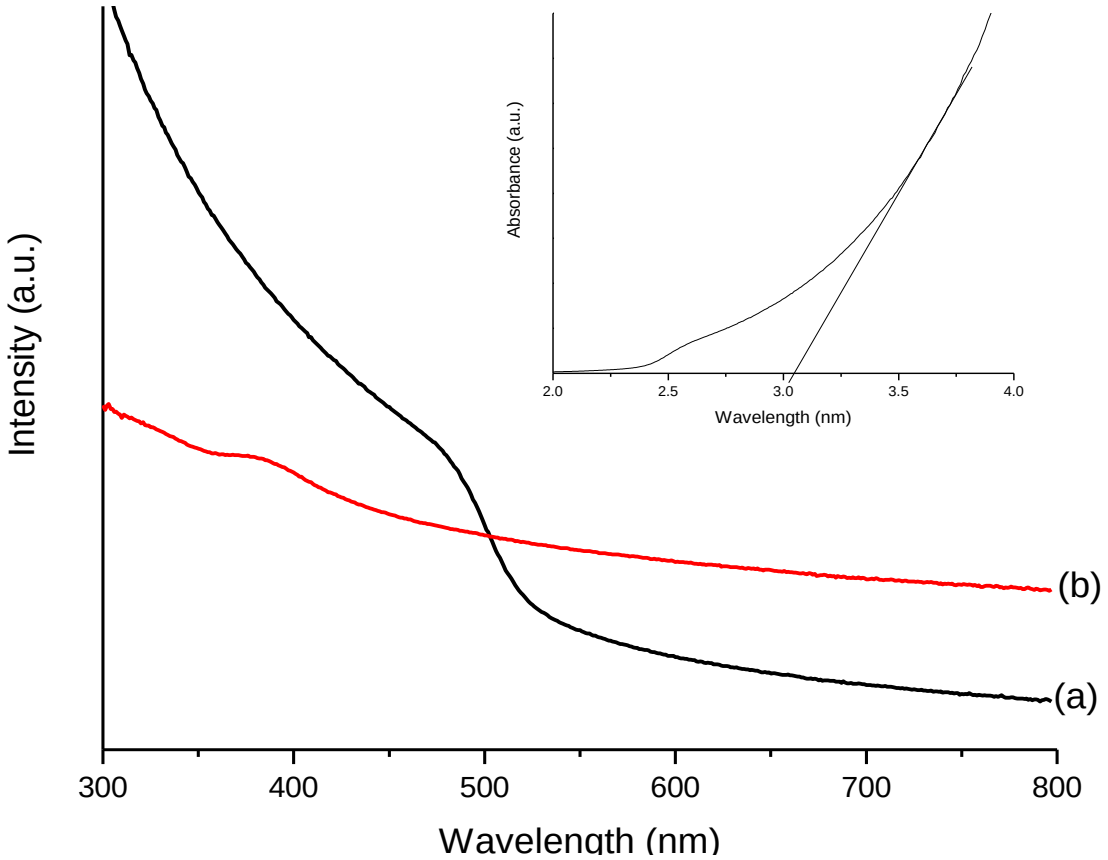

Figure 2.24: UV-vis spectra of CdS nanoparticles prepared at 270 °C (a) without DT (inset Tauc plot) and (b) with DT.

Figure 2.25 shows PL spectra of the as prepared nanoparticles. At this temperature (270 °C) there was no emission for the CdS nanoparticles prepared with dodecanethiol. However those obtained without this coordinating agent gave emission peaks at 435 nm and 528 nm. The peak located at 435 nm is related to the result obtained by Arora *et al.* where they had an emission at 425 nm, but due to Ostwald ripening the particle sizes are bigger in this case, hence the 10 nm shift in the emission peak.[54]

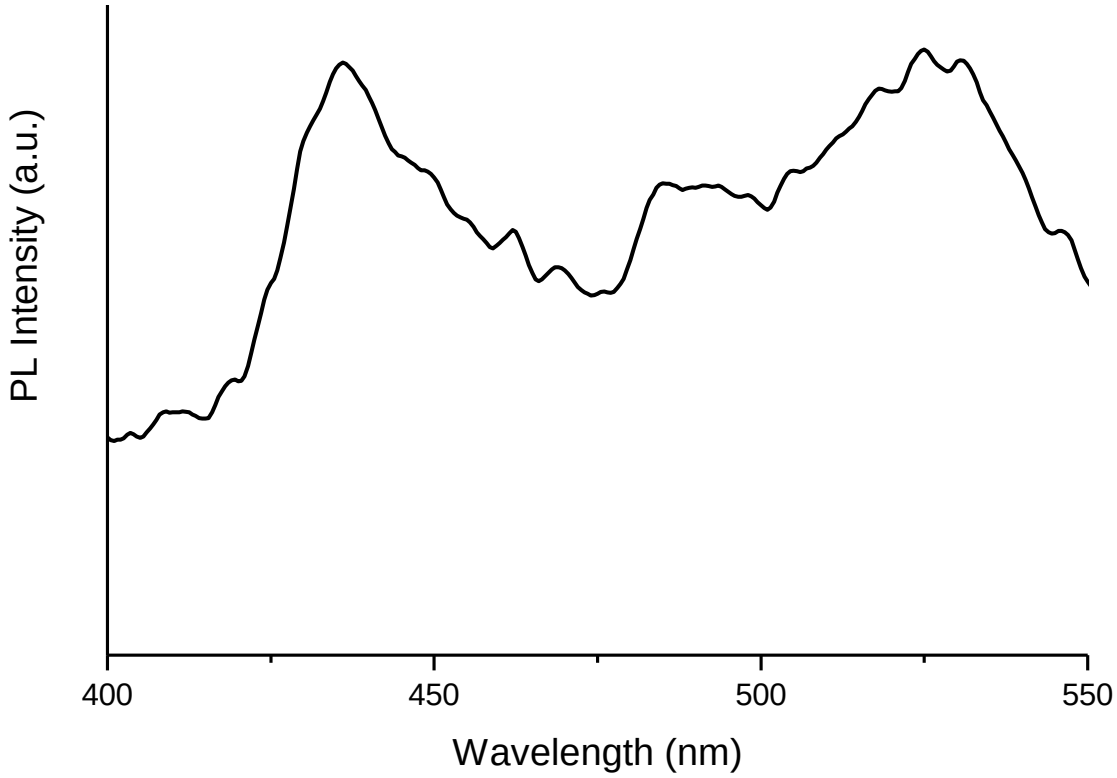

Figure 2.25: PL spectra of CdS nanoparticles prepared at 270 °C without the use of DT.

TEM images of the obtained nanoparticles at 270 °C are presented in Figure 2.26. The average sizes of these nanoparticles are 16.73 nm Figure 2.26 (a) and 44.27 nm Figure 2.26 (c) for nanoparticles prepared without DT and with DT respectively. The particles were all crystalline as evidenced by the SAED patterns.

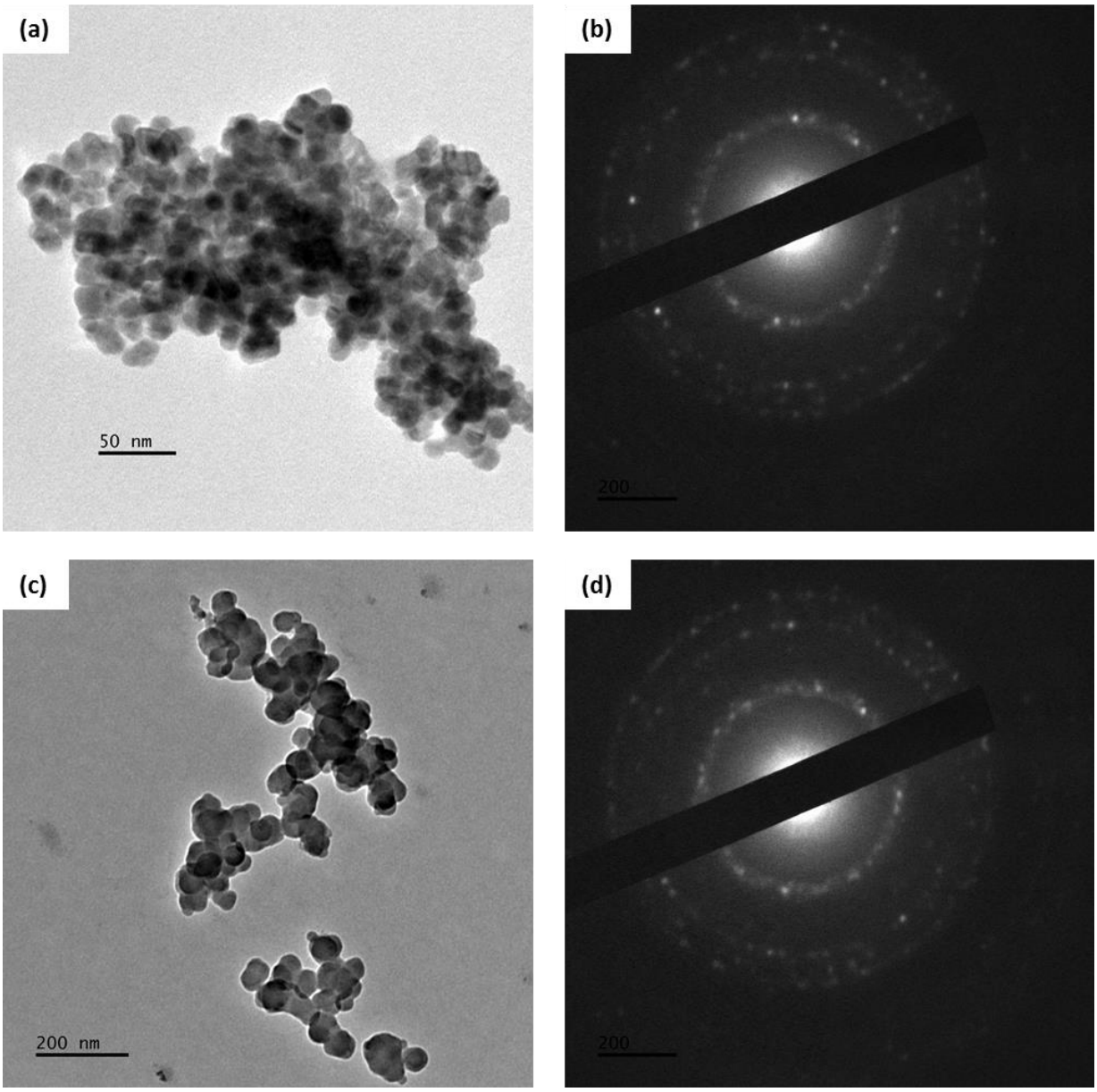

Figure 2.26: TEM images of CdS nanoparticles prepared from SSP at 270 °C (a) without DT, (c) with DT and their corresponding SAED (b) and (d) respectively.

2.4. Conclusion

Cadmium sulfide quantum dots have been successfully prepared by employing various thermolysis techniques using imidazolium based ionic liquid, where the reaction temperature and injection method were varied to tune both the optical and structural properties. At high temperatures hexagonal phases were obtained whereas for lower temperatures cubic phase has been observed. Morphological studies showed that relatively low temperatures gave particles of smaller sizes, which were further confirmed by the broadness of the diffraction patterns. The prepared nanoparticles have sizes ranging from 2.40 to 15.66 nm. The optical studies further revealed that the as-synthesized CdS quantum dots exhibited strong quantum size effect due to their sharp band for the dual source precursors. The nanoparticles synthesized from a single source precursor showed a mixture of both phases at higher temperatures, while at 190 °C only a cubic phase was observed. Optical analyses from this method (single source precursor) show much red shifted absorption compared to those of dual source precursors, while the intensities of the XRD patterns were more distinct resulting into less crystalline CdS nanoparticles. The mean sizes of these nanoparticles were found to be 44.27 nm. The use of IL has proved its efficiency because the synthetic reactions could be done in a decent environment with no volatility and flammability of the reactants and products. Also the results obtained are comparable to other literature findings which conforms to the stated effectiveness of the IL usage.

2.5. References

(1) Devendran, P.; Alagesan, T.; Pandian, K. Single pot microwave synthesis of CdS nanoparticles in ionic liquid and their photocatalytic application. *Asian Journal of Chemistry* **2013**, *25*, S79.

(2) Bansal, P.; Jaggi, N.; Rohilla, S. Green synthesis of CdS nanoparticles and effect of capping agent concentration on crystallite size. *Research Journal of Chemical Sciences* **2012**, *2*, 69-71.

(3) Singh, V.; Sharma, P.; Chauhan, P. Synthesis of CdS nanoparticles with enhanced optical properties. *Materials Characterization* **2011**, *62*, 43-52.

(4) Banerjee, R.; Jayakrishnan, R.; Ayyub, P. Effect of the size-induced structural transformation on the band gap in CdS nanoparticles. *Journal of Physics: Condensed Matter* **2000**, *12*, 10647.

(5) Bandaranayake, R.; Wen, G.; Lin, J.; Jiang, H.; Sorensen, C. Structural phase behavior in II–VI semiconductor nanoparticles. *Applied Physics Letters* **1995**, *67*, 831-833.

(6) Ricolleau, C.; Audinet, L.; Gandais, M.; Gacoin, T. Structural transformations in II-VI semiconductor nanocrystals. *The European Physical Journal D-Atomic, Molecular, Optical and Plasma Physics* **1999**, *9*, 565-570.

(7) Zhulai, D.; Fedorenko, D.; Kovalchuk, A.; Bugaychuk, S.; Klimusheva, G. V.; Mirnaya, T. A. Influence of semiconductor and metal nanoparticles on the dielectric properties of ionic matrix cadmium octanoate. *Nanoscale Research Letters* **2015**, *10*, 66.

(8) Singh, V.; Chauhan, P. Structural and optical characterization of CdS nanoparticles prepared by chemical precipitation method. *Journal of Physics and Chemistry of Solids* **2009**, *70*, 1074-1079.

(9) Lalayan, A. Formation of colloidal GaAs and CdS quantum dots by laser ablation in liquid media. *Applied Surface Science* **2005**, *248*, 209-212.

(10) Phuruangrat, A.; Thongtem, T.; Thongtem, S. Characterisation of one-dimensional CdS nanorods synthesised by solvothermal method. *Journal of Experimental Nanoscience* **2009**, *4*, 47-54.

(11) Pal, U.; Loaiza-González, G.; Bautista-Hernández, A.; Vázquez-Cuchillo, O. Synthesis of CdS nanoparticles through colloidal rout. *Superficies y Vacío* **2000**, *11*, 40-43.

(12) He, R.; Qian, X.-f.; Yin, J.; Xi, H.-a.; Bian, L.-j.; Zhu, Z.-k. Formation of monodispersed PVP-capped ZnS and CdS nanocrystals under microwave irradiation. *Colloids and Surfaces A: Physicochemical and Engineering Aspects* **2003**, *220*, 151-157.

(13) Alivisatos, A. P. Semiconductor clusters, nanocrystals, and quantum dots. *Science* **1996**, *271*, 933.

(14) Rajeswari Yogamalar, N.; Sadhanandam, K.; Chandra Bose, A.; Jayavel, R. Quantum confined CdS inclusion in graphene oxide for improved electrical conductivity and facile charge transfer in hetero-junction solar cell. *Royal Society of Chemistry Advances* **2015**, *5*, 16856-16869.

(15) Romeo, N.; Bosio, A.; Canevari, V.; Podesta, A. Recent progress on CdTe/CdS thin film solar cells. *Solar Energy* **2004**, *77*, 795-801.

(16) Nelson, J. The Physics of solar cells. *World Scientific Publishing Company* **2003,** 279-282.

(17) Cha, D.; Kim, S.; Huang, N. Study on electrical properties of CdS films prepared by chemical pyrolysis deposition. *Materials Science and Engineering: B* **2004**, *106*, 63-68.

(18) Duan, X.; Huang, Y.; Agarwal, R.; Lieber, C. M. Single-nanowire electrically driven lasers. *Nature* **2003**, *421*, 241-245.

(19) Wang, Y.; Ramanathan, S.; Fan, Q.; Yun, F.; Morkoc, H.; Bandyopadhyay, S. Electric field modulation of infrared absorption at room temperature in electrochemically self assembled quantum dots. *Journal of Nanoscience and Nanotechnology* **2006**, *6*, 2077-2080.

(20) Murai, H.; Abe, T.; Matsuda, J.; Sato, H.; Chiba, S.; Kashiwaba, Y. Improvement in the light emission characteristics of CdS: Cu/CdS diodes. *Applied Surface Science* **2005**, *244*, 351-354.

(21) Ma, R.-M.; Dai, L.; Qin, G.-G. High-performance nano-Schottky diodes and nano-MESFETs made on single CdS nanobelts. *Nano Letters* **2007**, *7*, 868-873.

(22) Jiang, J.; He, Y.; Wan, L.; Cui, Z.; Cui, Z.; Jessop, P. G. Synthesis of CdS nanoparticles in switchable surfactant reverse micelles. *Chemical Communications* **2013**, *49*, 1912-1914.

(23) Dameron, C.; Reese, R.; Mehra, R.; Kortan, A.; Carroll, P.; Steigerwald, M.; Brus, L.; Winge, D. R. Biosynthesis of cadmium sulphide quantum semiconductor crystallites. *Nature* **1989**, *338*, 596-597.

(24) Nithya, N.; Boopathi, G. Synthesis and characterization of CdS and Ag doped CdS nanoparticle. *International Journal of Science and Research* **2015**, *4*, 2319-7064

(25) Zelaya-Angel, O.; de L Castillo-Alvarado, F.; Avendano-Lopez, J.; Escamilla-Esquivel, A.; Contreras-Puente, G.; Lozada-Morales, R.; Torres-Delgado, G. Raman studies in CdS thin films in the evolution from cubic to hexagonal phase. *Solid State Communications* **1997**, *104*, 161-166.

(26) Wang, W.; Liu, Z.; Zheng, C.; Xu, C.; Liu, Y.; Wang, G. Synthesis of CdS nanoparticles by a novel and simple one-step, solid-state reaction in the presence of a nonionic surfactant. *Materials Letters* **2003**, *57*, 2755-2760.

(27) Knudson, M.; Gupta, Y.; Kunz, A. Transformation mechanism for the pressure-induced phase transition in shocked CdS. *Physical Review B* **1999**, *59*, 11704.

(28) Gleiter, H. Nanostructured materials: State of the art and perspectives. *Nanostructured Materials* **1995**, *6*, 3-14.

(29) Lavanya, T.; Jaya, N. V. Synthesis and characterization of pure CdS nanoparticles for ptoelectronic applications. *Transactions of the Indian Ceramic Society* **2011**, *70*, 119-123.

(30) Welton, T. Room-temperature ionic liquids. Solvents for synthesis and catalysis. *Chemical Reviews* **1999**, *99*, 2071-2084.

(31) Seddon, K. R. Ionic liquids for clean technology. *Journal of Chemical Technology and Biotechnology* **1997**, *68*, 351-356.

(32) Chauvin, Y.; Mussmann, L.; Olivier, H. A novel class of versatile solvents for two-phase catalysis: Hydrogenation, isomerization, and hydroformylation of alkenes catalyzed by rhodium complexes in liquid 1, 3-dialkylimidazolium salts. *Angewandte Chemie International Edition in English* **1996**, *34*, 2698-2700.

(33) Zheng, W.; Li, D.; Guo, W. Applications of ionic liquids (ILs) in synthesis of inorganic nanomaterials. *Materials Science* **2015**, 94-117.

(34) Jiang, N.; Xiu, Z.; Xie, Z.; Li, H.; Zhao, G.; Wang, W.; Wu, Y.; Hao, X. Reduced graphene oxide–CdS nanocomposites with enhanced visible-light photoactivity synthesized using ionic-liquid precursors. *New Journal of Chemistry* **2014**, *38*, 4312-4320.

(35) Biswas, K.; Rao, C. N. R. Use of ionic liquids in the synthesis of nanocrystals and nanorods of semiconducting metal chalcogenides. *Chemistry–A European Journal* **2007**, *13*, 6123-6129.

(36) Yao, K.; Lu, W.; Wang, J. Ionic liquid-assisted synthesis, structural characterization, and photocatalytic performance of CdS nanocrystals. *Materials Chemistry and Physics* **2011**, *130*, 1175-1181.

(37) Iimura, Y.; Ito, T.; Hagihara, H. The crystal structure of cadmium ethylxanthate. *Acta Crystallographica Section B: Structural Crystallography and Crystal Chemistry* **1972**, *28*, 2271-2279.

(38) Trindade, T.; O'Brien, P.; Zhang, X.-m.; Motevalli, M. Synthesis of PbS nanocrystallites using a novel single moleculeprecursors approach: X-ray single-crystal structure of Pb $(S_2CNEtPri)_2$. *Journal of Materials Chemistry* **1997**, *7*, 1011-1016.

(39) Oliva, A.; Solí, O.; Castro-Rodrí, R.; Quintana, P. Formation of the band gap energy on CdS thin films growth by two different techniques. *Thin Solid Films* **2001**, *391*, 28-35.

(40) Singh, V.; Singh, R.; Thompson, G.; Jayaraman, V.; Sanagapalli, S.; Rangari, V. Characteristics of nanocrystalline CdS films fabricated by sonochemical, microwave and solution growth methods for solar cell applications. *Solar Energy Materials and Solar Cells* **2004**, *81*, 293-303.

(41) Mthethwa, T.; Pullabhotla, V. S. R.; Mdluli, P. S.; Wesley-Smith, J.; Revaprasadu, N. Synthesis of hexadecylamine capped CdS nanoparticles using heterocyclic cadmium dithiocarbamates as single source precursors. *Polyhedron* **2009**, *28*, 2977-2982.

(42) Aguilar-Hernandez, J.; Contreras-Puente, G.; Morales-Acevedo, A.; Vigil-Galan, O.; Cruz-Gandarilla, F.; Vidal-Larramendi, J.; Escamilla-Esquivel, A.; Hernandez-Contreras, H.; Hesiquio-Garduno, M.; Arias-Carbajal, A. Photoluminescence and structural properties of cadmium sulphide thin films grown by different techniques. *Semiconductor Science and Technology* **2002**, *18*, 111.

(43) Mirnaya, T.; Asaula, V.; Volkov, S.; Tolochko, A.; Melnik, D.; Klimusheva, G. Synthesis and optical properties of liquid crystalline nanocomposites of cadmium octanoate with CdS quantum dots. *Physics and Chemistry of Solids* **2012**, *13*, 131-135.

(44) Fu, Z.; Zhou, S.; Shi, J.; Zhang, S. Effects of precursors on the crystal structure and photoluminescence of CdS nanocrystalline. *Materials Research Bulletin* **2005**, *40*, 1591-1598.

(45) Ghows, N.; Entezari, M. A novel method for the synthesis of CdS nanoparticles without surfactant. *Ultrasonics Sonochemistry* **2011**, *18*, 269-275.

(46) Pozina, G.; Bergman, J.; Monemar, B.; Takeuchi, T.; Amano, H.; Akasaki, I. Origin of multiple peak photoluminescence in InGaN/GaN multiple quantum wells. *Journal of Applied Physics* **2000**, *88*, 2677-2681.

(47) Nair, P. S.; Radhakrishnan, T.; Revaprasadu, N.; Kolawole, G.; O'Brien, P. Cadmium ethylxanthate: A novel single-source precursor for the preparation of CdS nanoparticles. *Journal of Materials Chemistry* **2002**, *12*, 2722-2725.

(48) Agrawal, V.; Jain, K.; Arora, L.; Chand, S. Synthesis of CdS nanocrystals in poly (3-hexylthiophene) polymer matrix: Optical and structural studies. *Journal of Nanoparticle Research* **2013**, *15*, 1697.

(49) Nyamen, L. D.; Pullabhotla, V. S. R.; Nejo, A. A.; Ndifon, P.; Revaprasadu, N. Heterocyclic dithiocarbamates: Precursors for shape controlled growth of CdS nanoparticles. *New Journal of Chemistry* **2011**, *35*, 1133-1139.

(50) Chestnoy, N.; Harris, T. D.; Hull, R.; Brus, L. E. Luminescence and photophysics of cadmium sulfide semiconductor clusters: The nature of the emitting electronic state. *The Journal of Physical Chemistry* **1986**, *90*, 3393-3399.

(51) Fojtik, A.; Weller, H.; Koch, U.; Henglein, A. Photo-chemistry of colloidal metal sulfides 8. Photo-physics of extremely small CdS particles: Q-state CdS and magic agglomeration numbers. *International Journal of Physical Chemistry* **1984**, *88*, 969-977.

(52) Qi, L.; Cölfen, H.; Antonietti, M. Synthesis and characterization of CdS nanoparticles stabilized by double-hydrophilic block copolymers. *Nano Letters* **2001**, *1*, 61-65.

(53) Malik, M. A.; O'Brien, P.; Revaprasadu, N. Synthesis of TOPO-capped Mn-doped ZnS and CdS quantum dots. *Journal of Materials Chemistry* **2001**, *11*, 2382-2386.

(54) Arora, S.; Manoharan, S. S. Size-dependent photoluminescent properties of uncapped CdS particles prepared by acoustic wave and microwave method. *Journal of Physics and Chemistry of Solids* **2007**, *68*, 1897-1901.

CHAPTER THREE

Synthesis of PbS nanoparticles using single and dual source precursors

3.1. Introduction

The use of ionic liquids in nanomaterial synthesis is in keeping with the principles of green chemistry.[1] These principles impart knowledge about the importance of designing chemical products and processes which are environmentally friendly and at the same time reducing negative impacts to human health.[2] Ionic liquids are associated with properties such as negligible vapor pressure, non-flammability, high ionic conductivity, good thermal and chemical stability, and tunable solubility for both organic and inorganic molecules.[3] These properties make them ideal substitutes for traditional organic solvents. The first use of ionic liquids as a solvent was reported by Dai and co-workers.[4] Green and co-workers reported the synthesis of CdSe nanocrystals passivated by an ionic liquid (trihexyl(tetradecyl)phosphonium bis(2,4,4-trimethylpentylphosphinate).[5] Cubic PbS nanoparticles have been prepared in 1-butyl-3-methylimidazolium tetrafluoroborate using an ionic liquid as the reaction medium.[6] Ionic liquids with BF_6^- as ions are known to decompose and produce toxic species such as hydrofluoric acid in the presence of water. Therefore the use of halogen free compounds such as alkyl sulfonate ions may be good alternatives.[7] Star-like PbS nanoclusters have been prepared in 1-ethyl-3-methylimidazolium ethyl sulfate.[8] Similar ionic liquids such as 1-butyl-3-methylimidazolium bis(triflylmethyl-sulfonyl) imide have been used for the synthesis of iron oxide nanorods and nanocubes.[9]

PbS is a IV- VI semiconductor that has a small direct band gap energy of 0.41 eV and large exciton Bohr radius of 18 nm.[10-13] Optical absorption and emission in the near infrared region require semiconductors with small band gap energy, making PbS a potential candidate for electronic devices.[2,14-18] Synthetic routes to this material are of great importance especially in aiding desired properties which are influenced by the shape and size of the material. These synthetic routes differ by varying reaction parameters which include type of precursors, conditions of the reactions and techniques used. Many reports exist which make use of dual precursors in synthesizing PbS nanomaterials. Hardman *et al*. prepared PbS nanoparticles using PbO and bistrimethylsilyl sulfide as their starting materials.[19] Ultrasound transient absorption measurements were used to study multiple exciton generation in solutions of the synthesized

nanoparticles in this study. $PbBr_2$ has been used with sulfur as the precursor in the fabrication of PbS quantum dots.[20] Using the bromide precursor rendered slow reaction kinetics which led to smaller quantum dots compared to another halide precursor thus giving a possible way to control quantum dot growth. PbS nanowires with ellipse and parallelogram structures have been synthesized from $Pb(NO_3)_2$ and thiourea in ethylenediamine/H_2O as a solvent.[21] Ji *et al*. used the hydrothermal route to control the morphology of PbS nanocrystals, by varying the lead and sulfur sources, PbS particles in the form of star shapes and rods were obtained.[14] Using a hot injection technique enhances the quality of nanoparticles, this method has been used for the preparation of highly luminescent PbS nanocrystals.[22] Oleic acid capped PbS nanocrystals of 1-2 nm were prepared using colloidal techniques.[23]

The use of single molecular precursors is a well reported route to nanomaterials. One of the advantages of the route is the elimination of defects as the metal is already coordinated to the chalcogenide source. Earlier research on the use of these precursors include a study by Fainer *et al.* where PbS thin films were grown by low pressure chemical vapour deposition using dithiocarbamates complexes.[24] A few years later, aerosol assisted chemical vapour dipostion was used for PbS thin film synthesis using similar precursors.[25] Trindade and co-workers reported nanodispersed PbS prepared from a thermolysis of lead dithiocarbomato complexes.[26] Different morphologies ranging from polyhedral to flower-like structures have been obtained from a solvothermal decomposition of lead diethyldithiocarbamate at 150- 180 ℃.[27] Apart from the extensively studied dithocarbamate complexes as precursors, heterocyclic lead dithiocarbamates,[13] lead dialkyldithiophosphates,[28] lead hydroxy thiocyanate[29] and lead xanthates[30,31] have been investigated for the synthesis of lead sulfide nanomaterials. It is well stipulated that variation of growth temperature, reaction time or capping agent can result in different nanoparticle morphology as reported by Lee and others, where they demonstrated shape evolution of PbS nanocrystals from star- shaped structures to truncated octahedron and cubes.[32] The concentration of the precursor also has an effect on modifying the morphology of nanomaterials. Plante *et al.* found an increasing degree of branching with the increase in the precursor concentration for lead sulfide nanocrystals.[33]

This chapter gives a description of the synthesis of PbS nanoparticles in 1-ethyl-3-methylimidazolium methanesulfonate, using single and dual source precursors. Furthermore, the effect of various parameters such as temperature, time and nature of precursors on synthesized

nanoparticles will be studied. A comparison between the two types of precursors (single and dual sources) will be carried to perceive the effect of each on the morphology and properties of the nanoparticles.

3.2. Experimental details

3.2.1. Materials

Lead acetate (≥99.9%, Sigma-Aldrich), 1-dodecanethiol (Sigma-Aldrich), 1-ethyl-3-methylimidazolium methanesulfonate (Sigma-Aldrich), sodium sulfide (60-62% Sigma Aldrich), potassium ethyl xanthate (96%, Sigma-Aldrich), acetone (Prestige laboratory) and ethanol (≥99.8%, Sigma-Aldrich) were used as received, with no further purification.

3.2.2. Synthesis of lead ethyl xanthate

Lead ethyl xanthate was synthesized by the method of Iimura *et al.*[34] In this method, lead ethyl xanthate powder was precipitated by mixing aqueous solutions of lead acetate and potassium ethyl xanthate slowly in a molar ratio of 1:2. The precipitate was filtered and dried in a vacuum desiccator.

Yield: 74 %. Elemental analysis: $C_6H_{10}PbO_2S_4$: Calculated (%): C, 16.01; H, 2.24; S, 28.16; Pb, 46.09. Found (%): C, 16.33; H, 2.44; S, 28.49; Pb, 46.18.

3.2.3. Synthesis of PbS nanoparticles

Two approaches were used for the synthesis of PbS nanoparticles from single source precursor and dual source precursors. Lead ethyl xanthate was used for the single source precursor route (method (**1**)) while lead acetate and dodecanethiol/ sodium sulfide were used as dual sources (method (**2**)) all in the presence of the ionic liquid (1-ethyl-3-methylimidazolium methanesulfonate). In both methods reaction parameters (temperature, time) were varied to observe their effect on the formation of the nanoparticles.

Method (**1**): in a three necked flask which is equipped with a reflux condenser, thermometer and a rubber septum, 5.0 mL of an ionic liquid was heated to a desired temperature (150 ℃ and 200 ℃). At the desired temperature, a suspension of the lead ethyl xanthate complex (0.130 g, 0.29 mmol) dispersed in 3.0 mL ionic liquid was injected into the hot liquid and the reaction was continued for 30 minutes. Afterward the content was removed from heating, allowed to cool to room temperature and then washed with a mixture of acetone and ethanol several times and centrifuged. The product was then dried in a desiccator and preserved for further analysis.

Method (**2**): in a three necked flask, lead acetate (0.098 g, 026 mmol) was added into 5.0 mL of the ionic liquid and the mixture was heated up to the desired temperature (200 ℃ and 250℃) followed by an injection of 1.0 mL (4.2 mmol) dodecanethiol, then the reaction was allowed to continue for 1 hour. The product was washed with a mixture of acetone and ethanol several times and water to ensure that the unreacted salts are removed. The product was then dried in a desiccator and dispersed in ethanol for further analysis. Alternatively, lead acetate (0.098 g, 026 mmol) and 5.0 mL 1-ethyl-3-methylimidazolium methanesulfonate were heated in a three necked flask. Sodium sulfide powder (0.020 g, 0.26 mmol) was dispersed in 3.0 mL of ionic liquid and injected into the hot solution of lead acetate at desired temperature (150 ℃ and 200 ℃). The reaction was allowed to continue for 30 minutes, after which the resulting dispersion was cooled to room temperature. After cooling, the solution was washed with a mixture of acetone and ethanol several times and finally with water to ensure the complete removal of unreacted salts and then centrifuged. The product was dried and dispersed in ethanol for further analysis.

3.2.4. Characterization techniques

The same instrumentation mentioned in chapter two was used in addition to the:

3.2.4.1. Raman spectroscopy

Raman spectra for few representative samples were recorded using Horiba Jobinyvon Raman spectrometer with 514.5 nm lasers, at room temperature.

3.2.4.2. Scanning electron microscopy (SEM) and Energy dispersive X-ray analysis (EDX)

The SEM and EDX measurements of the as-prepared nanoparticles were performed on a Zeiss Ultra Plus FEG (at 10 kV) and Oxford detector (at 20 kV) respectively.

3.3. Results and discussion

3.3.1. Synthesis of PbS nanoparticles from single source precursor

Lead ethyl xanthate complex has been used as a single source precursor and the ionic liquid, 1-ethyl-3-methylimidazolium methanesulfonate was used as a reaction medium in this approach (method (**1**)). Thermogravimetric analysis (Figure 3.1) of the complex (lead ethyl xanthate) showed that it decomposed in the temperature range of 110 ℃ to 150 ℃. Previous studies on the lead ethyl xanthate complexes also showed a one-step decomposition with a rapid weight loss between 129 ℃ and 156 ℃.[30,31] On the basis of the complex's decomposition temperature, thermolysis reactions were carried out at temperatures 150 ℃ and 200 ℃ to study the effect of temperature on the properties of the synthesized PbS nanoparticles. Solution hot injection route was followed, whereby an ionic liquid (1-ethyl-3-methylimidazolium methanesulfonate) preheated at desired temperatures was used as a thermolysis solvent, followed by the injection of the complex (dispersed in the same solvent).

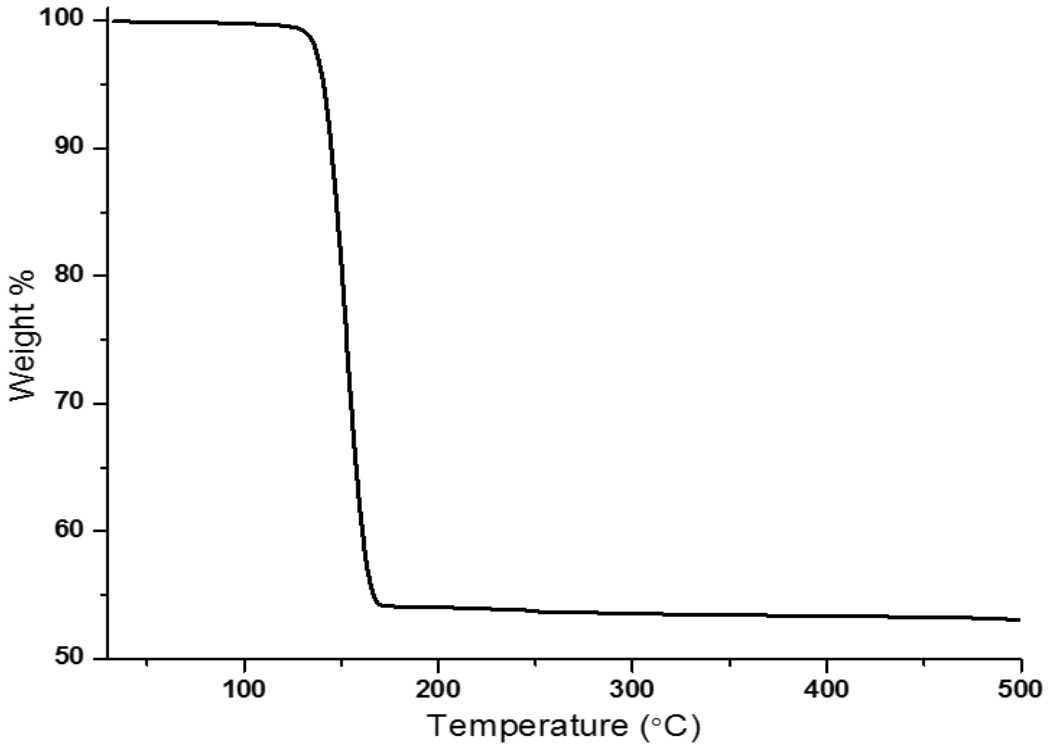

Figure 3.1: TGA plot of lead ethyl xanthate complex at a heating rate of 10 ℃/min under inert nitrogen atmosphere.

FTIR spectra of PbS nanoparticles in an ionic liquid and pure ionic liquid are shown in Figure 3.2. The FTIR analysis was done for the material prepared from dual sources (lead acetate and sodium sulfide). The bands located at 3154 cm^{-1} (IL) and 3021 cm^{-1} (IL capped PbS) are assigned to the ring antisymmetric stretching vibrations of HCCH. Bands located at 3095 cm^{-1} and 2931 cm^{-1} are proposed to be due to CH_3(N)HCH antisymmetric stretching for IL and IL capped PbS nanoparticles respectively.[35,36] Again the absorption bands found at 1574 cm^{-1} (IL) and 1422 cm^{-1} (IL capped PbS) are attributed to the C-N skeleton stretching vibrations of the imidazole ring.[37] 1460 cm^{-1} and 1345 cm^{-1} bands can be assigned to CCH HCH antisymmetric bends and CH_3(N) respectively.[35] The bands at 1179 cm^{-1}(IL) and 1133 cm^{-1} (IL capped PbS) are due to C-H of the imidazole ring in-plane deformation vibrations.[36] Similarly, the bands found at 1038 cm^{-1} and 1025 cm^{-1} can be attributed to imidazole ring symmetric stretching of CH_3(N) and CH_2(N). The overall shift in band positions may be due to the existence of hydrogen bonding and interaction between the ionic liquid and the as-prepared nanoparticles.

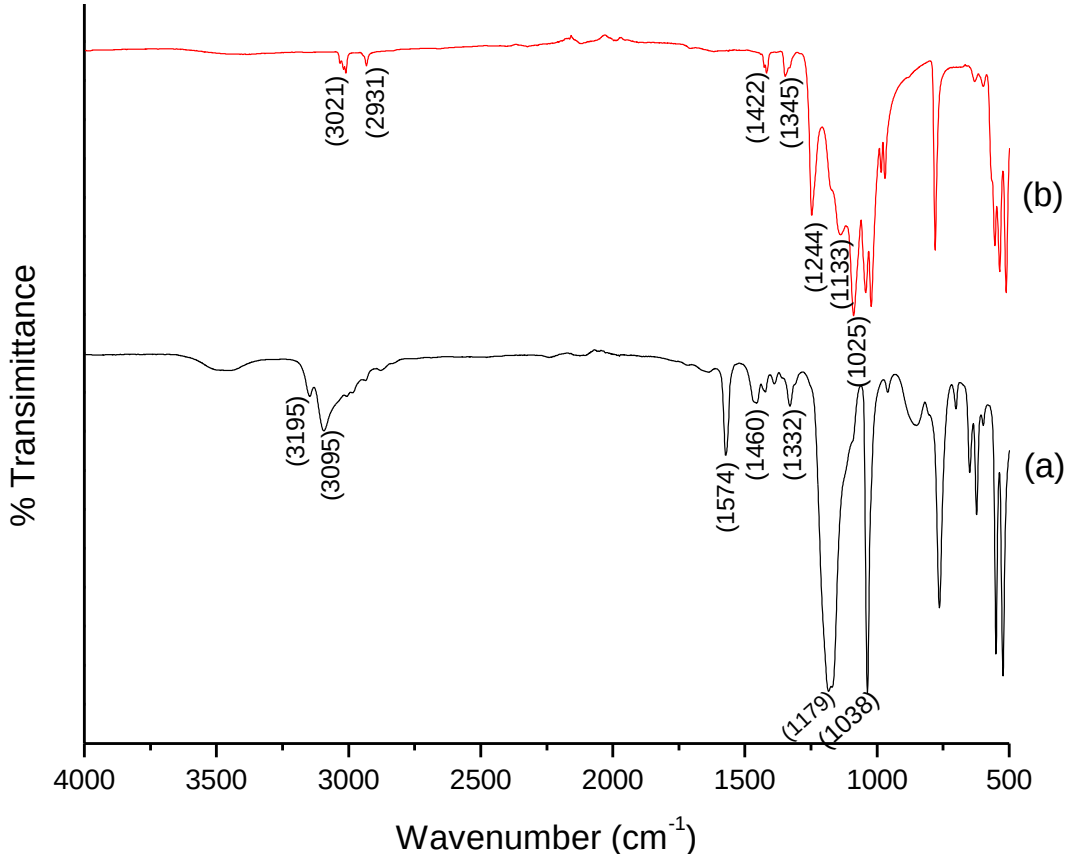

Figure 3.2: FTIR spectra of (a) pure ionic liquid and (b) ionic liquid capped PbS nanoparticles.

P-XRD patterns of the ionic liquid capped PbS nanoparticles synthesized from lead ethyl xanthate complex are shown in Figure 3.3. From both temperatures, a pure phase of PbS nanoparticles was obtained and the peaks confirm formation of the expected cubic rock salt phase of PbS. This phase has characteristic planes of (111), (200), (220), (311), (222), (400), (331), (420), (422) and (511) (Card #: 00-005-0592). The crystal growth preference is towards the (200) plane for the nanoparticles prepared at 150 ℃. The morphology is expected to differ from particles synthesized at a higher temperature (200 ℃) wherein the crystals grow dominantly on the (220 and 200) planes. O'Brien and co-workers studied the effect of temperature on the crystalline nature of the synthesized PbS using lead (II) n-butylxanthate, ($Pb(S_2COBu)_2$) complex from ambient temperature to 275 ℃, they found that low temperatures resulted to partial decomposition of the precursors.[38]

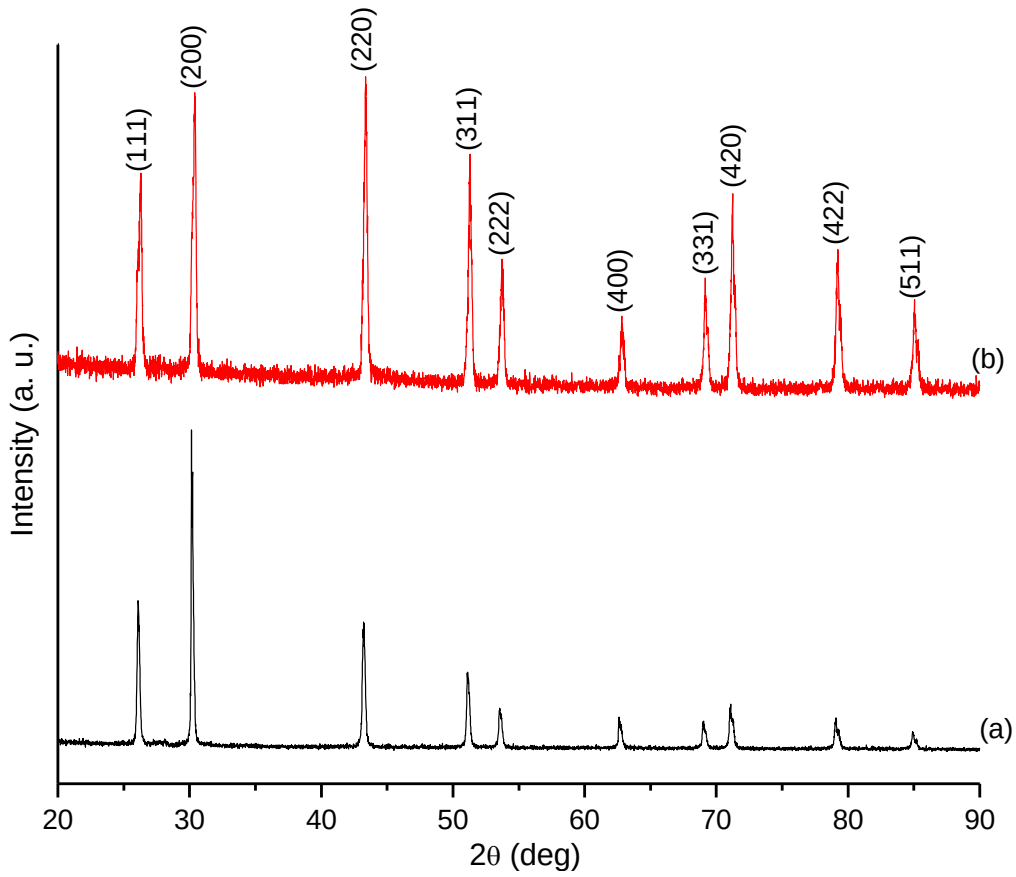

Figure 3.3: XRD patterns of PbS nanoparticles prepared from lead ethyl xanthate at (a) 150 ℃ and (b) 200 ℃.

In addition to the infrared spectroscopy, Raman spectroscopy is commonly used to afford a structural fingerprint by which molecules can be identified. The Raman spectrum of the PbS nanoparticles is shown in Figure 3.4. A prominent peak observed at 130 cm^{-1} (less than 10 cm^{-1} shift) can compared to earlier reports on PbS absorption in Raman scattering.[39,40] The blue shifted peak with a shoulder at 80 cm^{-1} can be assigned to a combination of longitudinal and transversal acoustic modes.[41] Crystallinity, surface roughness and particle sizes have a significant impact on the shift in wavenumbers hence the observed difference in peak position and intensity.[42]

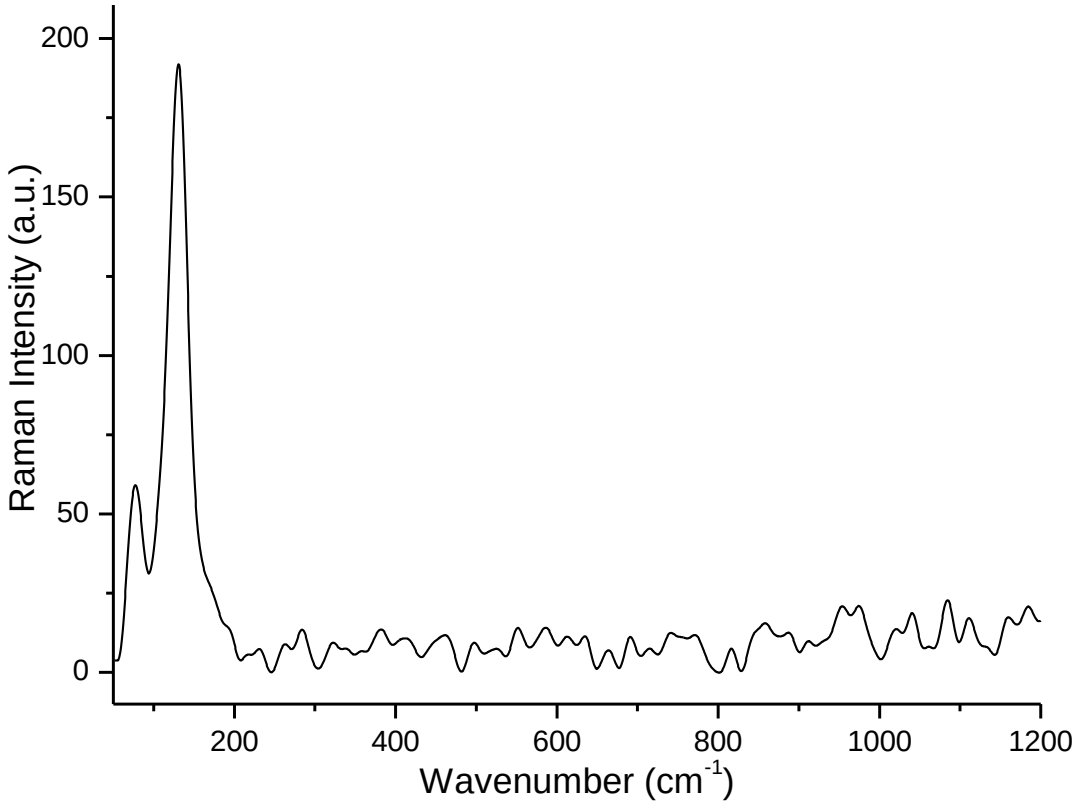

Figure 3.4: Raman Spectrum of PbS nanoparticles prepared from lead ethyl xanthate at 150 ℃.

TEM images of PbS nanoparticles synthesized by lead ethyl xanthate complex are presented in Figure 3.5. Well-defined cubic shaped particles with an average particle sizes of 102 ± 4.2 nm were observed for 150 ℃ reaction temperature (Figure 3.5(a) and (b)). At an elevated temperature of 200 ℃, the PbS nanoparticles appear agglomerated forming large irregular shaped particles with an average diameter of 160 ± 7.2 nm (Figure 3.5(c and d)). This is in agreement with the XRD results where the peaks are relatively narrow, suggesting larger sizes. Due to a fast consumption of the precursor, elevated temperatures promote the Ostwald ripening process, in which larger particles grow at the expense of smaller particles, and thereby both the average size and the size distribution of the particles are increased.

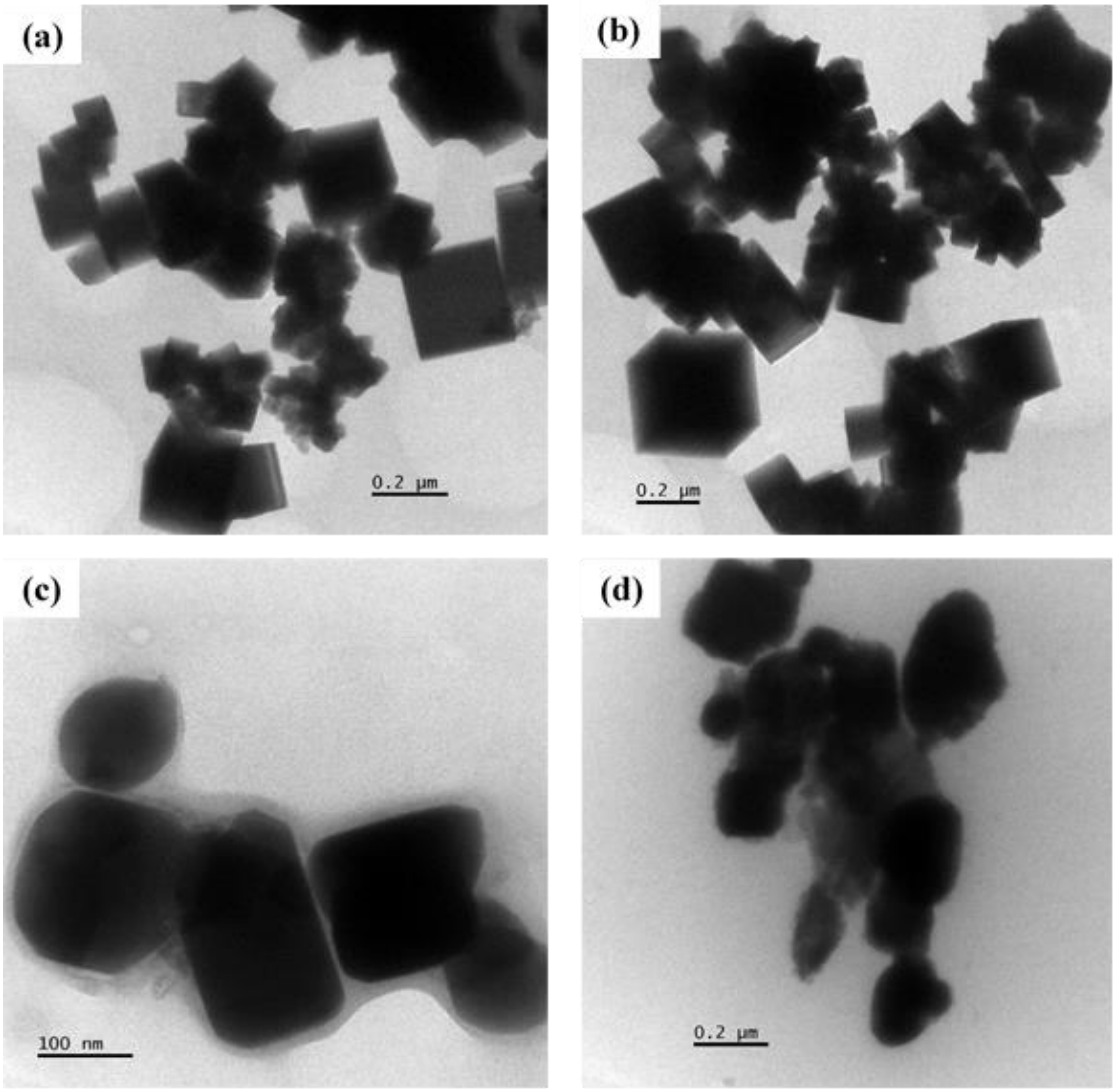

Figure 3.3: TEM images of PbS nanoparticles prepared from lead ethyl xanthate at (a), (b) 150 ℃ and (c), (d) 200 ℃.

SEM images confirm the formation of cubic shaped nanoparticles for PbS obtained at 150 ℃ (Figure 3.6(a and b)) while those obtained at 200 ℃ showed mixed cubic to spherical shaped morphology (Figure 3.6(c)). The size of these nanoparticles were estimated to be 64 ± 18.1 nm and 55 ± 29.2 nm for 150 ℃ and 200 ℃ reaction temperatures respectively. EDX composition showed a 1:1 ratio of Pb: S (Figure 3.6(d)).

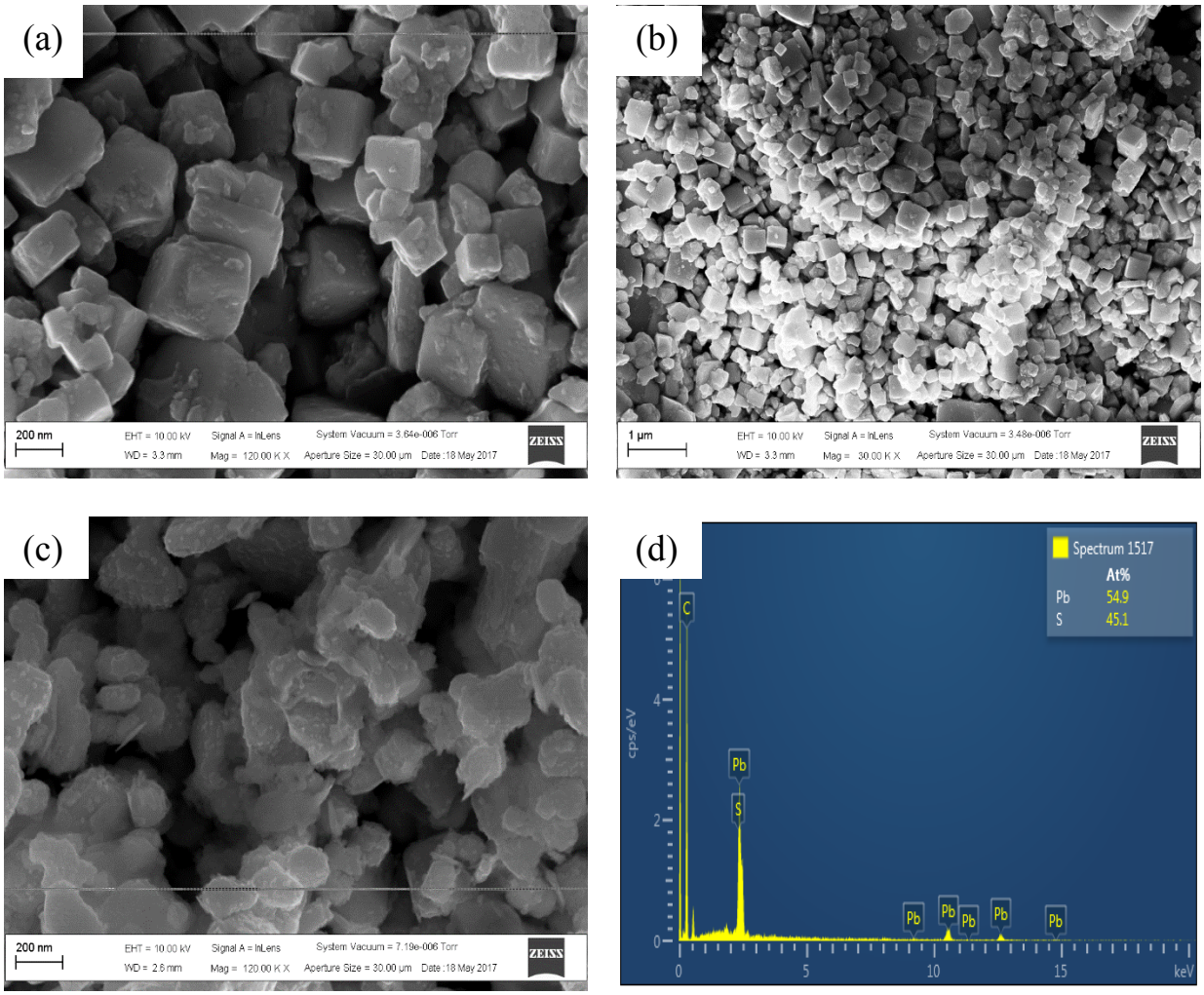

Figure 3.4: SEM images of PbS nanoparticles prepared by lead ethyl xanthate at (a), (b) 150 ℃ and (c), (d) 200 ℃.

3.3.2. Synthesis of PbS nanoparticles using dual source precursors

The use of dual source precursors was also explored in the experimental protocols. Two different sulfur sources (organic and inorganic) were used for the PbS preparation to observe the interaction and its effect on the morphological properties of the nanoparticles (method **2**). 1-dodecanethiol was used as the organic sulfur source while sodium sulfide was used as the inorganic source. Each of these two sulfur sources were used with lead acetate and 1-ethyl-3-methylimidazolium methanesulfonate as explained in the following sub-section. Lead acetate and the ionic liquid was preheated to a stable desired temperature followed by an injection of 1-dodecanethiol or sodium sulfide (dispersed in IL).

3.3.2.1. Lead acetate and sodium sulfide

The use of sodium sulfide which is an inorganic sulfur source was encouraged by its good solubility in ionic liquid, its ionic nature and high reactivity. The reaction was performed at comparatively lower temperatures of 150 and 200 °C. Figure 3.7(a) and (b) present the powder XRD patterns indicating the formation of a well-defined PbS fcc structure. The high intensity of the (200) peak shows that the nanoparticles have a preferred orientation towards the (200) plane which makes it the dominant reflection in the diffraction pattern. Pure PbS nanoparticles were obtained at both temperatures, and the XRD pattern does not show any trace of impurities. This suggests that use of sodium sulfide is more favourable and efficient as compared to thiol, seemingly because of its high reactivity. The preferential crystal growth at lower temperature of 150 °C is towards (200) plane, whereas that obtained at 200 °C prefers growth in the (220) plane.

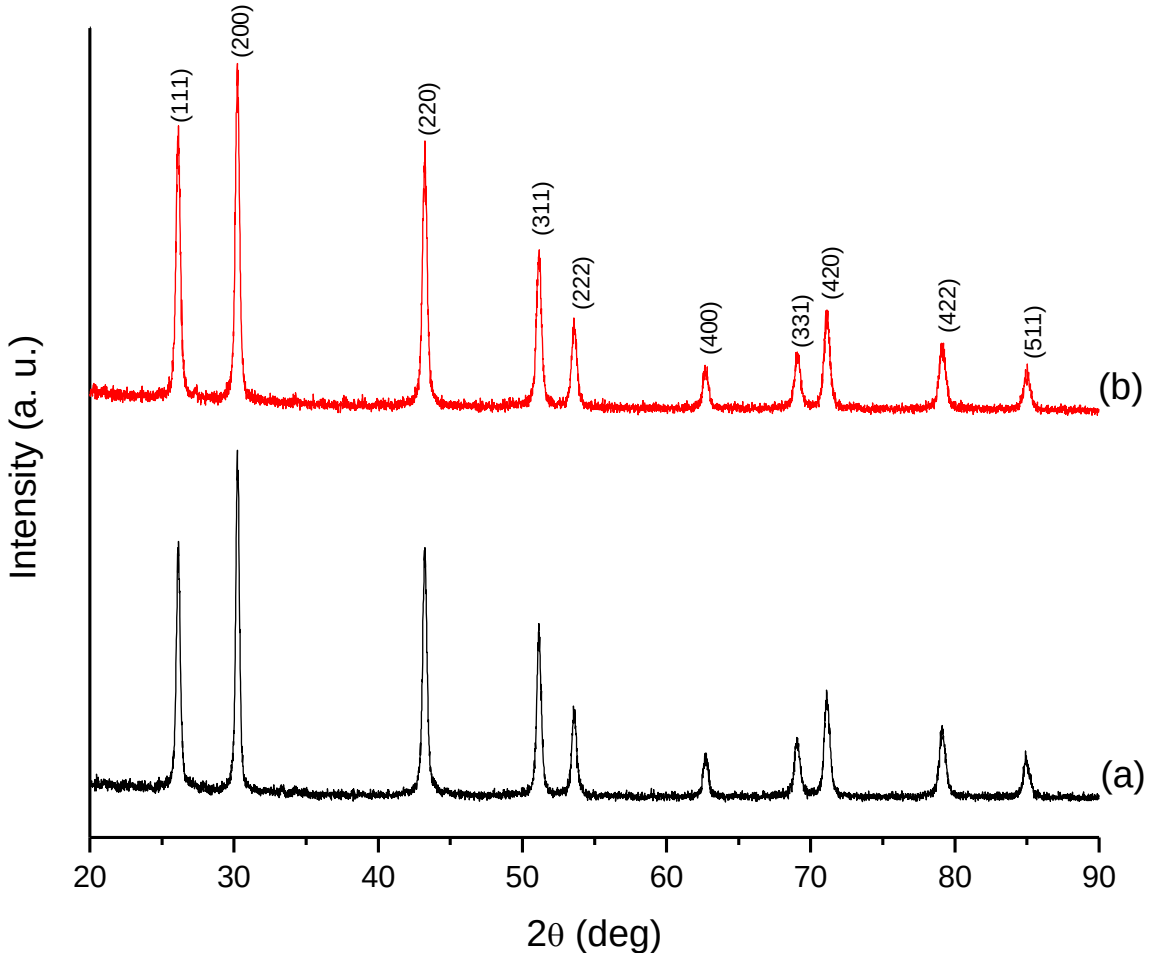

Figure 3.7: XRD patterns of PbS nanoparticles prepared from lead acetate and sodium sulfide at (a) 150 ℃ and (b) 200 ℃.

UV-visible spectra of the as prepared PbS nanoparticles are shown in Figure 3.8. A broad absorption observed from about 1000 nm shows a blue shift from the bulk material spectrum.[43] The result confirms indeed the formation of a material which is in the nano range. At an increased temperature a shift towards the higher wavelength values was realized which suggests an increase in particle size. The band gap estimation from the Tauc plot (inset in Figure 3.8) was found to be 1.26 eV, which is 0.85 eV larger than that of a bulk PbS material. Similar results have been reported by Thielsch *et al*. where a huge blue shift of band gap was observed.[44]

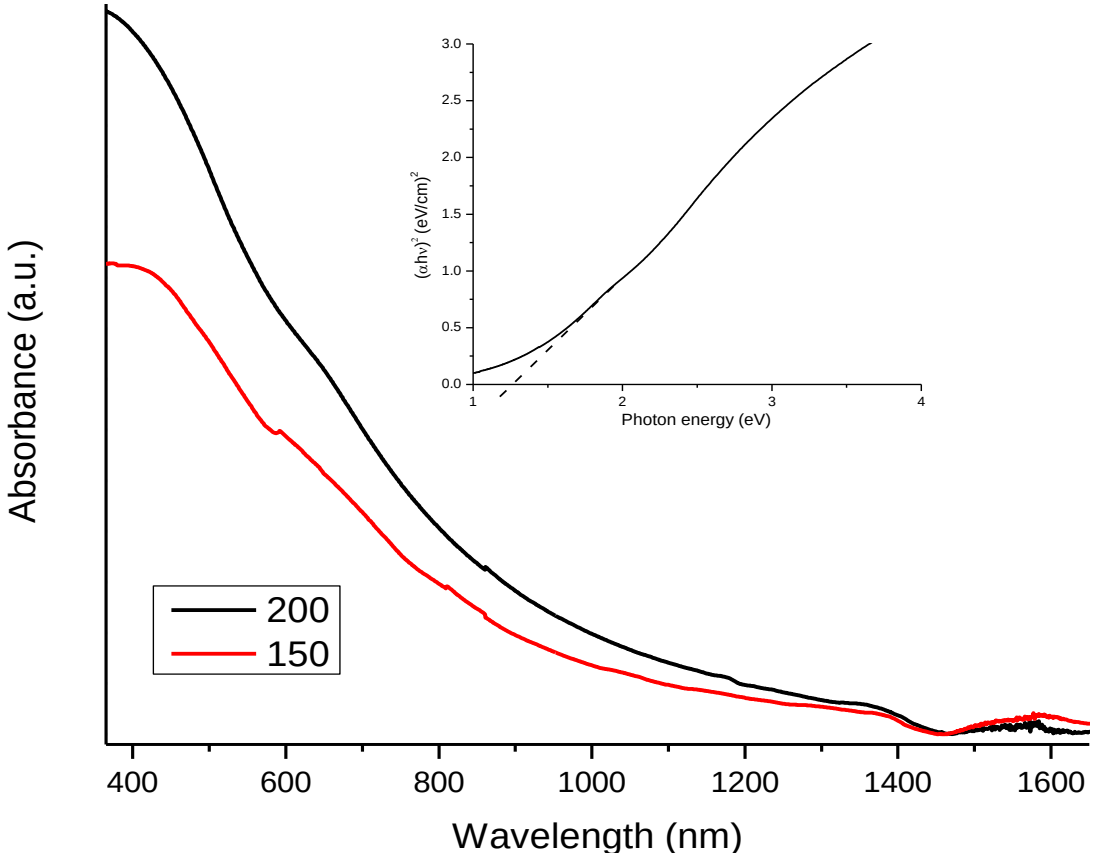

Figure 3.8: UV-vis spectra for PbS nanoparticles prepared from lead acetate and sodium sulfide at 150 ℃ and 200 ℃.

The change in morphology is evident in the TEM images. At low temperature, rectangular particles were observed, whereas at higher temperature comparatively small sized elongated particles were dominantly present (Figure 3.9). The morphology of the PbS particles obtained at both temperatures were polydisperse with broad size distribution as well, i.e. 38 ± 11.3 nm and 37 ± 6.80 nm at 150 ℃ and 200 ℃ temperatures respectively.

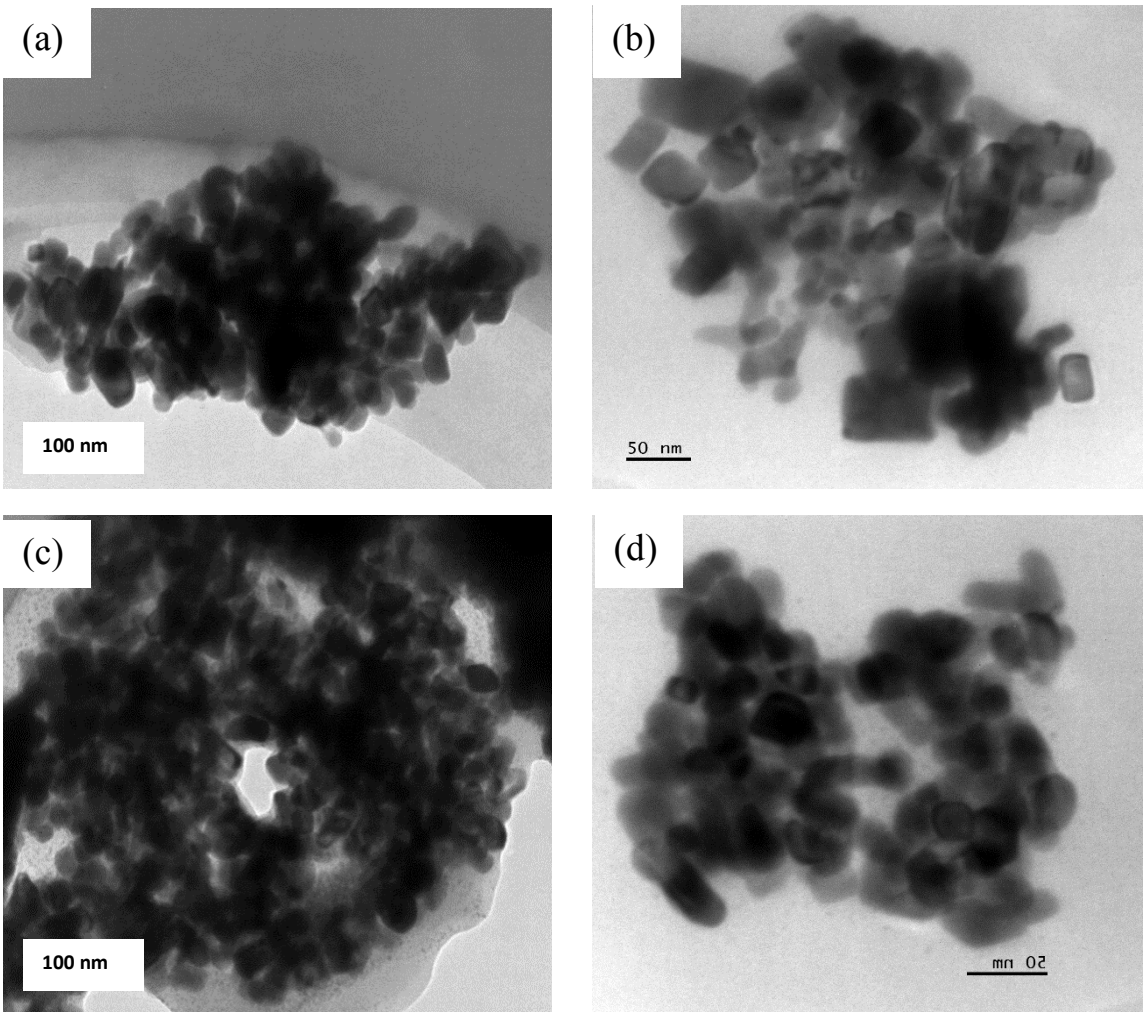

Figure 3.9: TEM images of PbS nanoparticles prepared from lead acetate and sodium sulfide at (a), (b) 150 ℃ and (c), (d) 200 ℃.

SEM images also show that the as prepared PbS nanoparticles are small in size with close to spherical spherical morphology (Figure 3.10). The mean particle sizes were estimated to be 44 ± 16 nm and 34 ± 6 nm for nanoparticles obtained from 150 ℃ and 200 ℃ respectively. EDX analysis shows that the product consists of only lead and sulfur in the ratio 1:0.8 (Pb:S) as shown in Table 3.1.

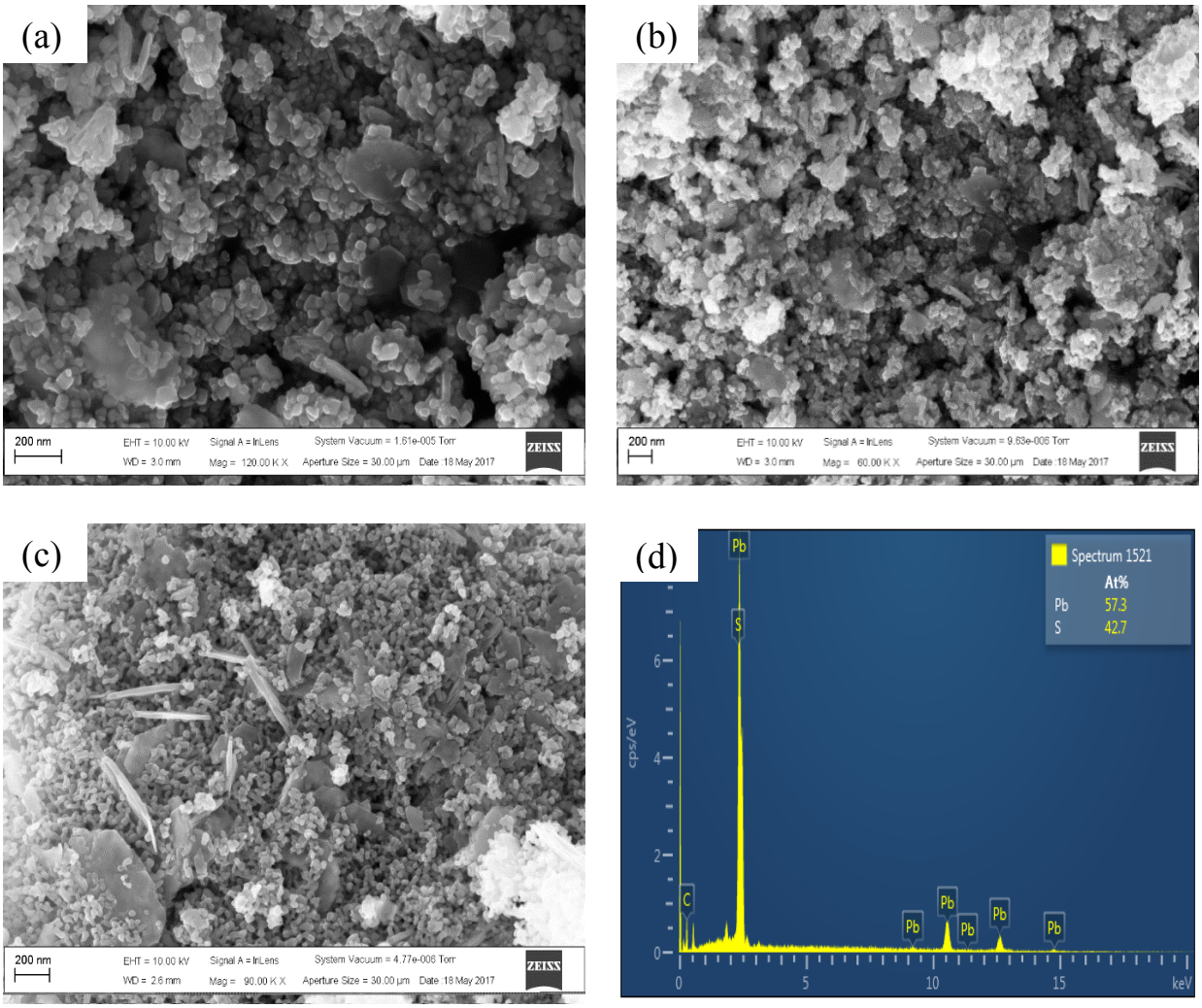

Figure 3.10: SEM images of PbS nanoparticles prepared from lead acetate and sodium sulfide at (a), (b) 150 ℃ and (c) 200 ℃, (d) a representative EDX spectrum.

3.3.2.2. Lead acetate and 1-dodecanethiol

It was observed that the reaction between lead acetate and dodecanethiol was not thermodynamically favoured at temperatures below 200 ℃. The addition of the thiol may lead to the formation of a lead thiolate complex because of the strong coordination between the mercapto group and lead ions.[45] This thiolate complex might not decompose easily to PbS, requiring an elevated reaction temperature. This is depicted in Figure 3.11(a) where the presence of extra impurity peaks along with PbS peaks indicate the partial decomposition of lead thiolate complex. Furthermore, the peaks were of low intensity which indicates an amorphous product at 200 ℃. When the reaction was performed at an elevated temperature of 250 °C (Figure 3.11(b)), complete decomposition of the lead thiolate complex was observed and pure crystalline PbS was obtained. The XRD pattern shows prominent peaks that can be indexed to exclusively cubic PbS without the presence of any impurities for the reaction carried at 250 ℃.

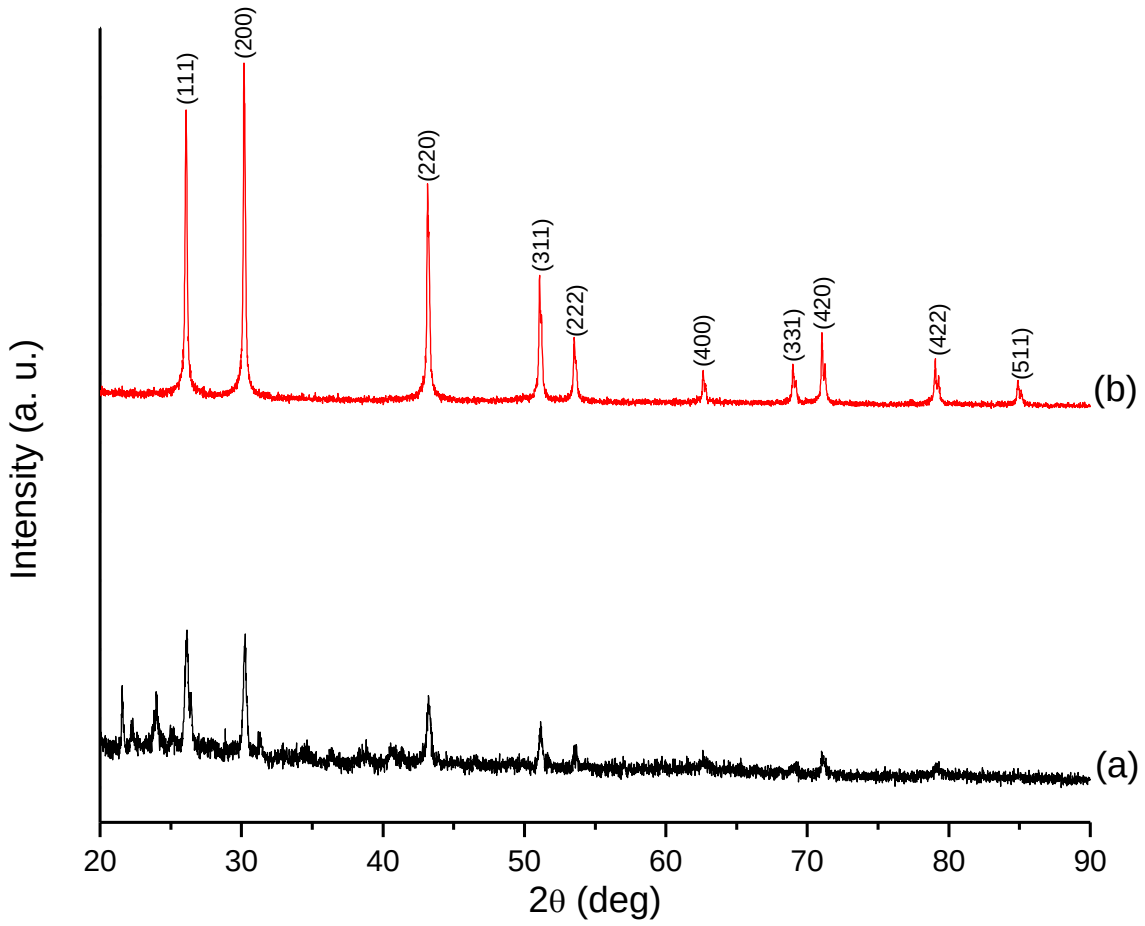

Figure 3.11: XRD pattern of PbS nanoparticles prepared from lead acetate and dodecanethiol at (a) 200 ℃ and (b) 250 ℃.

TEM image of PbS nanoparticles synthesized at lower temperature (200 ℃) (Figure 3.12(a)) using dodecanethiol shows a mixture of cubic and hexagonal shapes (most with sharp corners of hexagons) with an average size of 86 ± 27.2 nm. They are almost uniform in shape/size unlike those obtained at a higher temperature (250 ℃), where particles appear agglomerated (Figure 3.12(c)). It is clear that particle sizes increase with an increase in temperature. The selective area electron diffraction (SAED) pattern (Figure 3.12(b)) shows formation of highly crystalline PbS nanoparticles.

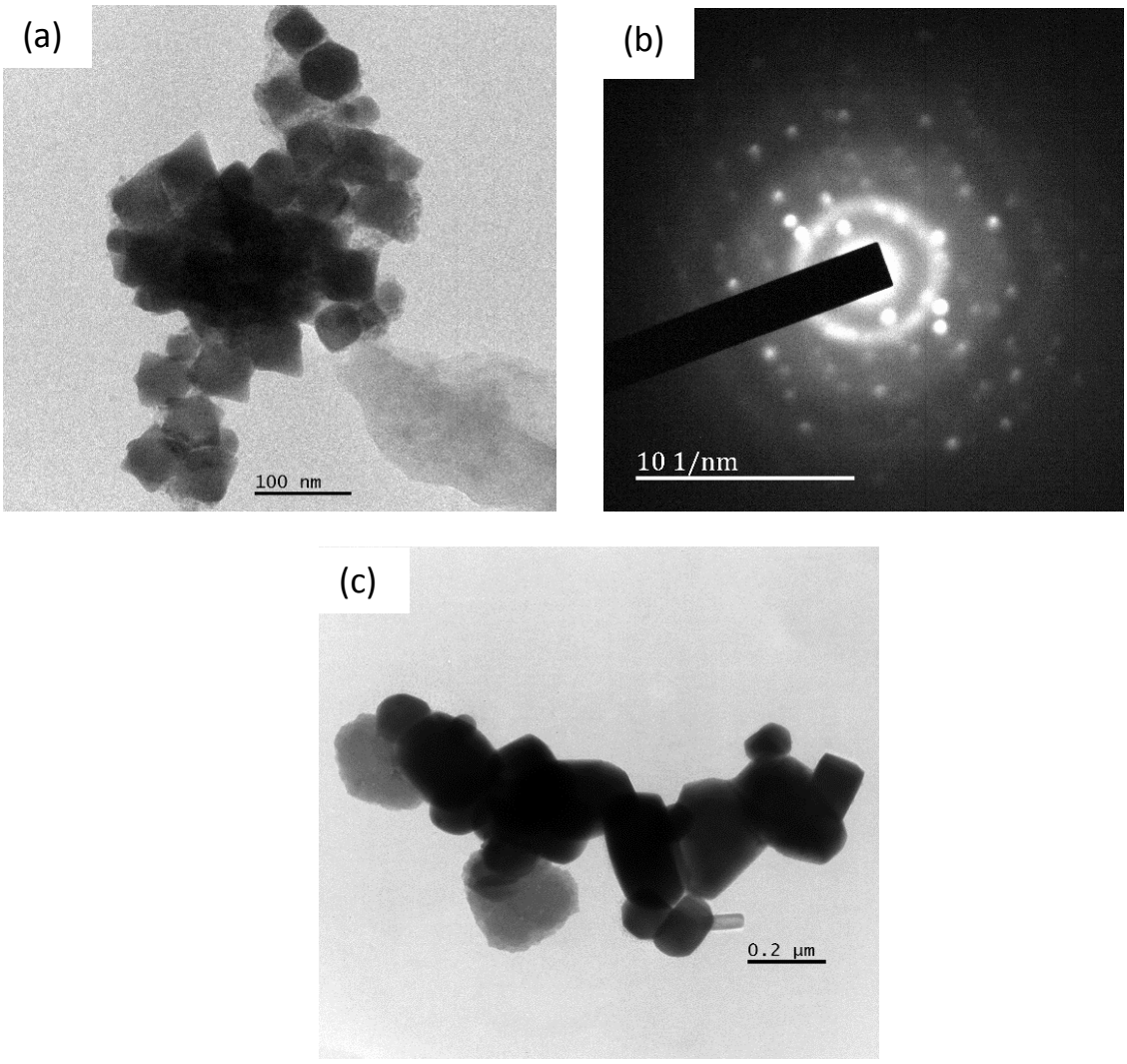

Figure 3.12: TEM images of PbS nanoparticles prepared from lead acetate and 1-dodecanethiol at (a) 200 ℃ and (b) its corresponding SAED and respectively and those prepared at (c) 250 ℃.

Representative SEM images of the PbS nanoparticles are shown in Figure 3.13. The morphology of the PbS nanoparticles changed vividly when the temperature was increased to 250 ℃. At the lower temperature irregular shapes were observed, while cubic like structures (with some holes inside) have been observed at high temperature. The holes can be attributed to the incomplete growth of the agglomerating nanoparticles from low temperature. The nanoparticle sizes changed from 41 ± 10.9 nm to 110 ± 22.1 nm for 200 ℃ and 250 ℃ respectively. Figure 3.14 shows the absorbance spectra of the nanoparticles synthesized from dual source precursors at 200 ℃ and 250 ℃ with 1-dodecanethiol as a sulfur source. Similar absorption bands were obtained from earlier method (where sodium sulfide was used as a source of sulfur). The broad absorption

starting 1200 nm corresponding to 1.03 eV shows a blue shift from that of the bulk PbS crystals.[46] The average nanoparticle sizes are smaller than the excitonic Bohr radius of the bulk PbS which indicates existence of quantum confinements.[47] The elemental composition of the samples was done through EDX analysis and the results are summarisesd in Table 3.1.It was observed that there was deficiency of sulfur in the obtained samples.

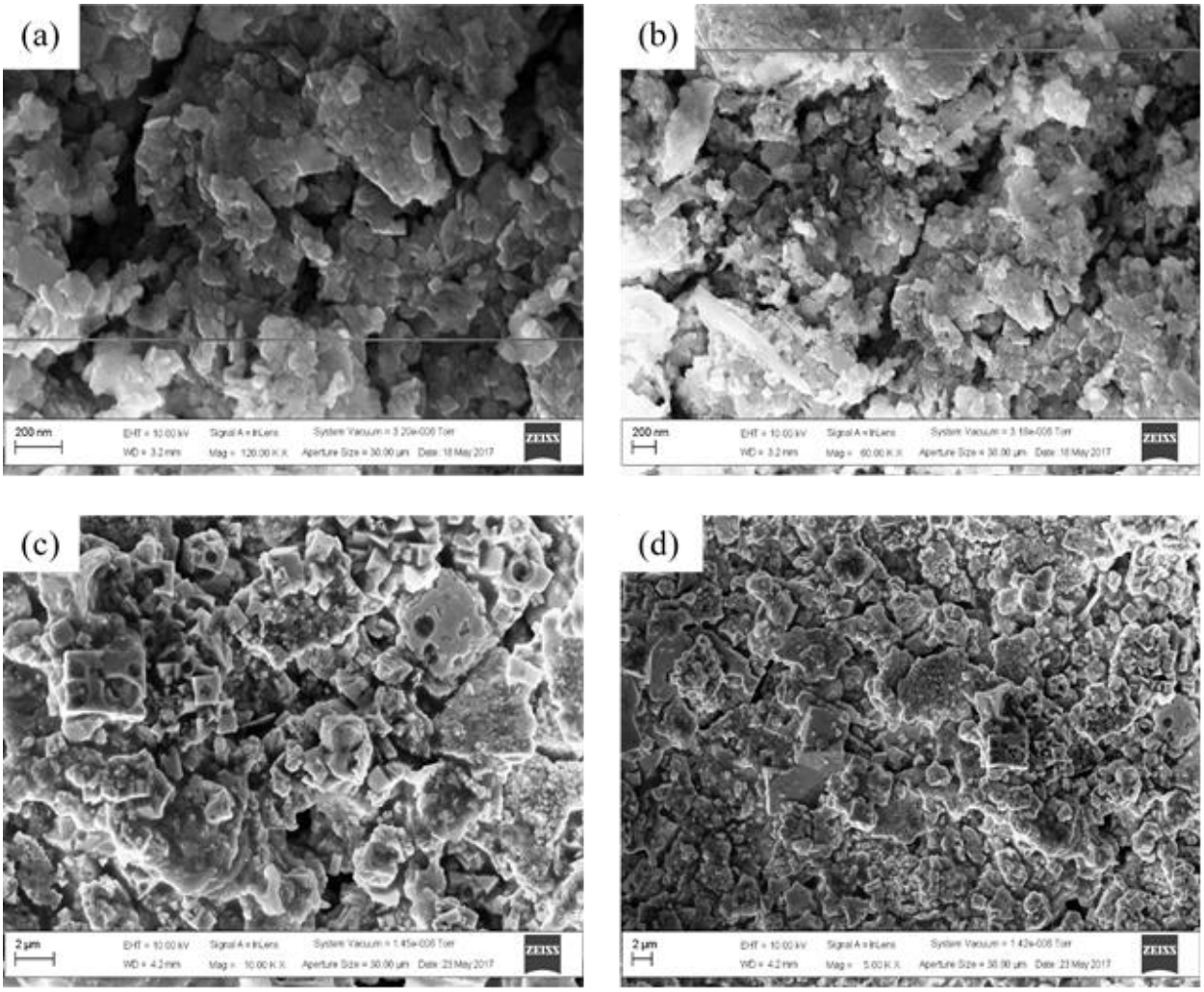

Figure 3.13: SEM images of PbS nanoparticles prepared from lead acetate and 1-dodecanethiol at (a), (b) 200 ℃ and (c), (d) 250 ℃.

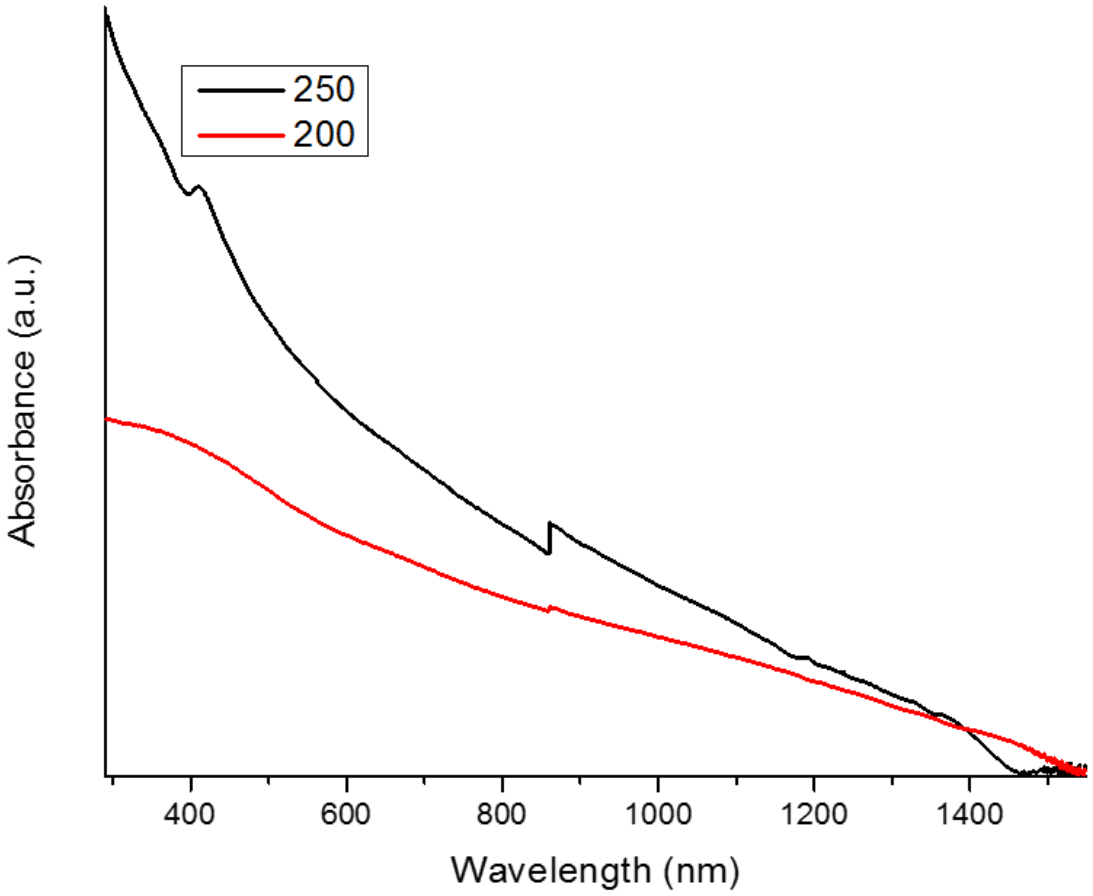

Figure 3.14: UV-vis spectra of PbS nanoparticles prepared from lead acetate and dodecanethiol at 200 ℃ and 250 ℃.

Table 3.1: Elemental composition of as synthesized PbS by EDX spectroscopy.

Precursors and temperature	**Pb**	**S**	**Pb:S**
Xan 150	54.9	45.1	1:0.8
Xan 200	51.7	48.1	1:0.9
Na_2S 150	56.1	43.9	1:0.8
Na_2S 200	57.3	42.7	1:0.8
DT 200	68.5	31.5	1:0.5
DT 250	52.0	48.0	1:0.9

3.4. Conclusion

PbS nanoparticles capped with ionic liquid (1-ethyl-3-methylimidazolium methanesulfonate) were successfully prepared using lead ethyl xanthate complex as a single source precursor and an organic (1-dodecanethiol) and inorganic (sodium sulfide) sulfur sources and lead acetate as dual source precursors. Different reaction parameters were established and used for this study to investigate their effect on the morphology and structural properties of the as-synthesized PbS nanoparticles. An increase in the reaction temperature resulted in the formation of larger particle sizes. The use of single source precursor produced well defined shaped PbS nanoparticles than dual sources route. For dual source precursors, thiol requires relatively high temperatures for a pure product to be obtained, whereas sodium sulfide reacts readily even at low temperatures. The present study further confirmed the effectiveness of an ionic liquid (1-ethyl-3-methylimidazolium methanesulfonate) as a green coordinating solvent for high quality nanoparticles synthesis.

3.5. References

(1) Nagaraju, G.; Ravishankar, T.; Manjunatha, K.; Sarkar, S.; Nagabhushana, H.; Goncalves, R.; Dupont, J. Ionothermal synthesis of TiO_2 nanoparticles: Photocatalytic hydrogen generation. *Materials Letters* **2013**, *109*, 27-30.

(2) Akhtar, J.; Malik, M. A.; O'Brien, P.; Wijayantha, K.; Dharmadasa, R.; Hardman, S. J.; Graham, D. M.; Spencer, B. F.; Stubbs, S. K.; Flavell, W. R. A greener route to photoelectrochemically active PbS nanoparticles. *Journal of Materials Chemistry* **2010**, *20*, 2336-2344.

(3) He, Z.; Alexandridis, P. Nanoparticles in ionic liquids: Interactions and organization. *Physical Chemistry Chemical Physics* **2015**, *17*, 18238-18261.

(4) Dai, S.; Ju, Y.; Gao, H.; Lin, J.; Pennycook, S.; Barnes, C. Preparation of silica aerogel using ionic liquids as solvents. *Chemical Communications* **2000**, 243-244.

(5) Green, M.; Rahman, P.; Smyth-Boyle, D. Ionic liquid passivated CdSe nanocrystals. *Chemical Communications* **2007**, 574-576.

(6) Biswas, K.; Rao, C. N. R. Use of ionic liquids in the synthesis of nanocrystals and nanorods of semiconducting metal chalcogenides. *Chemistry–A European Journal* **2007**, *13*, 6123-6129.

(7) Wasserscheid, P.; van Hal, R.; Bösmann, A. 1-n-butyl-3-methylimidazolium ([bmim]) octylsulfate- An even 'greener'ionic liquid. *Green Chemistry* **2002**, *4*, 400-404.

(8) Behboudnia, M.; Habibi-Yangjeh, A.; Jafari-Tarzanag, Y.; Khodayari, A. Facile and room temperature preparation and characterization of PbS nanoparticles in aqueous [EMIM][$EtSO_4$] ionic liquid using ultrasonic irradiation. *Bulletin of the Korean Chemical Society* **2009**, *30*, 53-56.

(9) Wang, Y.; Yang, H. Synthesis of iron oxide nanorods and nanocubes in an imidazolium ionic liquid. *Chemical Engineering Journal* **2009**, *147*, 71-78.

(10) Wang, N.; Cao, X.; Guo, L.; Yang, S.; Wu, Z. Facile synthesis of PbS truncated octahedron crystals with high symmetry and their large-scale assembly into regular patterns by a simple solution route. *American Chemical Society Nano* **2008**, *2*, 184-190.

(11) Yücel, E.; Yücel, Y.; Beleli, B. Optimization of synthesis conditions of PbS thin films grown by chemical bath deposition using response surface methodology. *Journal of Alloys and Compounds* **2015**, *642*, 63-69.

(12) Sathyamoorthy, R.; Kungumadevi, L. Facile synthesis of PbS nanorods induced by concentration difference. *Advanced Powder Technology* **2015**, *26*, 355-361.

(13) Nyamen, L. D.; Pullabhotla, V. S. R.; Nejo, A. A.; Ndifon, P. T.; Warner, J. H.; Revaprasadu, N. Synthesis of anisotropic PbS nanoparticles using heterocyclic dithiocarbamate complexes. *Dalton Transactions* **2012**, *41*, 8297-8302.

(14) Ji, Y.; Yang, D. R.; Zhang, H.; Ma, X. Y.; Xu, J.; Que, D. L. Morphology control of PbS nanocrystals by a novel hydrothermal process. *Trans Tech Publications*, **2004**, *99*, 197-202.

(15) Cao, Y.; Hu, P.; Jia, D. Solvothermal synthesis, growth mechanism, and photoluminescence property of sub-micrometer PbS anisotropic structures. *Nanoscale Research Letters* **2012**, *7*, 1-8.

(16) Tavakoli, M. M. Surface engineering of PbS colloidal quantum dots using atomic passivation for photovoltaic applications. *Procedia Engineering* **2016**, *139*, 117-122.

(17) Diacon, A.; Rusen, E.; Mocanu, A.; Nistor, L. C. Polymer photonic crystal band-gap modulation using PbS quantum dots. *Journal of Materials Chemistry C* **2013**, *1*, 4350-4357.

(18) Das, A.; Wai, C. M. Ultrasound-assisted synthesis of PbS quantum dots stabilized by 1,2-benzenedimethanethiol and attachment to single-walled carbon nanotubes. *Ultrasonics Sonochemistry* **2014**, *21*, 892-900.

(19) Hardman, S. J.; Graham, D. M.; Stubbs, S. K.; Spencer, B. F.; Seddon, E. A.; Fung, H.-T.; Gardonio, S.; Sirotti, F.; Silly, M. G.; Akhtar, J. Electronic and surface properties of PbS nanoparticles exhibiting efficient multiple exciton generation. *Physical Chemistry Chemical Physics* **2011**, *13*, 20275-20283.

(20) Yuan, L.; Patterson, R.; Cao, W.; Zhang, Z.; Zhang, Z.; Stride, J. A.; Reece, P.; Conibeer, G.; Huang, S. Air-stable PbS quantum dots synthesized with slow reaction kinetics via a $PbBr_2$ precursor. *Royal Society of Chemistry Advances* **2015**, *5*, 68579-68586.

(21) Yu, D.; Wang, D.; Meng, Z.; Lu, J.; Qian, Y. Synthesis of closed PbS nanowires with regular geometric morphologies. *Journal of Materials Chemistry* **2002**, *12*, 403-405.

(22) Hines, M. A.; Scholes, G. D. Colloidal PbS nanocrystals with size-tunable near-infrared emission: Observation of post-synthesis self-narrowing of the particle size distribution. *Advanced Materials* **2003**, *15*, 1844-1849.

(23) Warner, J. H.; Thomsen, E.; Watt, A. R.; Heckenberg, N. R.; Rubinsztein-Dunlop, H. Time-resolved photoluminescence spectroscopy of ligand-capped PbS nanocrystals. *Nanotechnology* **2004**, *16*, 175-179.

(24) Fainer, N.; Kosinova, M.; Rumyantsev, Y. M.; Salman, E.; Kuznetsov, F. Growth of PbS and CdS thin films by low-pressure chemical vapour deposition using dithiocarbamates. *Thin Solid Films* **1996**, *280*, 16-19.

(25) Afzaal, M.; Ellwood, K.; Pickett, N. L.; O'Brien, P.; Raftery, J.; Waters, J. Growth of lead chalcogenide thin films using single-source precursors. *Journal of Materials Chemistry* **2004**, *14*, 1310-1315.

(26) Trindade, T.; O'Brien, P.; Zhang, X.-m.; Motevalli, M. Synthesis of PbS nanocrystallites using a novel single moleculeprecursors approach: X-ray single-crystal structure of Pb $(S_2CNEtPri)_2$. *Journal of Materials Chemistry* **1997**, *7*, 1011-1016.

(27) Zhang, Y. C.; Qiao, T.; Hu, X. Y.; Wang, G. Y.; Wu, X. Shape-controlled synthesis of PbS microcrystallites by mild solvothermal decomposition of a single-source molecular precursor. *Journal of Crystal Growth* **2005**, *277*, 518-523.

(28) Duan, T.; Lou, W.; Wang, X.; Xue, Q. Size-controlled synthesis of orderly organized cube-shaped lead sulfide nanocrystals via a solvothermal single-source precursor method. *Colloids and Surfaces A: Physicochemical and Engineering Aspects* **2007**, *310*, 86-93.

(29) Duan, X.; Ma, J.; Shen, Y.; Zheng, W. A novel PbS hierarchical superstructure guided by the balance between thermodynamic and kinetic control via a single-source precursor route. *Inorganic Chemistry* **2012**, *51*, 914-919.

(30) Clark, J. M.; Kociok-Köhn, G.; Harnett, N.; Hill, M.; Hill, R.; Molloy, K. C.; Saponia, H.; Stanton, D.; Sudlow, A. Formation of PbS materials from lead xanthate precursors. *Dalton Transactions* **2011**, *40*, 6893-6900.

(31) McNaughter, P. D.; Saah, S. A.; Akhtar, M.; Abdulwahab, K.; Malik, M. A.; Raftery, J.; Awudza, J. A.; O'Brien, P. The effect of alkyl chain length on the structure of lead (II) xanthates and their decomposition to PbS in melt reactions. *Dalton Transactions* **2016**, *45*, 16345-16353.

(32) Lee, S.-M.; Jun, Y.-w.; Cho, S.-N.; Cheon, J. Single-crystalline star-shaped nanocrystals and their evolution: Programming the geometry of nano-building blocks. *Journal of the American Chemical Society* **2002**, *124*, 11244-11245.

(33) Jen-La Plante, I.; Zeid, T. W.; Yang, P.; Mokari, T. Synthesis of metal sulfide nanomaterials via thermal decomposition of single-source precursors. *Journal of Materials Chemistry* **2010**, *20*, 6612-6617.

(34) Iimura, Y.; Ito, T.; Hagihara, H. The crystal structure of cadmium ethylxanthate. *Acta Crystallographica Section B: Structural Crystallography and Crystal Chemistry* **1972**, *28*, 2271-2279.

(35) Kiefer, J.; Fries, J.; Leipertz, A. Experimental vibrational study of imidazolium-based ionic liquids: Raman and infrared spectra of 1-ethyl-3-methylimidazolium bis (trifluoromethylsulfonyl) imide and 1-ethyl-3-methylimidazolium ethylsulfate. *Applied Spectroscopy* **2007**, *61*, 1306-1311.

(36) Zhu, J.; Shen, Y.; Xie, A.; Qiu, L.; Zhang, Q.; Zhang, S. Photoinduced synthesis of anisotropic gold nanoparticles in room-temperature ionic liquid. *The Journal of Physical Chemistry C* **2007**, *111*, 7629-7633.

(37) Wang, L.; Chang, L.; Zhao, B.; Yuan, Z.; Shao, G.; Zheng, W. Systematic investigation on morphologies, forming mechanism, photocatalytic and photoluminescent properties of ZnO nanostructures constructed in ionic liquids. *Inorganic Chemistry* **2008**, *47*, 1443-1452.

(38) Lewis, E. A.; McNaughter, P. D.; Yin, Z.; Chen, Y.; Brent, J. R.; Saah, S. A.; Raftery, J.; Awudza, J. A.; Malik, M. A.; O'Brien, P. In situ synthesis of PbS nanocrystals in polymer thin films from lead (II) xanthate and dithiocarbamate complexes: Evidence for size and morphology control. *Chemistry of Materials* **2015**, *27*, 2127-2136.

(39) Nanda, K.; Sahu, S.; Soni, R.; Tripathy, S. Raman spectroscopy of PbS nanocrystalline semiconductors. *Physical Review B* **1998**, *58*, 15405-15407.

(40) Krauss, T. D.; Wise, F. W.; Tanner, D. B. Observation of coupled vibrational modes of a semiconductor nanocrystal. *Physical Review Letters* **1996**, *76*, 1376-1379.

(41) Pérez, R. G.; Tellez, G. H.; Rosas, U. P.; Torres, A. M.; Tecorralco, J. H.; Lima, L. C.; Moreno, O. P. Growth of PbS nanocrystals thin films by chemical bath. *Journal of Materials Science and Engineering: A* **2013**, *3*, 1-13.

(42) Batonneau, Y.; Brémard, C.; Laureyns, J.; Merlin, J. Microscopic and imaging Raman scattering study of PbS and its photo-oxidation products. *Journal of Raman Spectroscopy* **2000**, *31*, 1113-1119.

(43) Zhao, Y.; Liao, X.-H.; Hong, J.-M.; Zhu, J.-J. Synthesis of lead sulfide nanocrystals via microwave and sonochemical methods. *Materials Chemistry and Physics* **2004**, *87*, 149-153.

(44) Thielsch, R.; Böhme, T.; Reiche, R.; Schläfer, D.; Bauer, H.-D.; Böttcher, H. Quantum-size effects of PbS nanocrystallites in evaporated composite films. *Nanostructured Materials* **1998**, *10*, 131-149.

(45) Lü, C.; Guan, C.; Liu, Y.; Cheng, Y.; Yang, B. PbS/polymer nanocomposite optical materials with high refractive index. *Chemistry of Materials* **2005**, *17*, 2448-2454.

(46) Kane, R. S.; Cohen, R. E.; Silbey, R. Theoretical study of the electronic structure of PbS nanoclusters. *The Journal of Physical Chemistry* **1996**, *100*, 7928-7932.

(47) Wang, W.; Liu, Y.; Zhan, Y.; Zheng, C.; Wang, G. A novel and simple one-step solid-state reaction for the synthesis of PbS nanoparticles in the presence of a suitable surfactant. *Materials Research Bulletin* **2001**, *36*, 1977-1984.

CHAPTER FOUR

Room temperature and microwave synthesis of CdS and PbS nanoparticles

4.1. Introduction

The drawback of using many synthetic approaches for nanomaterials synthesis is the requirement of high reaction temperatures and the use of toxic precursors for longer times. The use of microwave heating seems to be a possible solution to some of these issues. Microwave heating has advantages which include being able to carry reactions in simple and fast manner while obtaining pure products.[1-3] The success of using microwave (MW) irradiation was first reported for organic reactions, however its slow expansion has spread to inorganic reactions.[4-6]

Different metal chalcogenides have been synthesized using the MW irradiation technique. The list includes a study by Wang *et al.* where they reported mercury sulfide nanocrystals preparation from mercury acetate, thiourea and sulfur powder.[7,8] Chen *et al.* have demonstrated MW synthesis as a straightforward route to the preparation of nanocrystalline metal sulfides using multiple source precursors.[9] CdS nanoribbons have been prepared by a MW irradiation of cadmium chloride and ethylenediamine solution under ambient air.[10] The size distribution of CdS nanocrystallites have been controlled by the microwave assisted reaction of cadmium acetate and thiourea in the presence of N,N-dimethylformamide.[11] MW irradiation has been identified as the novel synthetic route because it has produced nanomaterials which are pure and very small in size with interesting morphologies and improved properties.[12-14] The efficiency of the technique makes it easy to work with, its other advantages include better selectivity, reproducibility, larger reaction yields, increased rates and convenience of non-injection reactions.[15,16]

A good choice of solvent has an added advantage on the synthesis of nanomaterials, it is for this reason that the ionic liquid has been chosen as a reaction medium in this work. Room temperature ionic liquids act as excellent medium for absorption of microwave irradiation because of the presence of a large positively charged organic component and their high polarizability.[17]

4.2. Experimental details

4.2.1. Materials

The materials used in this section are the same as those mentioned in earlier chapters; chapter two and three.

4.2.2. Procedures

The complexes were prepared according to the method adopted from literature, which is explained in detail in Chapter 3, subsection 3.2.2.[18] Nanoparticles were prepared in a one pot setting via two routes namely; room temperature and microwave assisted reactions. The procedures are explained in the following sub-sections.

4.2.2.1. Synthesis of nanoparticles via room temperature protocol

PbS nanoparticles

In a one necked flask, 0.096 g (0.25 mmol) of lead acetate, 0.026 g (0.33 mmol) sodium sulfide and 5.0 mL of 1-ethyl-3-methylimidazolium methanesulfonate were added and the flask was placed on the magnetic stirrer, the contents were then stirred for 5 hours. A second path was the use of single source precursor i.e. lead ethyl xanthate where 0.130 g of the complex was dispersed in 5.0 mL 1-ethyl-3-methylimidazolium methanesulfonate and stirred at room temperature for 24 hours. The resultant solutions were then washed with ethanol, centrifuged and dried for analysis.

4.2.2.2. Synthesis via microwave irradiation

CdS nanoparticles

The microwave assisted reactions were done in an Anton Par microwave 50 at 150 ℃ for 1 minute hold time. In a reaction tube, 0.113 g (0.32 mmol) cadmium ethyl xanthate and 5.0 mL 1-ethyl-3-methylimidazolium methanesulfonate were heated via a microwave irradiation for 1 minute. In another reaction vessel, 0.100 g (0.38 mmol) cadmium acetate, 1.0 mL of 1-dodecanethiol and 3.0 mL 1-ethyl-3-methylimidazolium methanesulfonate were prepared. A third reaction was composed of 0.118 g (0.44 mmol) cadmium acetate, 0.036 g (0.46 mmol) sodium sulfide and 5.0 mL of 1-ethyl-3-methylimidazolium methanesulfonate which were heated with the same parameters as the other reactions. The products were washed several times with ethanol and dried for further analysis.

PbS nanoparticles

The same reaction settings and parameters mentioned above (for CdS preparation) were used for the synthesis of PbS nanoparticles in a microwave 50 device. Three different precursor types have been used with the first one being a dual source precursor method where 0.097 g (0.26 mmol) lead acetate, 0.026 g (0.33 mmol) sodium sulfide and 2.0 mL 1-ethyl-3-methylimidazolium methanesulfonate were employed for the synthesis. Secondly 0.099 g (0.26 mmol) lead acetate, 1.0 mL dodecanethiol and 2.0 mL 1-ethyl-3-methylimidazolium methanesulfonate were used and lastly a single source precursor was used which constituted of 0.115 g (0.26 mmol) lead ethyl xanthate which was dispersed in 5.0 mL 1-ethyl-3-methylimidazolium methanesulfonate for the formation of PbS nanoparticles.

4.3. Results and discussions

4.3.1. Room temperature synthesis of PbS nanoparticles

Under a room temperature condition (20 ± 1℃), two different types of precursors have been used *i.e*. single source precursor (lead ethyl xanthate) and dual source precursors (lead acetate and sodium sulfide) with the ionic liquid (1-ethyl-3-methylimidazolium methanesulfonate) as a capping and dispersing agent. Lead ethyl xanthate was used as the former and lead acetate and sodium sulfide have been used as the latter. In this synthesis protocol no heat was applied when carrying out the reactions. Figure 4.1 shows powder XRD patterns of PbS nanoparticles prepared from these two different precursors. The patterns obtained from dual source precursors (Figure 4.1(a)) show traces of impurities which are due to the unreacted precursors i.e. sodium sulfide which was in excess, however a cubic crystal phase can still be spotted from the patterns as the major peaks of such a phase prevail and are prominent. On the other hand, patterns attained from the single source precursor (Figure 4.1(b)) show a production of a much purer phase, all peaks could be indexed to the cubic crystal structure with (111), (200), (220), (311), (222), (400), (331), (420), (422) and (511) indices.[19]

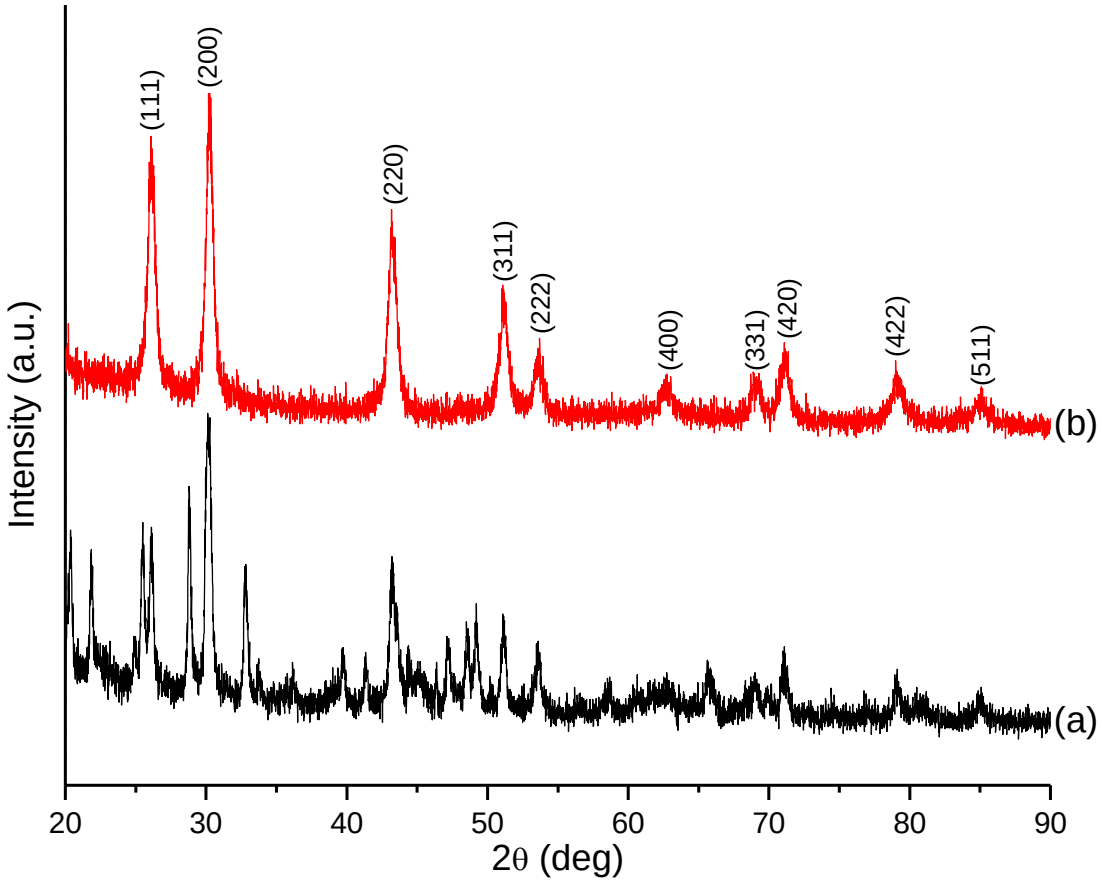

Figure 4.1: XRD patterns of PbS nanoparticles prepared at room temperature from (a) dual source precursors and (b) SSP.

Figure 4.2 shows TEM images of the as-prepared PbS nanoparticles obtained from the room temperature synthesis. The images reveal small sized nanoparticle formation from dual source precursors (Figure 4.2(a)) when compared to those obtained from the single source precursor (Figure 4.2(b)). The resultant particles from both types of precursors are dominated by cubic structured particles with sizes ranging from 23 ± 2.9 nm (Figure 4.2(a)) to 59 ± 17 nm (Figure 4.2(b)). A representative selective area electron diffraction patterns image shows high crystallinity of the prepared nanoparticles.

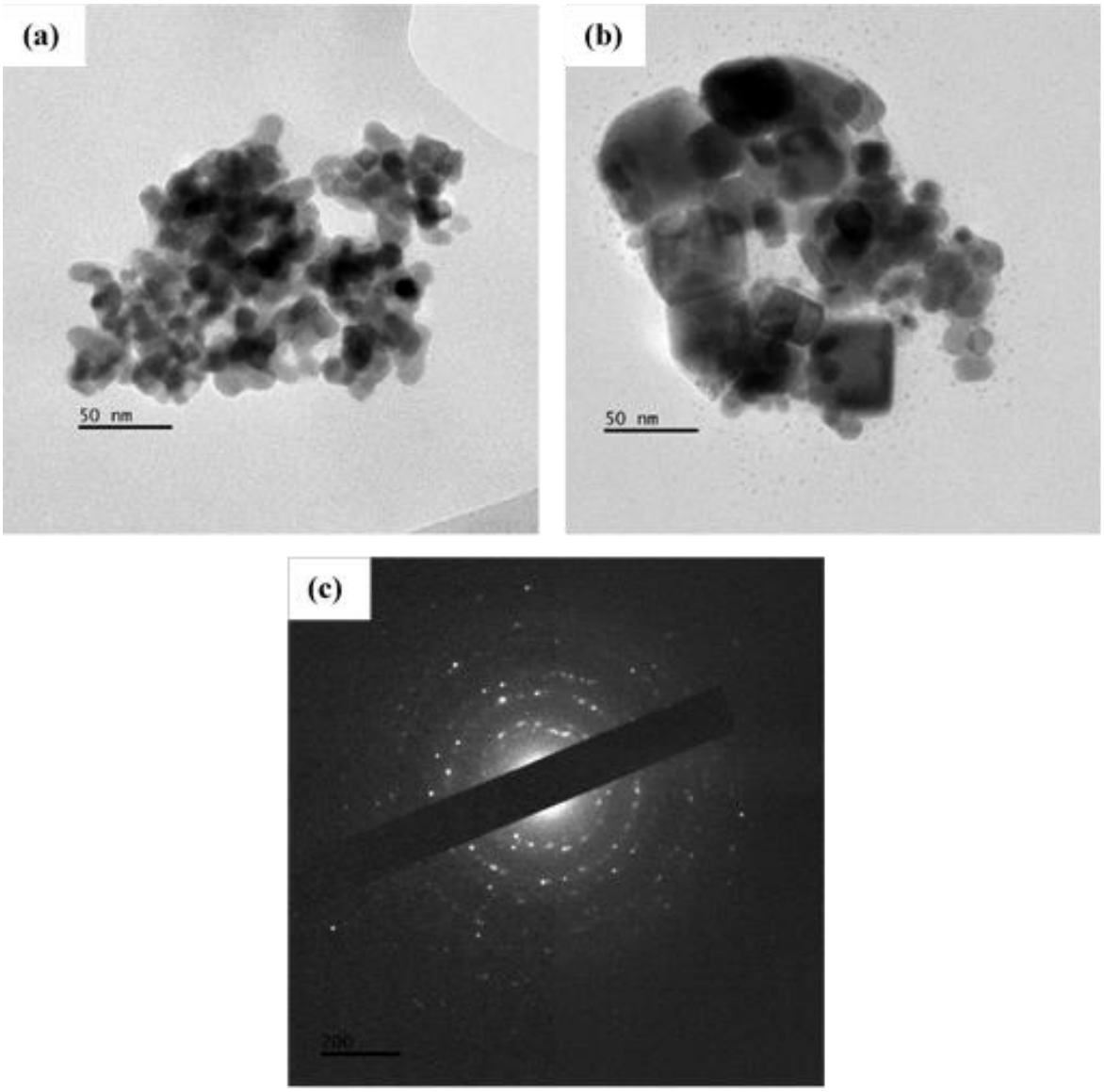

Figure 4.2: TEM images of PbS nanoparticles prepared at room temperature by (a) dual sources, (b) SSP and (c) their representative SAED patterns.

Figure 4.3 represents SEM images of as prepared PbS nanoparticles. Images obtained from dual source precursors (Figure 4.3(a) and (b)) conform with the TEM results of the same sample, they gave cubic structured nanoparticles with an average size of 44 ± 5.6 nm. Similar results have been obtained by Karami *et al.* when the same precursors (lead acetate and sodium sulfide with sodium dodecyl sulfate as a structural stabilizer) were used at relatively high temperatures.[20] The images in Figure 4.3(c) and d clearly show that the nanoparticles are uniform and spherical in shape with relatively smaller sizes (4.6 ± 2.1 nm). The spherical uniform shapes are in good

agreement with the ones reported in literature for PbS prepared at higher temperatures.[21] The percentage composition, EDX of the nanoparticles obtained from dual source precursors is shown in Figure 4.4 and the summary of all the methods reported in this chapter is listed in Table 4.1.

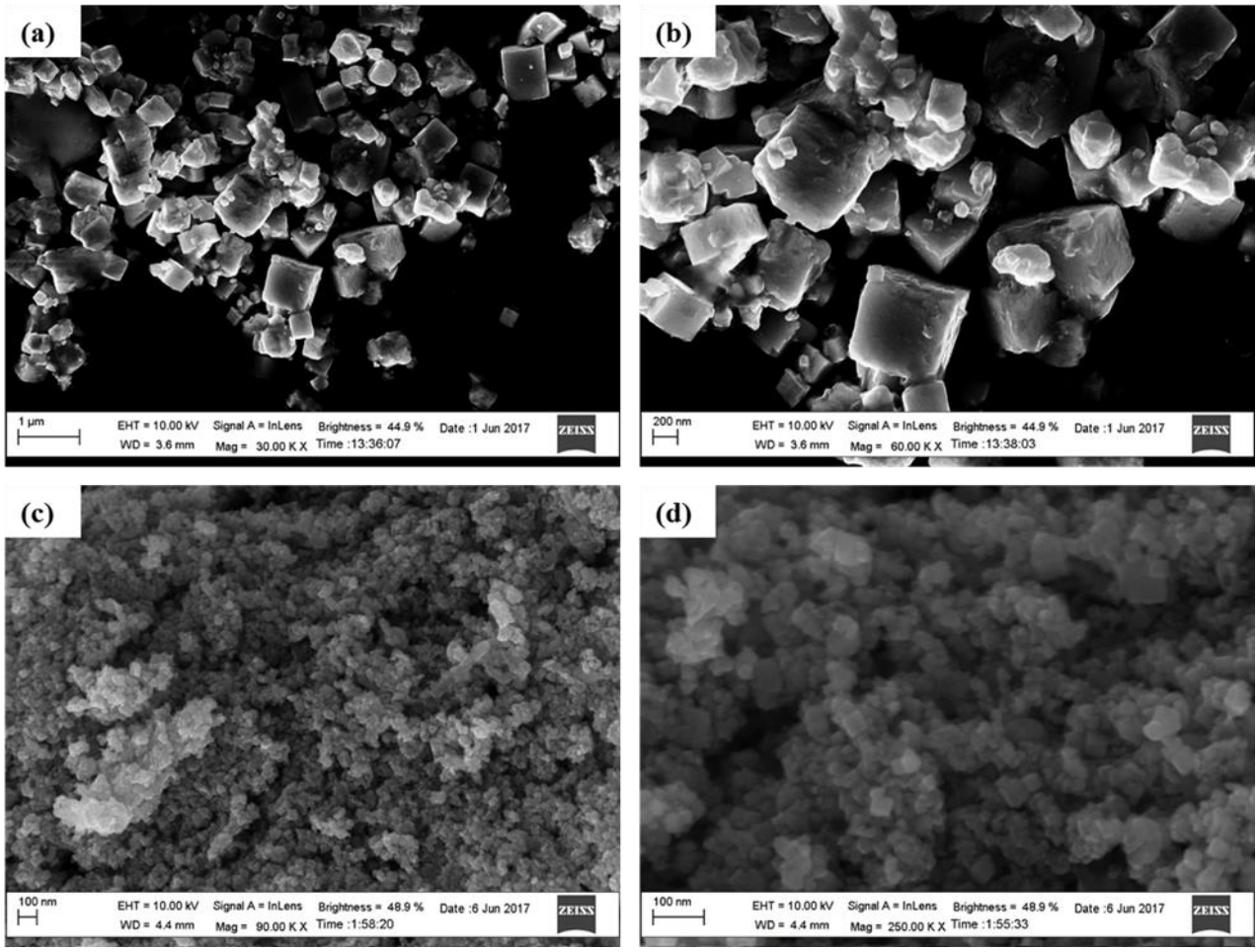

Figure 4.3: SEM images of PbS nanoparticles prepared from (a)-(b) dual sources and (c)-(d) SSP at room temperature.

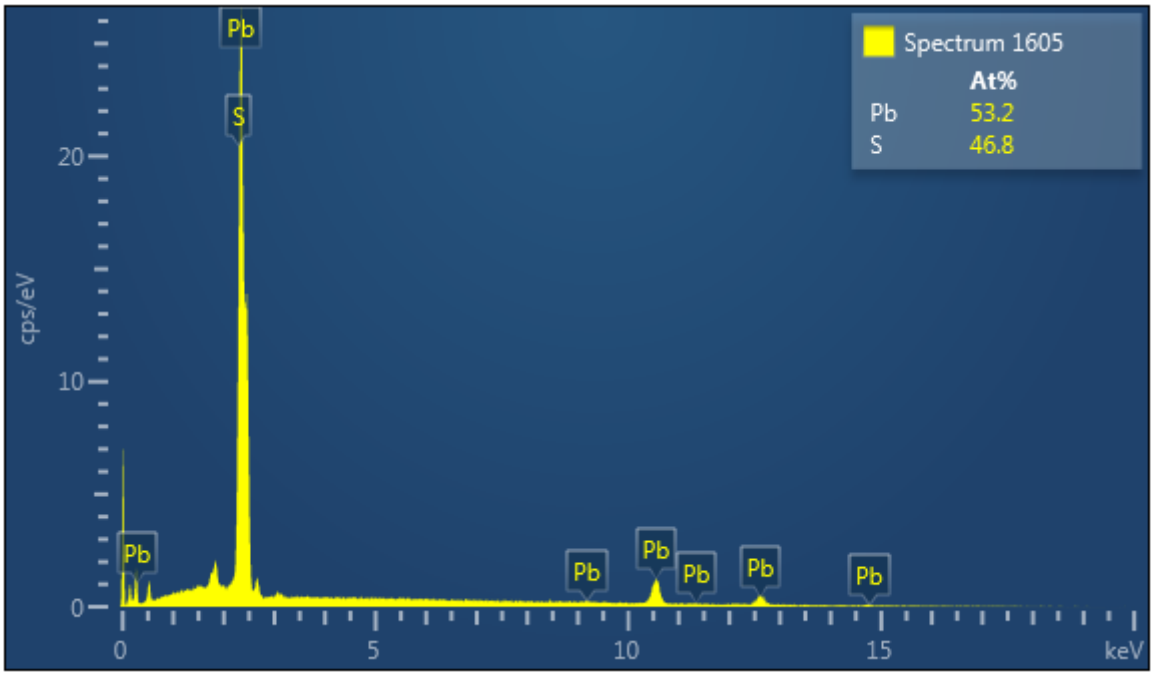

Figure 4.4: EDX analysis of PbS nanoparticles synthesized from dual sources at room temperature.

4.3.2. Microwave assisted synthesis of PbS nanoparticles

The microwave synthetic temperature was maintained at 150 ℃ for a 1 minute hold time duration for all materials discussed in this chapter. Again two types of starting materials (single and dual source precursors) were used independently. Figure 4.5 shows the XRD patterns of PbS nanoparticles prepared from both single and dual source precursors with the ionic liquid as a capping agent. The peaks of both samples (Figure 4.5(a) and (b)) could be readily indexed to the PbS cubic crystal structure with very small traces of impurities. There were no major impurities found on the analysed material and the results are comparable to other reported research findings.[22] TEM images (Figure 4.6(a)) reveal close to uniform sized nanoparticles obtained from dual source precursors while those obtained from single source precursors (Figure 4.6(c)) formed different shapes with high crystallinity as shown by the SAED patterns. The mean particle sizes of the images are 27 ± 5.2 nm and 28 ± 2.5 nm for the single source precursor and dual source precursors respectively. The shapes of these nanoparticles can be clearly seen from the SEM images (Figure 4.7). Mixed shapes i.e. spherical and cubic structured nanoparticles are observed for dual source precursors (Figure 4.7(a) and (b)) while lead ethyl xanthate (Figure 4.7(c) and (d)) produced perfect cubic shaped nanoparticles with EDX percent composition of 1:0.91 Pb:S ratio (Figure 4.8). The summary of EDX compositions of both SSP and dual souces is outlined in Table 4.1. From the table it is clearly visible that there is little sulfur deficiency.

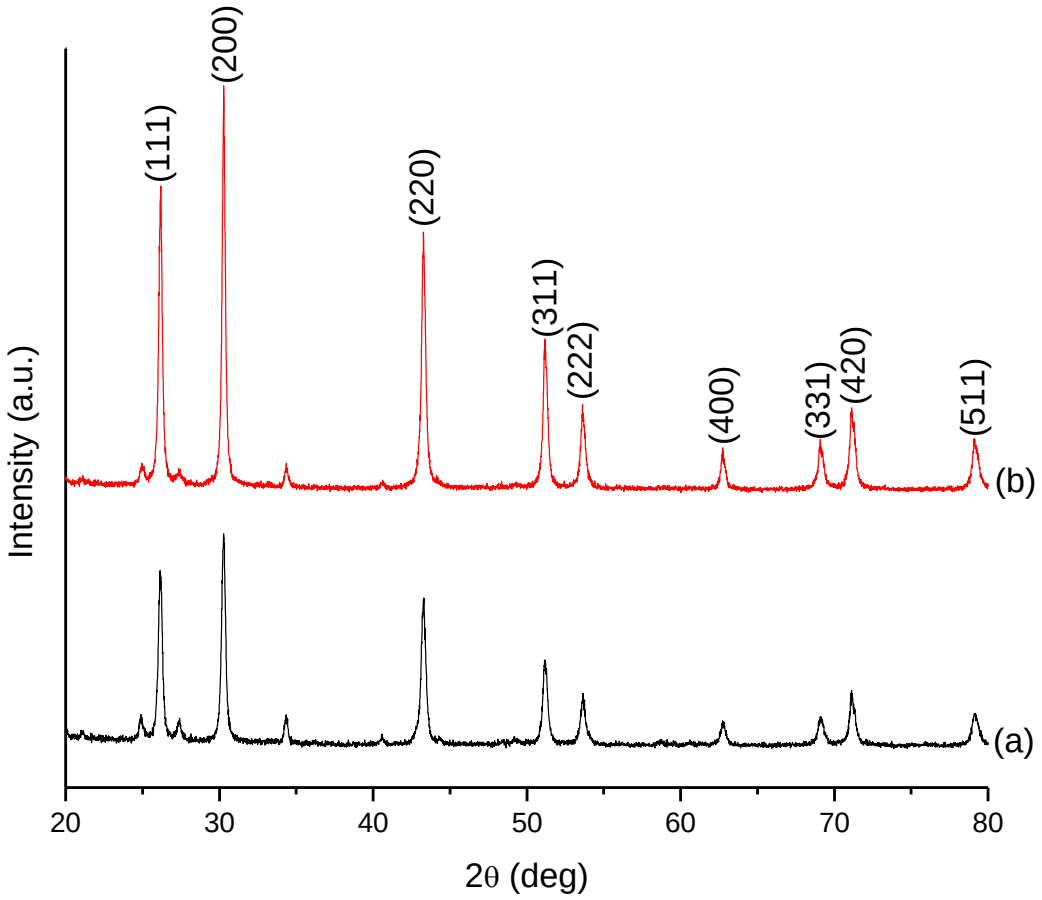

Figure 4.5: XRD patterns of PbS nanoparticles from (a) dual sources and (b) SSP by microwave irradiation.

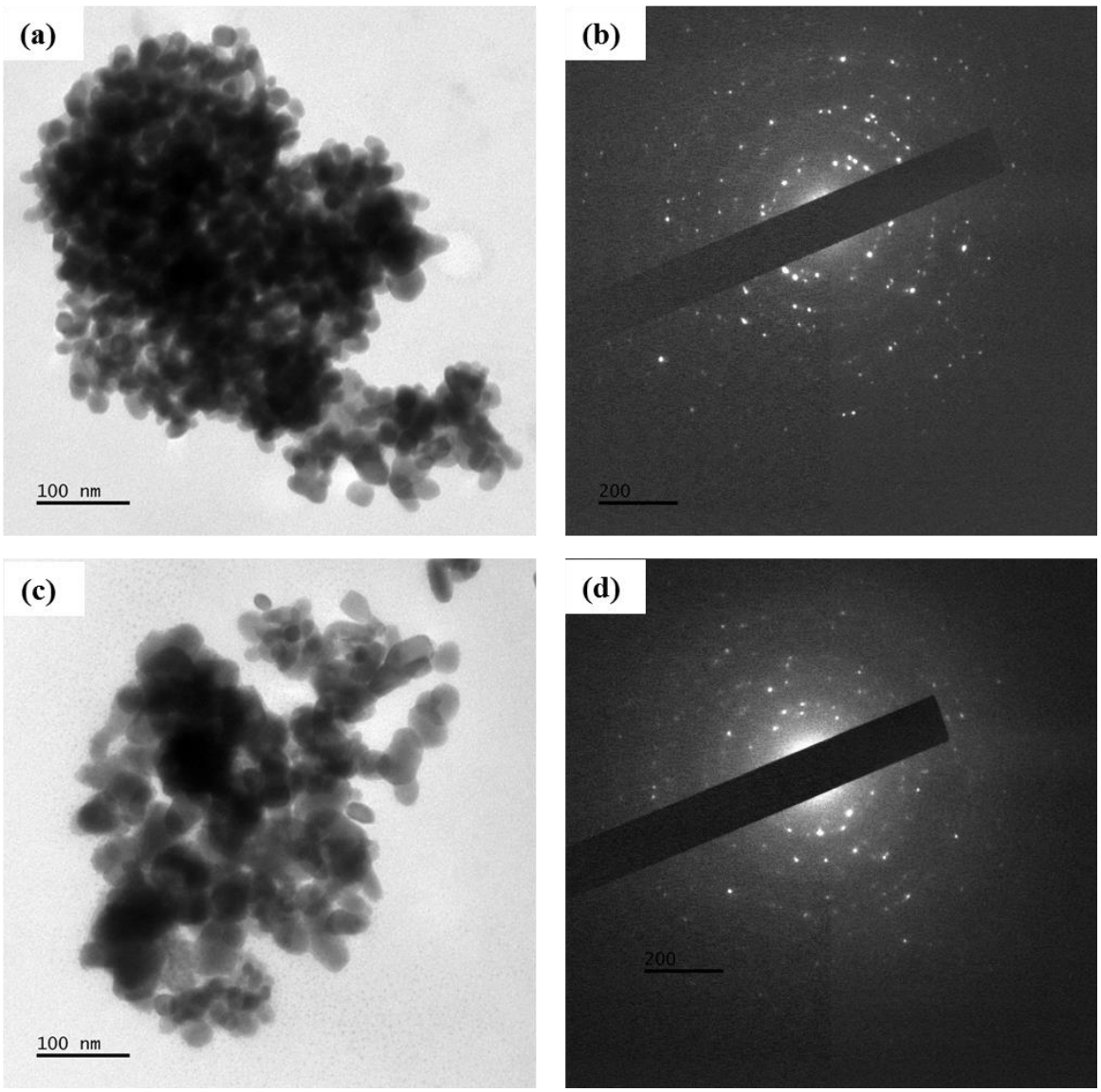

Figure 4.6: TEM images of PbS nanoparticles prepared through microwave irradiation by (a) dual sources and (c) SSP and their corresponding SAED patterns (b) and (d) respectively.

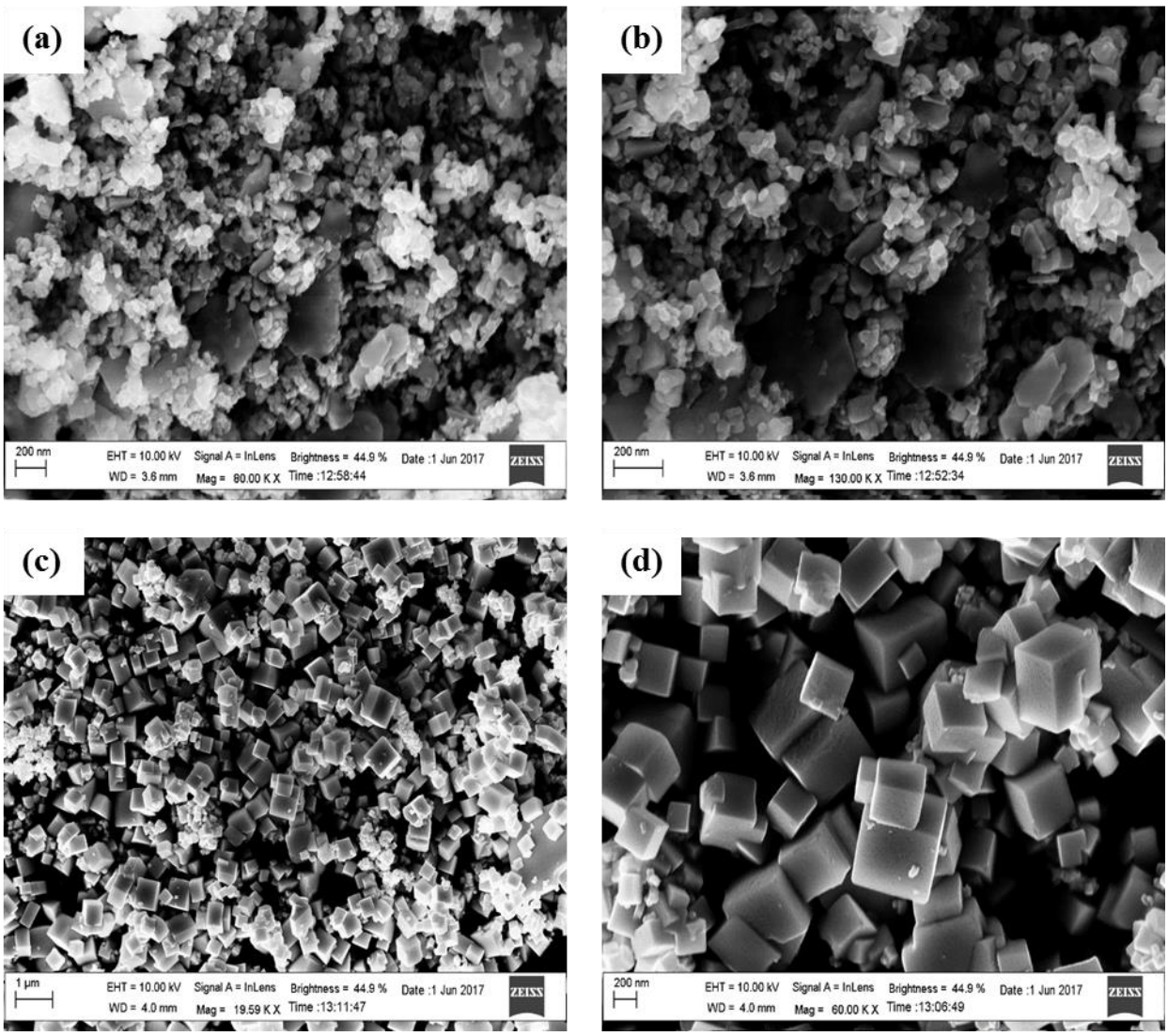

Figure 4.7: SEM images of PbS nanoparticles prepared through microwave irradiation by (a), (b) dual sources and (c), (d) SSP at different magnifications.

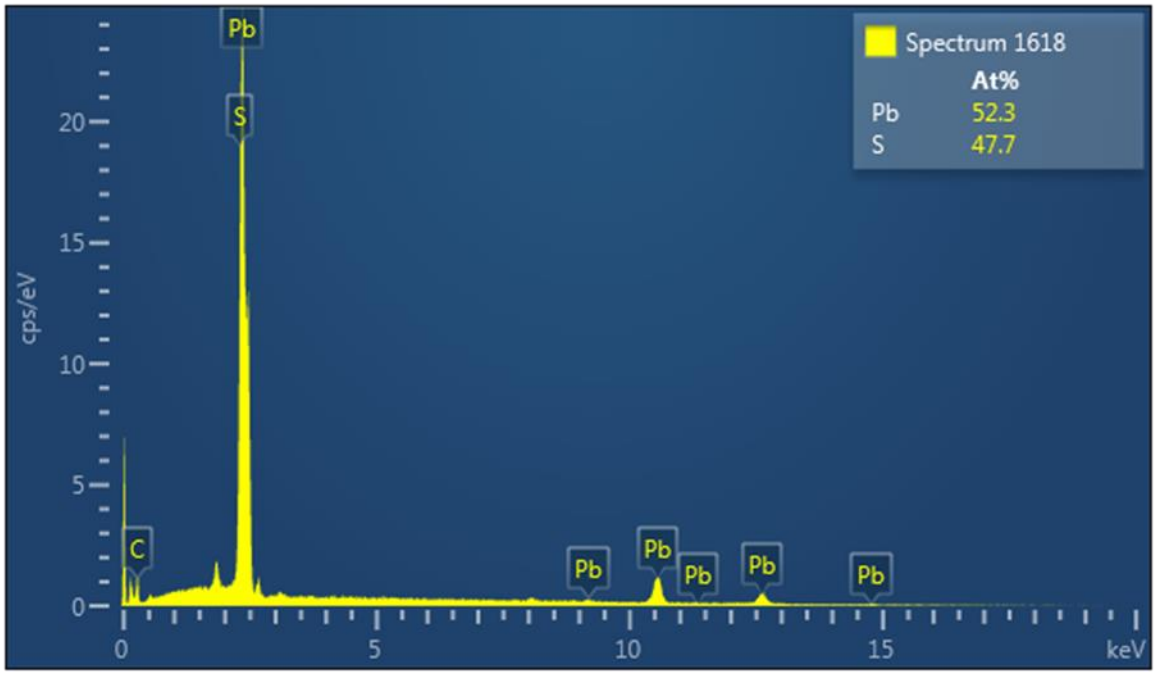

Figure 4.8: EDX analysis of PbS nanoparticles synthesized from SSP using microwave irradiation.

Table 4.1: Elemental composition of as synthesized PbS by EDX spectroscopy.

Precursor type	**Pb:S ratio**	
	Room temperature	**Microwave**
SSP	1:0.99	1:0.91
Dual sources	1:0.88	1:0.72

4.3.3. Microwave assisted synthesis of CdS nanoparticles

Figure 4.9 shows XRD patterns of CdS nanoparticles obtained from dual source and single source precursors respectively with ionic liquid being used as the capping agent for all reactions. The reactions were carried at 150 ℃ for a duration of 1 minute for CdS synthesis reported in this section. CdS is known to exist in two different crystal structures, the stable hexagonal wurtzite and the cubic zinc blende.[23] Both these phases have been obtained in this study and the transformation was influenced by the use of different precursors. The pattern in Figure 4.9(a) shows a formation of cubic CdS phase and in the latter (Figure 4.9(b)), a hexagonal phase was obtained. For both cases the samples showed no trace of impurities and could be indexed to their respective crystal phases. The peak broadness (more pronounced in Figure 4.9 (a)) is an indication that the nanoparticles are very small in size. Particle growth preference is towards the (111) plane for the cubic phase whereas for the hexagonal phase (002) orientation was preferred.

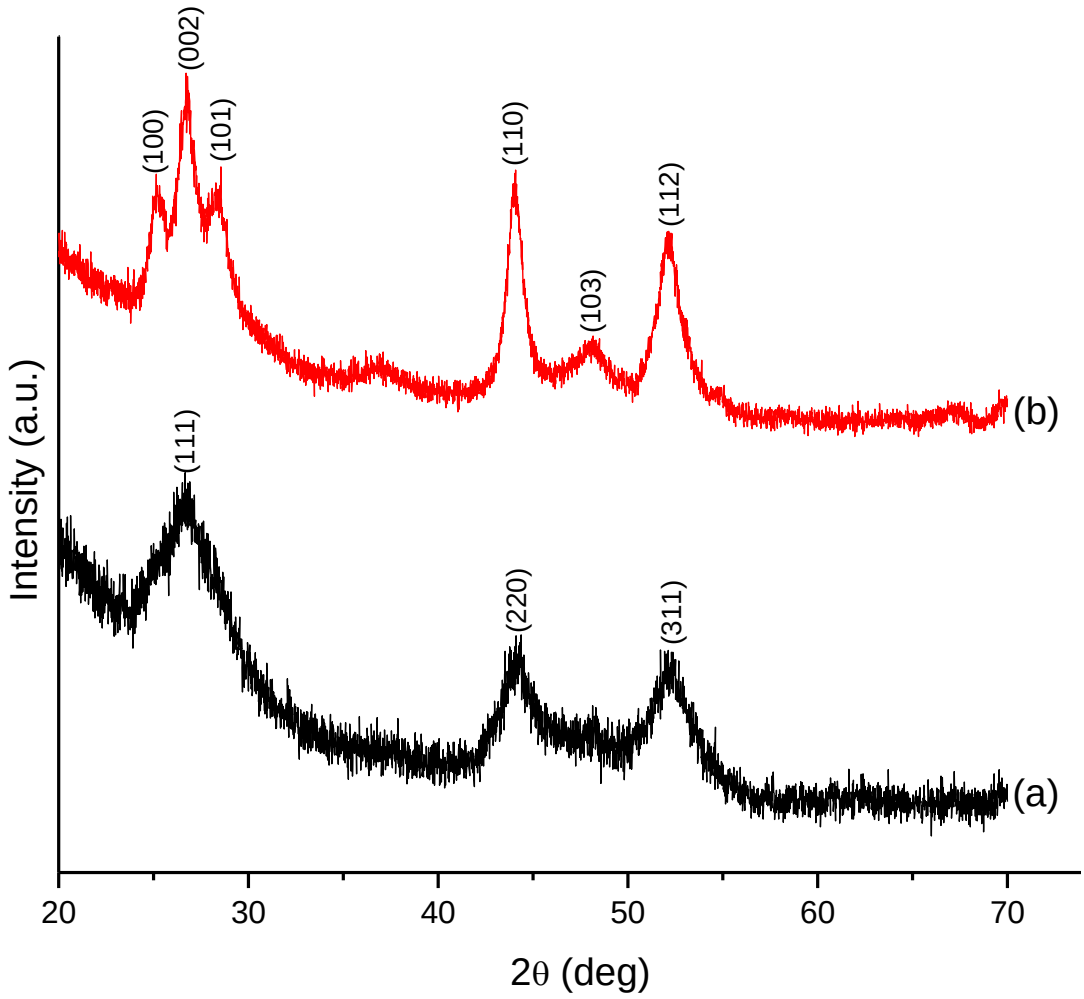

Figure 4.9: XRD patterns of CdS nanoparticles prepared from (a) dual sources and (b) SSP.

Figure 4.10 are ultraviolet visible spectra of CdS nanoparticles obtained from the use of single source precursor and dual source precursors at 150 ℃ for 1 minute hold time using a microwave. From the spectra (Figure 4.10(a) and (b)) it can be observed that nanoparticles obtained from both types of precursors show broad absorption 500 nm. This region is classified as the nanorange region and these results are further corroborated by the particle sizes obtained from XRD and TEM analyses. The production of small sized stable nanoparticles is an indication of the efficiency of the ionic liquid capping ability to the nanoparticles.[24,25]

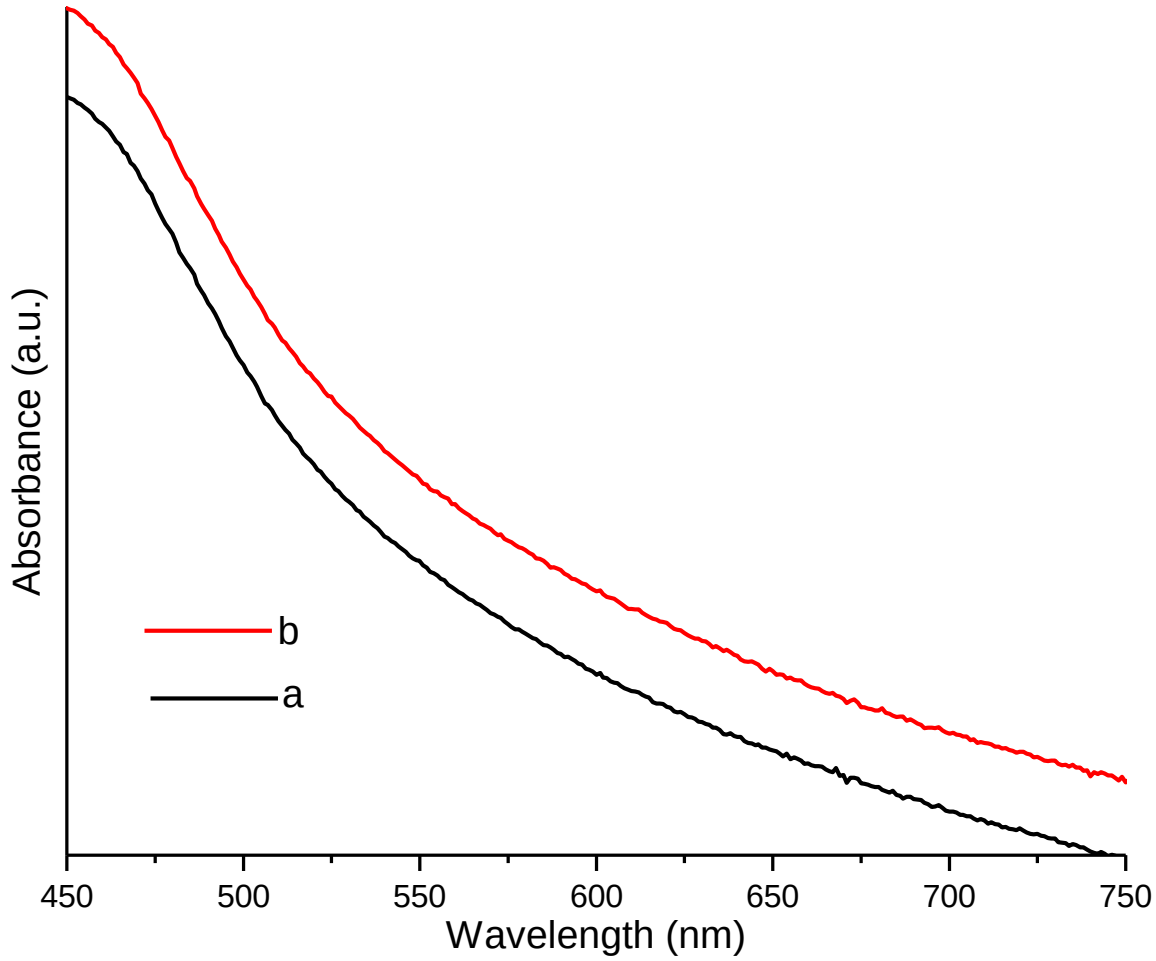

Figure 4.10: UV-vis spectrum of CdS nanoparticles synthesized from (a) dual sources and (b) SSP.

Photoluminescence spectra of the as-synthesized CdS nanoparticles are shown in Figure 4.11. The emission peak is observed at 515 nm with a shoulder at 492 nm (Figure 4.11(a)), the shoulder can be attributed to the trap state emission.[26] Again the emission peak observed at 534 nm (Figure 4.11(b)) which is associated with green band luminescence.[37] The nanoparticles obtained from the two precursors molecules differ in phases as observed in XRD analysis and hence the difference in the emission wavelength. Single source precursor produced nanoparticles which emit at a longer wavelength which indicates the formation of larger nanoparticle sizes, this results conforms with the XRD analysis.

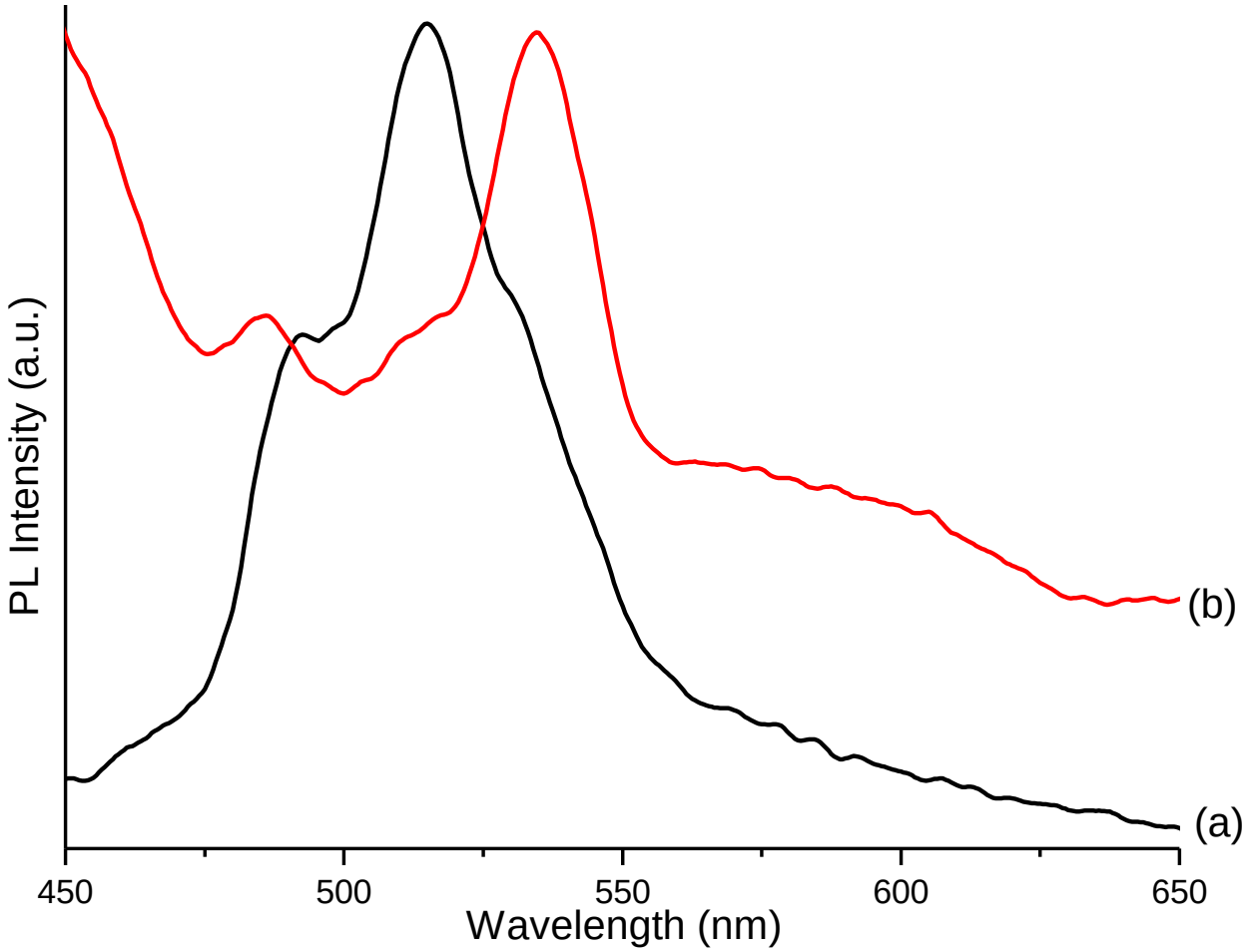

Figure 4.11: PL spectrum of CdS nanoparticles synthesized from (a) dual sources and (b) SSP.

TEM images CdS nanoparticles shown in Figure 4.12(a)-(d) reveal very small and spherical particles. The ionic liquid, [EMIM][$MeSO_4$], comprises of $[EMIM]^+$ cations and $[MeSO_4]^-$ anions. When a solution of the ionic liquid is used as a reaction medium, the sulfide moieties of the CdS nuclei are expected to be highly solvated by $[EMIM]^+$ ions through electrostatic and hydrogen bonding interactions.[28] Since ionic liquids have low interface tensions which results in high nucleation rates, small nanoparticles are formed.[29] The size of these nanoparticles conforms with the earlier reported results which are in the nano range region. The slow growth of the nanoparticles may be due to the hydrogen bond formed between the hydrogen atom at position 2 of the imidazole ring (Figure 1.8) and the sulfur atom of the CdS which serves as an effective bridge to connect the S^- terminated plane of the produced nuclei of metal sulfide and cations of ionic liquid.[30]

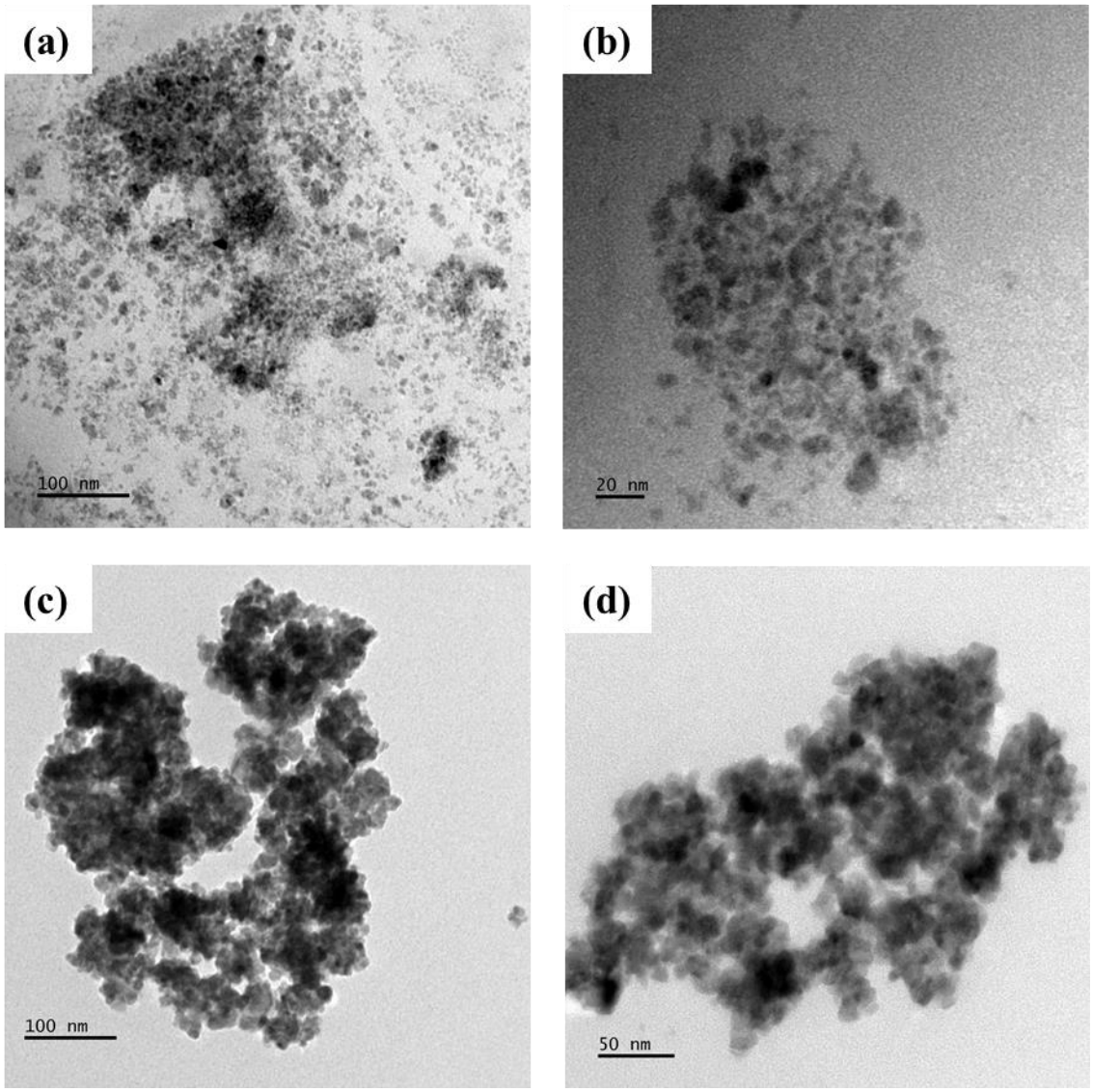

Figure 4.12: TEM images of CdS nanoparticles prepared from (a)-(b) dual sources and (c)-d) SSP.

The recorded FTIR spectra of the ionic liquid and CdS nanoparticles prepared in the ionic liquid are illustrated in Figure 4.13. The bands located at 3091 cm^{-1} (IL) and 3021 cm^{-1} (IL capped CdS) are assigned to the stretching vibrations of C(2)-H in an imidazole ring. Adsorption bands found at 1575 cm^{-1} (IL) and 1549 cm^{-1} (IL capped CdS) are attributed to the skeleton stretching vibrations of the imidazole ring.[30] The bands at 1179 cm^{-1}(IL) and 1191 cm^{-1}(IL capped CdS) are due to C-H of the imidazole ring in-plane deformation vibrations.[31] The difference in bands is an indication of the existence of hydrogen bonding and interaction between the ionic liquid and the as-prepared nanoparticles.

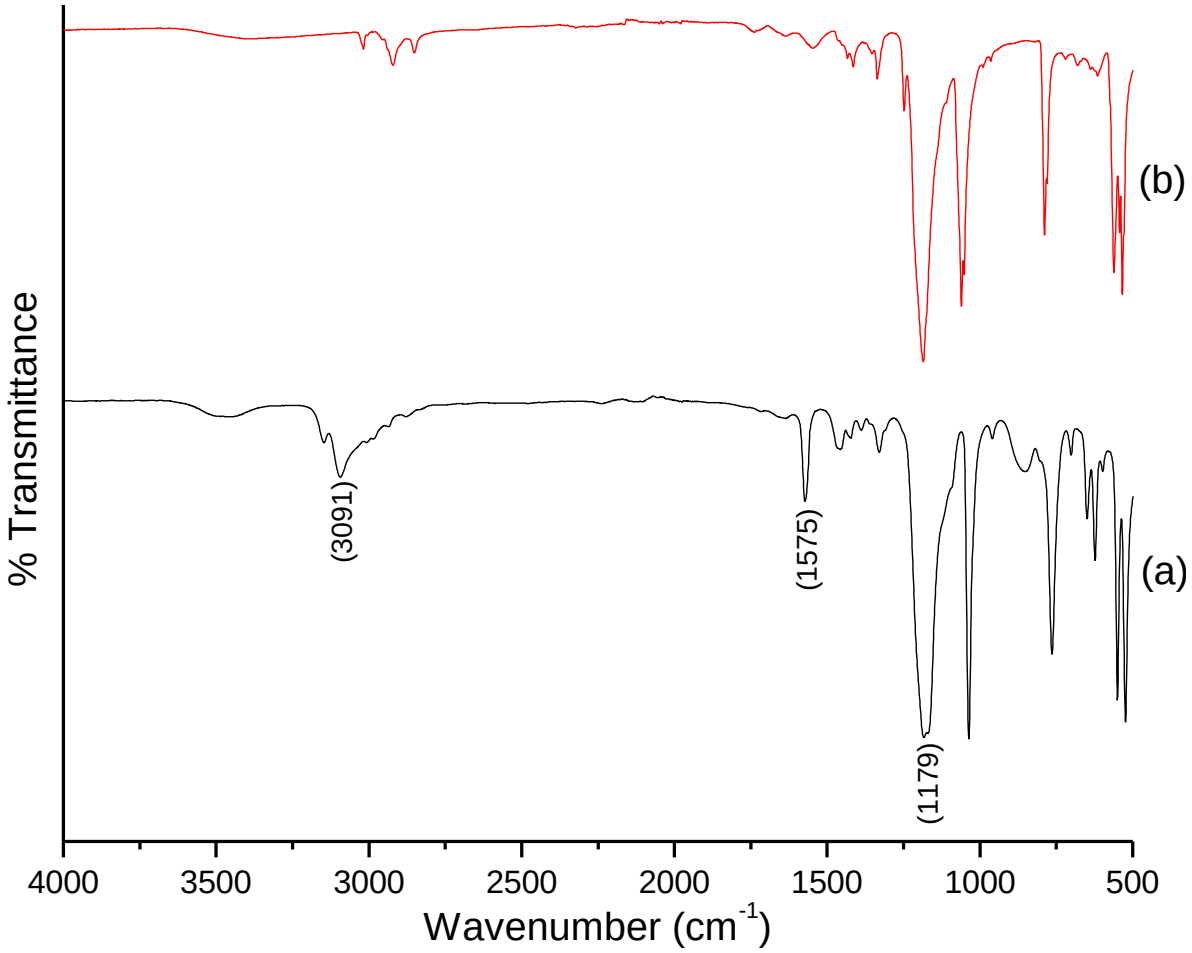

Figure 13: FTIR spectra of (a) IL and (b) IL capped CdS nanoparticles synthesized from dual source precursors.

Figure 4.14 is a demonstration of FTIR spectra of the CdS nanoparticles prepared from the SSP. The shift in bands from 3091 cm^{-1}, 1575 cm^{-1}, 1179 cm^{-1} of the pure IL (a) to 1626 cm^{-1}, 1370 cm^{-1}, 1108 cm^{-1} of the IL capped CdS (b) nanoparticles is an illustration of the formation of new bonds which indicates the interaction between the ionic liquid and the CdS nanoparticles.

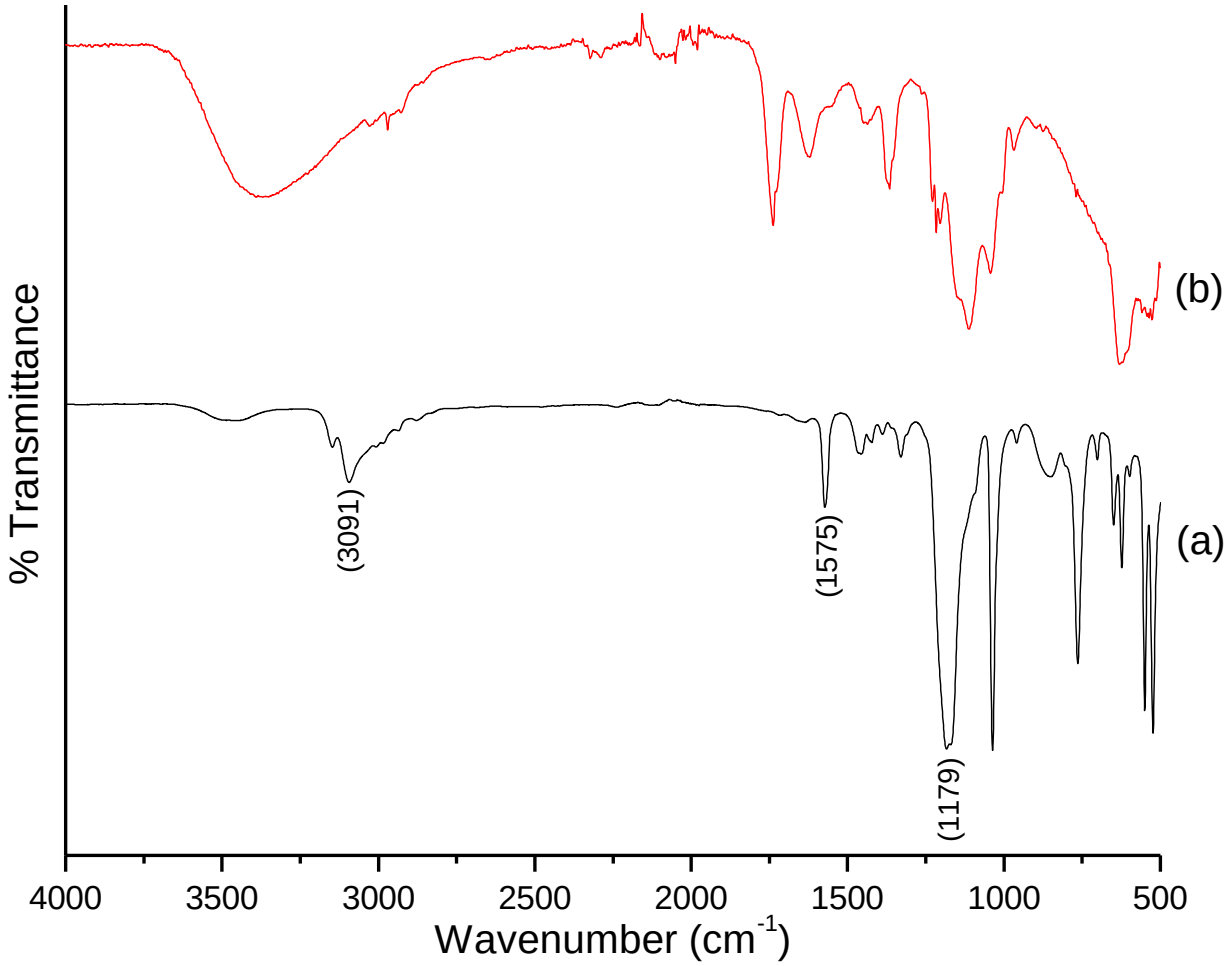

Figure 14: FTIR spectra of (a) IL and (b) IL capped CdS nanoparticles synthesized from SSP.

Conclusion

Facile synthesis of CdS and PbS nanoparticles has been reported. Two different routes i.e. room temperature synthesis (for PbS) and the microwave assisted synthesis (for both CdS and PbS) were employed. In each route two groups of precursors were used i.e. single and dual source precursors. Results obtained from the XRD study show a production of PbS nanoparticles with some impurities which are attributed to the unreacted components of the precursors of the dual precursors. A pure product was achieved from the single source precursor synthesis which is indexed to a cubic crystal phase from the same synthetic route. UV-vis analysis showed absorption in the nanorange region which confirms formation of very small nanoparticles. TEM images revealed crystalline nanoparticles with sizes ranging from 29 to 53 nm and SEM images confirmed these nanoparticles to be cubic in shape. Under the microwave assisted synthesis similar results were obtained however, the SEM images were more proper in shape when compared with those obtained from the former synthetic method. CdS synthesis was carried via the microwave irradiation only and the results differed significantly as different sets of precursors were used. Both known forms of CdS phases have been obtained, the hexagonal phase from the single source precursors and the cubic phase for the dual sources. In both cases, the sizes of the nanoparticles were very small. The two synthetic routes showed different results and properties have been obtained from them discretely, however microwave synthesis is the most efficient as products are obtained at very short time periods with high purity. The success of capping the nanoparticles by the ionic liquid has been confirmed by the FTIR results.

References

(1) Zhu, J.; Palchik, O.; Chen, S.; Gedanken, A. Microwave assisted preparation of CdSe, PbSe, and Cu_{2-x} Se nanoparticles. *The Journal of Physical Chemistry B* **2000**, *104*, 7344-7347.

(2) Zhu, J.; Zhou, M.; Xu, J.; Liao, X. Preparation of CdS and ZnS nanoparticles using microwave irradiation. *Materials Letters* **2001**, *47*, 25-29.

(3) Murugan, A. V.; Sonawane, R.; Kale, B.; Apte, S.; Kulkarni, A. V. Microwave–solvothermal synthesis of nanocrystalline cadmium sulfide. *Materials Chemistry and Physics* **2001**, *71*, 98-102.

(4) Gedye, R.; Smith, F.; Westaway, K.; Ali, H.; Baldisera, L.; Laberge, L.; Rousell, J. The use of microwave ovens for rapid organic synthesis. *Tetrahedron Letters* **1986**, *27*, 279-282.

(5) Caddick, S. Microwave assisted organic reactions. *Tetrahedron* **1995**, *51*, 10403-10432.

(6) Giguere, R. J.; Bray, T. L.; Duncan, S. M.; Majetich, G. Application of commercial microwave ovens to organic synthesis. *Tetrahedron Letters* **1986**, *27*, 4945-4948.

(7) Wang, H.; Zhang, J.-R.; Zhu, J.-J. A microwave assisted heating method for the rapid synthesis of sphalrite-type mercury sulfide nanocrystals with different sizes. *Journal of Crystal Growth* **2001**, *233*, 829-836.

(8) Ding, T.; Zhang, J.-R.; Long, S.; Zhu, J.-J. Synthesis of HgS and PbS nanocrystals in a polyol solvent by microwave heating. *Microelectronic Engineering* **2003**, *66*, 46-52.

(9) Chen, D.; Tang, K.; Shen, G.; Sheng, J.; Fang, Z.; Liu, X.; Zheng, H.; Qian, Y. Microwave-assisted synthesis of metal sulfides in ethylene glycol. *Materials Chemistry and Physics* **2003**, *82*, 206-209.

(10) Zhu, J.-J.; Wang, H.; Zhu, J.-M.; Wang, J. A rapid synthesis route for the preparation of CdS nanoribbons by microwave irradiation. *Materials Science and Engineering: B* **2002**, *94*, 136-140.

(11) Wada, Y.; Kuramoto, H.; Anand, J.; Kitamura, T.; Sakata, T.; Mori, H.; Yanagida, S. Microwave-assisted size control of CdS nanocrystallites. *Journal of Materials Chemistry* **2001**, *11*, 1936-1940.

(12) He, J.; Zhao, X.-N.; Zhu, J.-J.; Wang, J. Preparation of CdS nanowires by the decomposition of the complex in the presence of microwave irradiation. *Journal of Crystal Growth* **2002**, *240*, 389-394.

(13) Zhao, Y.; Liao, X.-H.; Hong, J.-M.; Zhu, J.-J. Synthesis of lead sulfide nanocrystals via microwave and sonochemical methods. *Materials Chemistry and Physics* **2004**, *87*, 149-153.

(14) Liao, X.-H.; Zhu, J.-J.; Chen, H.-Y. Microwave synthesis of nanocrystalline metal sulfides in formaldehyde solution. *Materials Science and Engineering: B* **2001**, *85*, 85-89.

(15) Caponetti, E.; Martino, D. C.; Leone, M.; Pedone, L.; Saladino, M. L.; Vetri, V. Microwave-assisted synthesis of anhydrous CdS nanoparticles in a water–oil microemulsion. *Journal of Colloid and Interface Science* **2006**, *304*, 413-418.

(16) Washington II, A. L.; Strouse, G. F. Microwave synthesis of CdSe and CdTe nanocrystals in nonabsorbing alkanes. *Journal of the American Chemical Society* **2008**, *130*, 8916-8922.

(17) Zhu, Y. J.; Wang, W. W.; Qi, R. J.; Hu, X. L. Microwave-assisted synthesis of single-crystalline tellurium nanorods and nanowires in ionic liquids. *Angewandte Chemie* **2004**, *116*, 1434-1438.

(18) Iimura, Y.; Ito, T.; Hagihara, H. The crystal structure of cadmium ethylxanthate. *Acta Crystallographica Section B: Structural Crystallography and Crystal Chemistry* **1972**, *28*, 2271-2279.

(19) Zhang, Y. C.; Qiao, T.; Hu, X. Y.; Wang, G. Y.; Wu, X. Shape-controlled synthesis of PbS microcrystallites by mild solvothermal decomposition of a single-source molecular precursor. *Journal of Crystal Growth* **2005**, *277*, 518-523.

(20) Karami, H.; Ghasemi, M.; Matini, S. Synthesis, characterization and application of lead sulfide nanostructures as ammonia gas sensing agent. *International Journal Electrochemical Science* **2013**, *8*, 11661-11679.

(21) Salavati-Niasari, M.; Sobhani, A.; Davar, F. Synthesis of star-shaped PbS nanocrystals using single-source precursor. *Journal of Alloys and Compounds* **2010**, *507*, 77-83.

(22) Afzaal, M.; O'Brien, P. Silica coated PbS nanowires. *Journal of Materials Chemistry* **2006**, *16*, 1113-1115.

(23) Zhai, T.; Fang, X.; Li, L.; Bando, Y.; Golberg, D. One-dimensional CdSnanostructures: Synthesis, properties, and applications. *Nanoscale* **2010**, *2*, 168-187.
(24) Manojkumar, K.; Sivaramakrishna, A.; Vijayakrishna, K. A short review on stable metal nanoparticles using ionic liquids, supported ionic liquids, and poly (ionic liquids). *Journal of Nanoparticle Research* **2016**, *18*, 1-22.
(25) He, Z.; Alexandridis, P. Nanoparticles in ionic liquids: Interactions and organization. *Physical Chemistry Chemical Physics* **2015**, *17*, 18238-18261.
(26) Xiao, Q.; Xiao, C.; Ouyang, L. Strong enhancement of band-edge photoluminescence in CdS nanocrystals prepared by one-step aqueous synthesis method. *Journal of Luminescence* **2008**, *128*, 1942-1947.
(27) Mirnaya, T.; Asaula, V.; Volkov, S.; Tolochko, A.; Melnik, D.; Klimusheva, G. Synthesis and optical properties of liquid crystalline nanocomposites of cadmium octanoate with CdS quantum dots. *Physics and Chemistry of Solids* **2012**, 131-135.
(28) Esmaili, M.; Habibi-Yangjeh, A. Microwave-assisted preparation of CdS nanoparticles in a halide-free ionic liquid and their photocatalytic activities. *Chinese Journal of Catalysis* **2011**, *32*, 933-938.
(29) Antonietti, M.; Kuang, D.; Smarsly, B.; Zhou, Y. Ionic liquids for the convenient synthesis of functional nanoparticles and other inorganic nanostructures. *Angewandte Chemie International Edition* **2004**, *43*, 4988-4992.
(30) Wang, L.; Chang, L.; Zhao, B.; Yuan, Z.; Shao, G.; Zheng, W. Systematic investigation on morphologies, forming mechanism, photocatalytic and photoluminescent properties of ZnO nanostructures constructed in ionic liquids. *Inorganic Chemistry* **2008**, *47*, 1443-1452.
(31) Zhu, J.; Shen, Y.; Xie, A.; Qiu, L.; Zhang, Q.; Zhang, S. Photoinduced synthesis of anisotropic gold nanoparticles in room-temperature ionic liquid. *The Journal of Physical Chemistry C* **2007**, *111*, 7629-7633.

CHAPTER FIVE

Conclusion and future work

5.1. Conclusion

Synthesis of ionic liquid (1-ethyl-3-methylimidazolium methanesulfonate) capped CdS and PbS nanoparticles using different synthetic methods i.e. thermolysis, microwave and room temperature (where no heat was applied for the reactions to continue) syntheses is reported. Temperature and precursor types were used as comparison tools in each route followed for the synthesis. At first three sets of temperatures viz 190 °C, 230 °C and 270 °C were used against single source precursor and dual sources independently. Hexagonal and cubic crystal phases have been obtained for CdS nanoparticles synthesized at high and low temperatures respectively. These nanoparticles were spherical in shape with sizes ranging from 2.40 to 15.66 nm. Their crystallinity was confirmed by XRD and SAED analyses and the optical studies (UV-vis and PL) revealed strong quantum size effect due to their sharp absorption bands.

A further study of the effect of sulfur source (for dual source precursors) on the morphology (with respect to temperature) of the nanoparticles was carried for the fabrication of PbS but only one type of single source precursor (ethyl xanthate) was used in this study for both CdS and PbS. The results have shown that an increase in the reaction temperature results in the formation of larger particle sizes. Use of single source precursor produced well defined shaped PbS nanoparticles (cubes) than dual sources route (irregular shapes). Again for dual source precursors, dodecanethiol required relatively high temperatures (250 °C) for production of pure PbS phase whereas sodium sulfide reacts readily even at low temperatures. The ionic liquid capping ability has been studied by FTIR and results showed that the nanoparticles have been capped.

A facile synthetic route for the preparation of both CdS and PbS nanoparticles was established under which microwave and room temperature syntheses were done. From room temperature synthesis, a pure product was achieved when lead ethyl xanthate (single source precursor) was used. The diffraction patterns obtained from XRD could be indexed to a cubic crystal phase of PbS. UV-vis analysis showed absorption in the nanorange region which confirms formation of very small nanoparticles. TEM images revealed crystalline nanoparticles with sizes ranging from 29 to 53 nm and SEM images confirmed these nanoparticles to be cubic in shape. Under the

microwave assisted synthesis similar results were obtained however, the SEM images were more pronounced in shape when compared with those obtained from the former synthetic method. CdS synthesis was carried via the microwave irradiation only and the results differed significantly as different sets of precursors were used. Both known forms of CdS phases have been obtained, the hexagonal phase from the single source precursors and the cubic phase for the dual sources. In both cases very small sizes of the nanoparticles were obtained. The two synthetic routes showed different results and properties have been obtained from them discretely, however microwave synthesis is the most efficient as products are obtained at very short time periods with high purity. The success of capping the nanoparticles by the ionic liquid has been confirmed by the FTIR results.

Several factors have been explored for the synthesis of CdS and PbS nanoparticles in the presence of the imidazolium based ionic liquid which showed the effectiveness of its capping capacity. From varying these factors it can be concluded that microwave synthesis gave the best results for PbS and the best optical results are obtained from thermolysis for CdS. Other materials can also be synthesized from the methods outlined in this study.

5.2. Suggestions for future work

Many synthetic routes have been established for the synthesis of CdS and PbS nanoparticles including the ones used in the present study, however thorough screening for the "proposed" applications (in solar cells) still needs to be done. Again a detailed mechanism for the obtained ionic liquid capped nanoparticle and some detailed spectroscopic analysis (NMR) may be done in future to provide valid binding sites between the IL and the nanoparticles.

Appendices: List of publications and conferences

List of publications

1. **Zikhona Tshemese**, Sixberth Mlowe, Neerish Revaprasadu, Deenadayalu. **Synthesis of CdS quantum dots using imidazolium based ionic liquid.** MSSP 71 (2017) 258–262.
2. **Zikhona Tshemese**, Malik Dilshad Khan, Sixberth Mlowe, Neerish Revaprasadu. **Synthesis and characterization of PbS nanoparticles in an ionic liquid using single and dual source precursors.** Materials Science & Engineering B 227 (2017) 116-121.

Conferences

1. Oral presenter: Synthesis and characterization of PbS nanoparticles using a xanthate single source precursor in an imidazolium based ionic liquid. 7th Annual Gauteng Nanosciences Young Researchers' Symposium (2017 SANi-NYRS).
2. Poster presenter: Synthesis and characterization of CdS nanoparticles using cadmium ethyl xanthate in an imidazolium based ionic liquid. SACI Inorganic 2017.
3. Poster presenter: Synthesis and chacterization of CdS nanoparticles in an imidazolium based ionic liquid. SACI 2015.